1980

Digital modeling of synchronous machines for transient stability studies

Kamran Behnam-Guilani
Iowa State University

BEHNAM-GUILANI, KAMRAN

DIGITAL MODELING OF SYNCHRONOUS MACHINES FOR TRANSIENT STABILITY STUDIES

Iowa State University PH.D. 1980

Digital modeling of synchronous machines for transient stability studies

by

Kamran Behnam-Guilani

A Dissertation Submitted to the
Graduate Faculty in Partial Fulfillment of the
Requirements for the Degree of
DOCTOR OF PHILOSOPHY

Major: Electrical Engineering

Approved:

Signature was redacted for privacy.

In Charge of Major Work

Signature was redacted for privacy.

For the Major Department

Signature was redacted for privacy.

For the Graduate College

Iowa State University
Ames, Iowa

1980

TABLE OF CONTENTS

LIST OF SYMBOLS AND DEFINITIONS

abc	Subscripts, denoting variables in abc-components
$\cdot$	Dot, denoting time-derivative operator, d/dt
d	Subscript, denoting variables on d-axis
δ_i	Angular deviation of rotor i with respect to synchronous reference frame
Δ	Prefix, denoting incremental value of a variable
$E' = E'_q + jE'_d$	Voltage behind the transient reactance
E_{FD}	Field voltage referred to armature side
H_i	Moment of inertia of mass i
i_i	Current at node i
K_A	Amplifier gain
K_E	Exciter gain
K_F	Stabilizing circuit gain
KM_D	Mutual coupling inductance between d-axis circuit and d-axis damper winding
KM_f	Mutual coupling inductance between d-axis circuit and field circuit
KM_{Qi}	Mutual coupling inductance between q-axis circuit and damper circuit i
L_{AD}	Magnetizing inductance on d-axis
L_{AQ}	Magnetizing inductance on q-axis
ℓ_D	d-axis damper winding leakage inductance
ℓ_d	d-axis circuit leakage inductance

$L_d = L_{AD} + \ell_d$	d-axis circuit self-inductance
ℓ_f	Field circuit leakage inductance
$L_f = L_{AD} + \ell_f$	Field circuit self-inductance
L_{ii}	Self-inductance of circuit i
$L_{ij} = L_{ji}$	Mutual inductance between circuits i and j
ℓ_{Qi}	q-axis damper winding i leakage inductance
$L_{Qi} = L_{AQ} + \ell_{Qi}$	q-axis damper winding i self-inductance
ℓ_q	q-axis circuit leakage inductance
$L_q = L_{AQ} + \ell_q$	q-axis circuit self-inductance
λ_i	Flux-linkage of circuit i
ω_R	Synchronous speed (377 rad/sec)
ω_i	Velocity of mass i
P_o	Generator (active) power output
P_{lo}	Load (active) power
q	Subscript, denoting variable on q-axis
Q_o	Generator (reactive) power output
Q_{lo}	Load (reactive) power
r_a	Armature resistance
r_e	Line resistance
r_D	D-damper winding resistance
r_f	Field circuit resistance
r_{Qi}	q-axis damper winding i resistance
RR	Exciter response ratio
r_t	Transformer resistance
τ_A	Amplifier time constant

τ_a	Armature time constant
t_c	Clearing time
T_e	Electrical developed torque
τ_E	Exciter time constant
τ_d''	d-axis subtransient short circuit time constant
τ_d'	d-axis transient short circuit time constant
τ_{do}''	d-axis subtransient open circuit time constant
τ_{do}'	d-axis transient open circuit time constant
T_m	Prime-mover torque
τ_q''	q-axis subtransient short circuit time constant
τ_q'	q-axis transient short circuit time constant
τ_{qo}''	q-axis subtransient open circuit time constant
τ_{qo}'	q-axis transient open circuit time constant
τ_R	Regulator input filter time constant
t_s	Switching time
v_f	Field voltage applied to field winding
v_H	Voltage on the high side of the station transformer
v_i	Voltage at node i
v_∞	Infinite bus voltage
V_{RMAX}	Maximum regulator output
V_{RMIN}	Minimum regulator output
v_t	Generator terminal voltage
x_d''	d-axis subtransient reactance
x_d'	d-axis transient reactance
x_d	d-axis synchronous reactance

x_e	Line reactance
x_ℓ	Armature leakage reactance
x_q''	q-axis subtransient reactance
x_q'	q-axis transient reactance
x_q	q-axis synchronous reactance
x_t	Transformer reactance
$\bar{y}$	Phasor
$\underline{Y}$	Matrix

I. INTRODUCTION

An important tool in power system planning is the examination of dynamic characteristics of alternative system designs, which involves time simulation of system's response to a disturbance, using a digital computer program. These studies, generally referred to as power system transient stability studies, are essential for proper power system planning.

In transient stability studies, mathematical models are developed for the components of power system, such as loads, generators, and interconnecting network (Figure 1). The power system's transient behavior

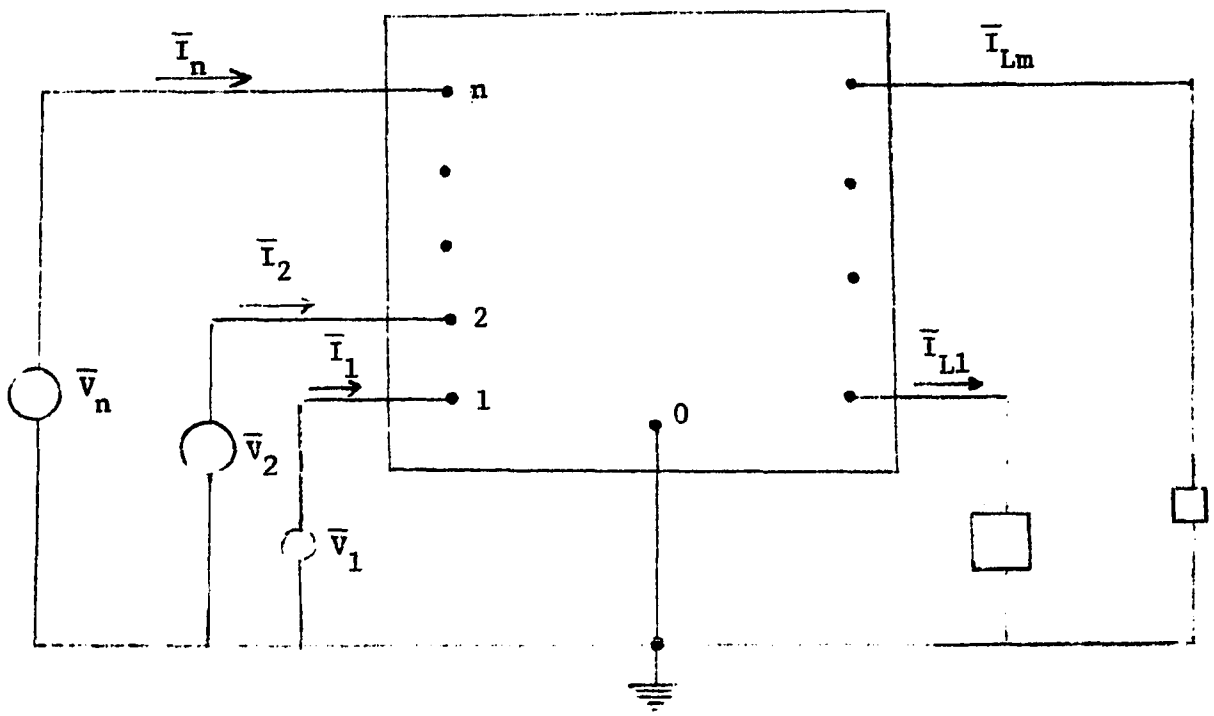

Figure 1. Multimachine power system with constant impedance loads

under the influence of a disturbance is then determined by obtaining time solutions using digital computer simulation. The information thus obtained can be used to graphically depict the transient performance of the power system. However, the steady increase in size and complexity of modern power systems has made these studies very expensive.

This dissertation is concerned with the development of efficient methods for accurate representation of synchronous machines, in power systems, for transient stability studies. There are a number of mathematical models that could be used to estimate the dynamic performance of synchronous machines. In selecting a model for a particular transient stability study, the trade-off is between accuracy versus computational cost. These models could range from the simple classical model to very complex models.

The work consists of three main parts:

1. To identify the least complex mathematical model that would approximate the basic dynamic characteristics of synchronous machines. These characteristics are indicated by a benchmark model considered to be accurate.
2. To develop and examine simulation techniques that will improve the efficiency of transient stability studies.
3. To develop efficient methods for selective modeling approach that will be used in a three tiered modeling strategy.

In this study, a complex model was chosen as the benchmark and is referred to as the FULL model. Numerous studies were made to find a

simple model that would approximate the basic dynamic characteristics of synchronous machines, as indicated by the benchmark model. This model will be referred to as the Approximate (APP) model.

Detailed examples of agreements and disagreements between these two models (FULL and APP) are given. The study describes how a combination of these two models could be used to improve the efficiency of simulation. Finally, a criterion based on fault location, clearing time, parameters, and initial loading of each machine is presented that could be used to determine the proper model (FULL or APP) to be selected to represent each synchronous machine.

It is hoped that this research work would contribute toward improving system study techniques, and thus make it possible for power system engineers to plan and operate these systems in a more efficient manner.

II. LITERATURE REVIEW

Mathematical modeling of electric power systems is an established method for the evaluation of power system's transient performance and control techniques. Since the main goal of these studies is to determine whether or not the various synchronous machines in the disturbed power system will remain in synchronism with one another, the dynamic characteristics of those synchronous machines obviously play a crucial part in the outcome of the study (1).

In this chapter is presented a review of the trends in power system transient stability studies, a description of the state of the art, and how this research work relates to it. Mathematical models for synchronous machines are given in Chapter III.

A. Trends in Transient Stability Studies

The dynamic performance of interconnected synchronous machines became of major interest to power system engineers approximately fifty-five years ago with the recognition of transient instability phenomenon (2). Early transient stability studies represented synchronous machines by a very simple model that neglected all internal dynamic characteristics of these machines (the classical model). This model was based on the assumption that field winding flux linkages tend to remain constant during transient disturbance and was therefore useful only for simulation of transients of limited duration. The limitation

was acceptable since in the great majority of cases the concern was whether the generator survived the first rotor swing following a disturbance.

Development of synchronous machine theory since the 1920s made it clear that the internal dynamic characteristics of these machines influenced the results of transient stability studies, if modern automatic voltage regulators are adopted. In addition, the concern for greater accuracy of simulation of faults near machine terminals demanded the use of more complex generator models in transient stability studies.

The high-speed digital computer proved to be of invaluable assistance to the system planning engineers. It made it possible to carry out electric power system computations which previously were accomplished with the aid of sliderule or network analyzer. Since the early 1960s, digital computer programs for transient stability studies allowed improvements in the representation of generator characteristics and the size of power systems that could be studied. Reference 3 describes one of the earlier commercially available computer programs with provisions to represent 96 generators (using the one-axis model), voltage regulator, and speed governor. Typical of the more recently available computer programs is the stability program developed by Philadelphia Electric Company which made it possible to simulate a 1500-bus, 250-machine power system (4).

The rapid growth in digital computer memory capacity and computational speed has encouraged a greater degree of emphasis on more accurate modeling of synchronous machines. This, however, is not a

universally accepted viewpoint. Synchronous machine modeling at transient phenomenon level is generally regarded to be adequate for transient stability studies. On the other hand, the ability to simulate generator internal dynamics at the level of the so called stator transients and subtransient phenomenon is regarded by some to be necessary for accurate representation of synchronous machines for transient stability studies. A report published in 1973 (5) concludes that the synchronous machine models presently used in transient stability studies do adequately represent the dynamic characteristics of these machines. On the other hand, a number of published papers indicate that more complex models may be needed in order to accurately simulate synchronous machines for power system transient stability studies (6; 7). This latter view is supported by results of experiments which were conducted in laboratory (on micromachines) and in the field (on actual generators). In these experiments three-phase short circuits were placed at the terminals of the test machines and power angle, and thus swing curves were measured (8; 9).

1. Choice of machine data

There is increasing evidence that the choice of machine data used in any of synchronous machine models could heavily influence the accuracy of the results of power system studies (10).

There are basically two sets of machine data that are presently suggested, one set calculated on the basis of standard ANSI definitions, and the second set obtained from frequency response measurements (11).

Reference 12 provides a comparison between the calculated performance of 555 MVA turboalternators, using both the standard data and data obtained from frequency response measurements and actual operating tests. These studies indicate that results obtained with data derived from frequency response tests are superior to results obtained using standard data with actual operating test results used as the benchmark.

It is hoped that such studies would encourage synchronous machine manufacturers to adopt frequency response methods for determining machine constants and thus contribute to improved accuracy in power system studies.

2. Cost reducing techniques

The steady growth in the size of electric power systems has made it extremely expensive to study these systems in detail. Consequently, a great deal of time and effort has been devoted to the development of cost reducing techniques for these studies (13).

There are basically two possibilities: a) reduction of the actual system to a smaller equivalent system, and b) improvements in numerical solution algorithms. Reduction of the size of the system is achieved by dividing the power system into two areas - a study area and an external area. The number of generators in the external area is then reduced through the use of one of the available approaches to the problem of equivalents (14; 15; 16; 17). The procedure involves identification of the dynamically coherent generators that could be replaced by an equivalent machine. Also, the (equivalent) generators, in the external area,

are represented by very simple models which would further reduce the order of the system.

Improvements of numerical solution techniques can be achieved by identifying the fundamental dynamic characteristics of power system models and to relate these to appropriate numerical algorithms. There are a number of numerical integration techniques that could be used in power system stability studies (18; 19; 20), and it is imperative that the appropriate algorithm be selected for this purpose.

The interest in this area of research is reflected in the fact that Electric Power Research Institute sponsored the development of a diagnostic transient stability program by Boeing Computer Services, Inc. (21). This program makes it possible to evaluate the performance of the selected numerical method while conducting transient stability computations. It analyzes the numerical algorithms for efficiency, reliability, and numerical stability, thus making it possible to select the best numerical technique for conducting power system dynamic computations.

It is hoped that such research efforts will lead to the development of highly efficient computer programs for power system studies.

B. Scope of the Work

The steady increase in the demand for electric power, and the need for reliable and inexpensive electricity, is normally met by construction of additional power plants and power pooling through extensive interconnections. Consequently, modern power systems are constantly growing in size and complexity. Therefore, increasingly larger and more complex

mathematical models are needed for power system dynamic studies, which in turn require ever increasing computational resources. Thus power system studies have grown extremely expensive and at the same time highly essential for operating and planning purposes. The electric power industry is therefore facing two conflicting requirements:

1. Reduce the cost of system studies without sacrificing reliability.
2. Allow for more accurate studies through the use of more detailed modeling.

These requirements indicate the need for more efficient system study techniques, which inspired this research work.

It is the aim of this dissertation to present efficient methods for accurate representation of synchronous machines in transient stability studies. This will be achieved through the use of the model switching technique accompanied by a selective modeling approach that will be used in a three-tiered modeling strategy.

III. MATHEMATICAL MODELS

A. Synchronous Machine Models

A three-phase synchronous machine generally has four windings, the field winding and three armature, or stator, windings. These windings form a group of inductively coupled circuits as seen in Figure 2.

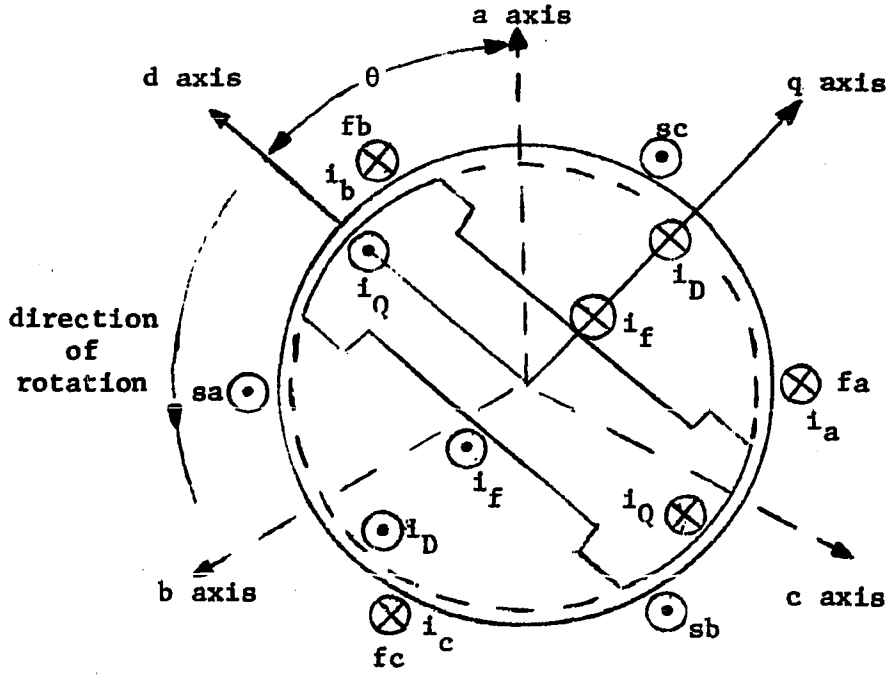

Figure 2. Schematic representation of a synchronous machine

The instantaneous terminal voltage of any of these circuits may be written in the form (22; 23)

$$v = ri + \dot{\lambda} \tag{1}$$

where r is the resistance of the winding, i is the current, and λ is the flux linkage of the winding, which depends upon the self-inductance

of the winding, the mutual inductances between it and other windings, and currents in all the coupled windings. Thus,

$$v_a = r_a i_a + \dot{\lambda}_a$$

$$v_b = r_b i_b + \dot{\lambda}_b$$

$$v_c = r_c i_c + \dot{\lambda}_c$$

$$v_f = r_f i_f + \dot{\lambda}_f \tag{2}$$

where, normally, $r_a = r_b = r_c$. If damper windings are also considered, the corresponding equations are

$$r_D i_D + \dot{\lambda}_D = 0$$

$$r_Q i_Q + \dot{\lambda}_Q = 0 \tag{3}$$

More damper windings could be considered if it is so desired. The flux linkage equations for these circuits are given by

$$\begin{bmatrix} \lambda_a \\ \lambda_b \\ \lambda_c \\ \lambda_f \\ \lambda_D \\ \lambda_Q \end{bmatrix} = \begin{bmatrix} L_{aa} & L_{ab} & L_{ac} & L_{af} & L_{aD} & L_{aQ} \\ L_{ba} & L_{bb} & L_{bc} & L_{bf} & L_{bD} & L_{bQ} \\ L_{ca} & L_{cb} & L_{cc} & L_{cf} & L_{cD} & L_{cQ} \\ L_{fa} & L_{fb} & L_{fc} & L_{ff} & L_{fD} & L_{fQ} \\ L_{Da} & L_{Db} & L_{Dc} & L_{Df} & L_{DD} & L_{DQ} \\ L_{Qa} & L_{Qb} & L_{Qc} & L_{Qf} & L_{QD} & L_{QQ} \end{bmatrix} \begin{bmatrix} i_a \\ i_b \\ i_c \\ i_f \\ i_D \\ i_Q \end{bmatrix} \tag{4}$$

Since many of the inductances vary periodically with the angular position of the rotor, it is extremely difficult to solve the differential equations of synchronous machines in the form presented so far.

However, if certain assumptions are made, a relatively simple transformation of variables will greatly simplify these equations.

The first assumption is that the stator windings are sinusoidally distributed along the air-gap so as to minimize all harmonics in the air-gap flux as much as is feasible. The second assumption is that the stator slots cause no appreciable variation of any of the rotor inductances with rotor angle. The principal justification for these assumptions comes from the comparison of calculated performance with actual performance obtained by test. The third assumption is that saturation of magnetic circuits can be neglected (24).

These assumptions make it possible to describe synchronous machine inductances as follows (25; 26):

Stator self-inductances are given by

$$L_{aa} = L_s + L_m \cos 2\theta$$
$$L_{bb} = L_s + L_m \cos 2(\theta - 2\pi/3)$$
$$L_{cc} = L_s + L_m \cos 2(\theta + 2\pi/3) \qquad (5)$$

Rotor self-inductances may be written as

$$L_{ff} = L_f \qquad L_{DD} = L_D \qquad L_{QQ} = L_Q \qquad (6)$$

which are all constant because saturation and slot effect are neglected.

Phase-to-phase mutual inductances are as follows:

$$L_{ab} = L_{ba} = -M_s - L_m \cos 2(\theta + \pi/6)$$
$$L_{bc} = L_{cb} = -M_s - L_m \cos 2(\theta - \pi/2)$$
$$L_{ca} = L_{ac} = -M_s - L_m \cos 2(\theta + 5\pi/6) \qquad (7)$$

Mutual inductances between stator and rotor are given by

$$L_{af} = L_{fa} = M_f \cos\theta$$

$$L_{bf} = L_{fb} = M_f \cos(\theta - 2\pi/3)$$

$$L_{cf} = L_{fc} = M_f \cos(\theta + 2\pi/3)$$

$$L_{aD} = L_{Da} = M_D \cos\theta$$

$$L_{bD} = L_{Db} = M_D \cos(\theta - 2\pi/3)$$

$$L_{cD} = L_{Dc} = M_D \cos(\theta + 2\pi/3)$$

$$L_{aQ} = L_{Qa} = M_Q \sin\theta$$

$$L_{bQ} = L_{Qb} = M_Q \sin(\theta - 2\pi/3)$$

$$L_{cQ} = L_{Qc} = M_Q \sin(\theta + 2\pi/3) \qquad (8)$$

Finally, rotor mutual inductances are given by

$$L_{fD} = L_{Df} = M_R$$

$$L_{fQ} = L_{Qf} = 0$$

$$L_{DQ} = L_{QD} = 0 \qquad (9)$$

The transformation, generally referred to as Park's transformation (27, 28), introduces a set of fictitious currents, voltages, and flux linkages, which are functions of actual currents, voltages, and flux linkages, and replaces them in the equations of synchronous machines. A modified version of Park's transformation(26) is defined as

$$\underline{P} = \sqrt{2/3} \begin{bmatrix} \frac{1}{\sqrt{2}} & \frac{1}{\sqrt{2}} & \frac{1}{\sqrt{2}} \\ \cos\theta & \cos(\theta - 2\pi/3) & \cos(\theta + 2\pi/3) \\ \sin\theta & \sin(\theta - 2\pi/3) & \sin(\theta + 2\pi/3) \end{bmatrix} \qquad (10)$$

which transforms all stator quantities from phases a, b, and c into new variables the frame of reference of which moves with the rotor. Thus, we get the relations

$$\underline{i}_{odq} = \underline{P}\ \underline{i}_{abc} \qquad \underline{v}_{odq} = \underline{P}\ \underline{v}_{abc} \qquad \underline{\lambda}_{odq} = \underline{P}\ \underline{\lambda}_{abc} \tag{11}$$

where

$$\underline{i}_{odq} = \begin{bmatrix} i_o \\ i_d \\ i_q \end{bmatrix} \qquad \underline{i}_{abc} = \begin{bmatrix} i_a \\ i_b \\ i_c \end{bmatrix} \tag{12}$$

and $\underline{v}_{odq}$, $\underline{v}_{abc}$, $\underline{\lambda}_{odq}$, and $\underline{\lambda}_{abc}$ are defined in a similar manner.

With the help of Park's transformation, the flux linkage equations may be written as

$$\begin{bmatrix} \lambda_o \\ \lambda_d \\ \lambda_q \\ \lambda_f \\ \lambda_D \\ \lambda_Q \end{bmatrix} = \begin{bmatrix} L_o & 0 & 0 & 0 & 0 & 0 \\ 0 & L_d & 0 & KM_f & KM_D & 0 \\ 0 & 0 & L_q & 0 & 0 & KM_Q \\ 0 & KM_f & 0 & L_f & M_R & 0 \\ 0 & KM_D & 0 & M_R & L_D & 0 \\ 0 & 0 & KM_Q & 0 & 0 & L_Q \end{bmatrix} \begin{bmatrix} i_o \\ i_d \\ i_q \\ i_f \\ i_D \\ i_Q \end{bmatrix} \tag{13}$$

where all of the inductances are constant. The inductance matrix is also symmetric which means it is physically realizable by an equivalent circuit. When remaining synchronous machine equations are similarly transformed, the so called Park's model will be obtained. Manufacturers

furnish data for synchronous machines sufficient to determine Park's model with two rotor circuits in the direct axis, and, in some cases (solid iron rotor machines), two rotor circuits in the quadrature axis. This model will be used as the benchmark model and will be referred to as the FULL model. This model is described by a set of eight first order differential equations as follows:

$$\dot{\lambda}_d = -r_a\, i_d - \omega\lambda_q - v_d$$

$$\dot{\lambda}_f = v_f - r_f\, i_f$$

$$\dot{\lambda}_D = -r_D\, i_D$$

$$\dot{\lambda}_q = -r_a\, i_q + \omega\lambda_d - v_q$$

$$\dot{\lambda}_{Q1} = -r_{Q1}\, i_{Q1}$$

$$\dot{\lambda}_{Q2} = -r_{Q2}\, i_{Q2}$$

$$\frac{2H\dot{\omega}}{\omega_R} = (T_m - T_e)$$

$$\dot{\delta} = \omega - \omega_R \qquad (14)$$

Notice that for hydro-generators

$$\dot{\lambda}_{Q1} = 0 \qquad (15)$$

Where

$$\lambda_d = L_d\, i_d + KM_f\, i_f + KM_D\, i_D$$

$$\lambda_f = L_f\, i_f + KM_f\, i_d + M_R\, i_D$$

$$\lambda_D = L_D\, i_D + KM_D\, i_D + M_R\, i_f$$

$$\lambda_q = L_q\, i_q + KM_{Q1}\, i_{Q1} + KM_{Q2}\, i_{Q2}$$

$$\lambda_{Q1} = L_{Q1}\, i_{Q1} + KM_{Q1}\, i_q + M_Q\, i_{Q2}$$

$$\lambda_{Q2} = L_{Q2}\, i_{Q2} + KM_{Q2}\, i_q + M_Q\, i_{Q1} \qquad (16)$$

As could be seen from the differential equations that describe the FULL model, this model accounts for the so called stator transients ($\dot{\lambda}_d$ and $\dot{\lambda}_q$) subtransient phenomenon ($\dot{\lambda}_D$ and $\dot{\lambda}_{Q2}$), transient phenomenon ($\dot{\lambda}_f$ and $\dot{\lambda}_{Q1}$), and mechanical transients ($\dot{\omega}$ and $\dot{\delta}$). Figure 3a illustrates equivalent circuit of the FULL model for a hydro-machine. The corresponding circuit for a turbo-generator is shown in Figure 3b.

The FULL model accounts for the so called stator transients ($\dot{\lambda}_d$ and $\dot{\lambda}_q$) which are caused by the dc-offset in stator short circuit current (29; 30; 31). Since flux produced by the dc-offset is stationary in space, it will induce sinusoidal voltages in the rotor circuits, frequencies of which are approximately 60 Hz. As a direct consequence of this fact, all electrical state variables in the FULL model will be oscillatory with near 60 Hz frequencies, thus making the FULL model extremely expensive for use in synchronous machine simulation.

The FULL model could, however, be reduced to much simpler models if certain simplifications were made. The most commonly made simplifications involve neglecting the stator transients and the subtransient phenomenon. The model thus obtained would have one rotor circuit in the direct axis and, for solid iron rotor machines, one rotor circuit in the quadrature axis. This model will be referred to as the approximate (APP) model.

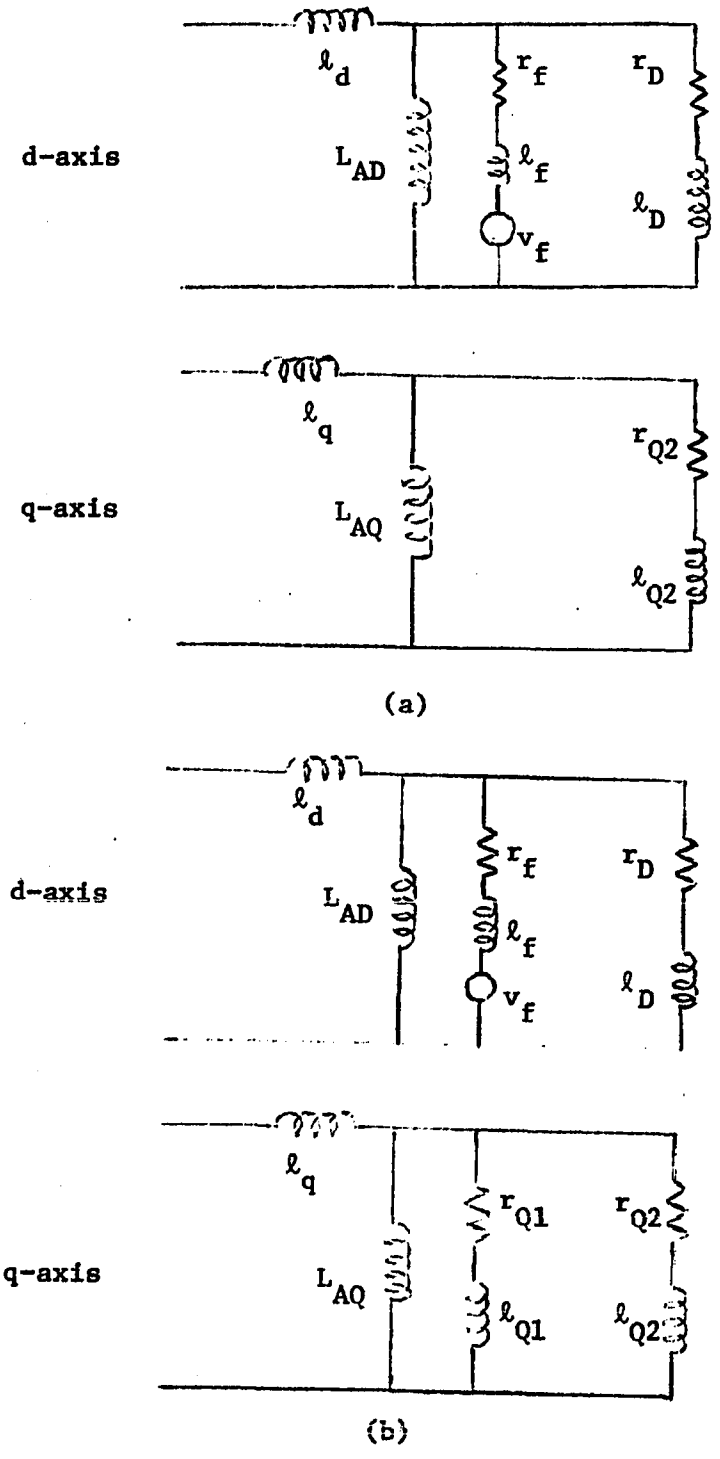

Figure 3. Equivalent circuits of the FULL model

The equivalent circuit for the APP model of a hydro-machine is given in Figure 4a. The corresponding circuit for a turbo-generator is illustrated in Figure 4b.

The differential equations describing the APP model are:

$$\begin{aligned}
\dot{\lambda}_f &= v_f - r_f\, i_f \\
\dot{\lambda}_{Q1} &= -r_{Q1}\, i_{Q1} \\
\frac{2H\dot{\omega}}{\omega_R} &= T_m - T_e \\
\dot{\delta} &= \omega - \omega_R
\end{aligned} \tag{17}$$

Notice that for hydro-machines

$$\dot{\lambda}_{Q1} = 0 \tag{18}$$

If the differential equations of the APP model are written in terms of stator variables, i.e., $\dot{E}'_q$ and $\dot{E}'_d$ instead of $\dot{\lambda}_f$ and $\dot{\lambda}_{Q1}$, the two-axis model will be obtained, which is described as follows:

$$\begin{aligned}
\dot{E}'_d &= \frac{-E'_d - (x_q - x'_q) I_q}{\tau'_{qo}} \\
\dot{E}'_q &= \frac{E_{FD} - E}{\tau'_{do}} \\
\frac{2H}{\omega_R}\dot{\omega} &= T_m - T_e \\
\dot{\delta} &= \omega - \omega_R
\end{aligned} \tag{19}$$

where

$$E = E'_q + (x'_d - x_d)\, I_d \tag{20}$$

In Equations 19 and 20, capital letters are used to indicate equivalent RMS quantities as per Reference [26], e.g., $I_q = i_q/\sqrt{3}$, etc.

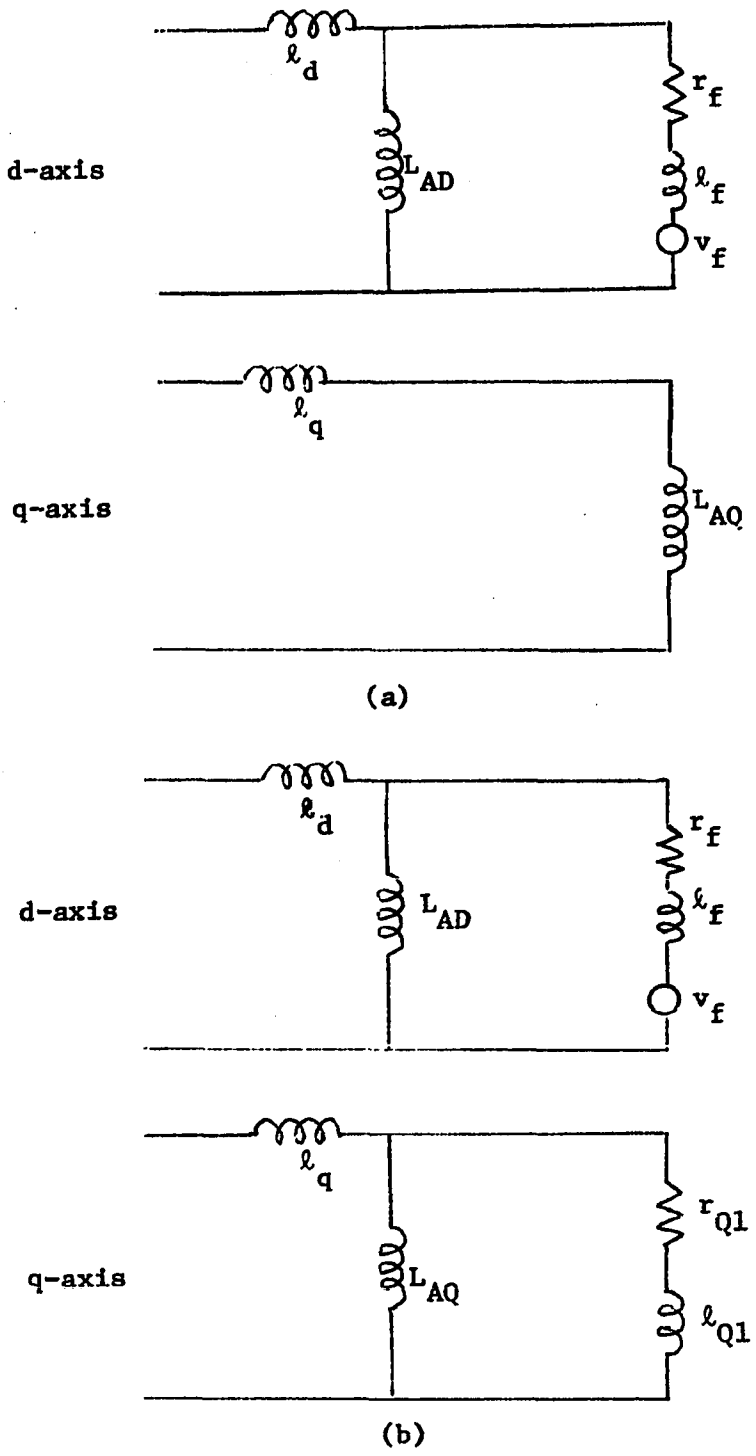

Figure 4. Equivalent circuits of the APP model

Notice that when $\dot{\lambda}_{Q1} = 0$, i.e., for hydro-machines, the one-axis model will be obtained, i.e., $\dot{E}'_d = 0$. Finally, if both $\dot{E}'_d$ and $\dot{E}'_q$ could be assumed to be zero, the synchronous machine can be represented by a constant voltage source behind a transient reactance. In this type of representation, it is further assumed that the mechanical angle of the synchronous machine rotor coincides with the electrical phase angle of the voltage behind transient reactance. The model that would thus be obtained is called the classical model. This model, due to its simplicity, was extensively used in the early stability studies, and is described by two first order differential equations as follows:

$$\frac{2H}{\omega_R}\dot{\omega} = T_m - T_e$$

$$\dot{\delta} = \omega - \omega_R \qquad (21)$$

B. Interface Equations

In this section, interface equations for a multimachine power system in the special case where loads are represented by constant impedances are developed. This was the only type of load representation considered in this research work. In such cases, it has been found adequate to represent the interconnecting network as a collection of lumped resistors, inductors, and capacitors, and to neglect the short lived electrical transients in the transmission system (26; 28). As a consequence of this fact, the terminal constraints imposed by the interconnecting network appear as a set of algebraid equations which may be solved by matrix methods as follows (see Chapter IX of Reference [26]):

$$\underline{\bar{T}}\,\underline{\bar{I}} = \underline{\bar{Y}}\,\underline{\bar{T}}\,\underline{\bar{V}} \tag{22}$$

where

$$\underline{\bar{V}} \triangleq \begin{bmatrix} v_{q1} + jv_{d1} \\ v_{q2} + jv_{d2} \\ \vdots \\ v_{qn} + jv_{dn} \end{bmatrix} = \begin{bmatrix} \bar{V}_1 \\ \bar{V}_2 \\ \vdots \\ \bar{V}_n \end{bmatrix} \tag{23}$$

$$\underline{\bar{I}} \triangleq \begin{bmatrix} i_{q1} + ji_{d1} \\ i_{q2} + ji_{d2} \\ \vdots \\ i_{qn} + ji_{dn} \end{bmatrix} = \begin{bmatrix} \bar{I}_1 \\ \bar{I}_2 \\ \vdots \\ \bar{I}_n \end{bmatrix} \tag{24}$$

where $\underline{\bar{Y}}$ is the short circuit admittance matrix of the interconnecting network, and $\underline{T}$ is a transformation matrix that transforms the d and q quantities of all machines to a common frame of reference rotating at synchronous speed. Premultiplying by $\underline{T}^{-1}$,

$$\underline{\bar{I}} = (\underline{T}^{-1}\,\underline{\bar{Y}}\underline{T})\underline{\bar{V}} = \underline{\bar{M}}\,\underline{\bar{V}} \tag{25}$$

and if $\underline{\bar{M}}^{-1}$ exists,

$$\underline{\bar{V}} = (\underline{T}^{-1}\,\underline{\bar{Y}}\underline{T})^{-1}\underline{\bar{I}} = (\underline{T}^{-1}\,\underline{\bar{Z}}\underline{T})\underline{\bar{I}} = \underline{\bar{M}}^{-1}\,\underline{\bar{I}} \tag{26}$$

where $\underline{\bar{Z}}$ is the matrix of the open circuit driving point and transfer impedances of the interconnecting network.

IV. SINGLE MACHINE STUDIES

In the early stages of this research work, numerous studies were made to compare the performance of various (synchronous machine) models. The results of these studies were used to identify the least complex model that would approximate the dynamic characteristics of the synchronous machines, as indicated by the benchmark model. Due to multiple-frequency behavior of multimachine systems, the differences between the performance of the various models are difficult to detect. On the other hand, the one machine-infinite-bus system model possesses only one mode of rotor angle oscillation. This system was therefore chosen for the preliminary studies, as shown in Figure 5.

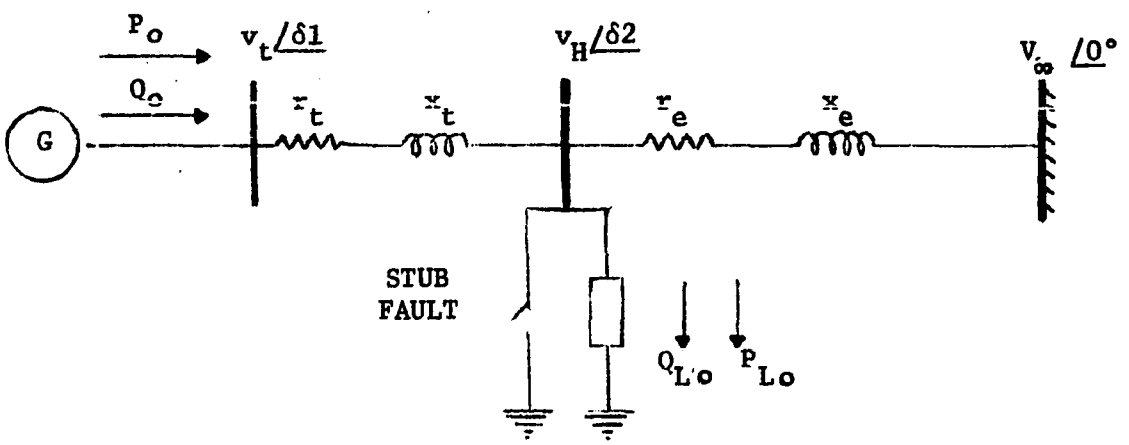

Figure 5. One-machine infinite-bus system

A two-pole 3600 rpm generator, typical of fossil fuel thermal units, was chosen for these studies. Data for the system are given in Table 1.

Table 1. System data[a]

x_d	x'_d	x''_d	τ'_{do}	τ''_{do}	x_q	x'_q	x''_q	τ'_{qo}	τ''_{qo}
1.75	.285	.24	.52	.0107	1.68	.47	.24	1.965	.053

τ_a	L_{AD}	L_{AQ}	r_a	H	MVA	r_t	x_t	r_e	x_e
.172	1.562	1.492	.0037	3.82	800	.0064	.1248	1.2880	2.6560

[a]Reactances and resistances are given in p.u. based on rated machine MVA and kV. H is in MW-sec/MVA. All time constants are in seconds.

The dynamic characteristics of a generator is a non-linear function of the electrical load on that generator. Therefore, transient performance of synchronous machines must be examined over a wide range of operating conditions. In this study, three different operating conditions, which are described in Table 2, were considered.

Table 2. Operating conditions

Case	I	II	III
δ, degrees	62	-6.4	9.8
$v_t/\underline{\delta_1}$	1.0255/6.7	1.055/-15.8	1.00/-15
P_o, MW	800	80	80
Q_o, MVAR	13.57	-40	-40
P_{Lo}, MW	795	145	149
Q_{Lo}, MVAR	-81.7	-96	-74
$v_H/\underline{\delta_2}$	1.025/-.15	1.055/-16.4	1.005/-15.5
$v_\infty/\underline{o}$	1.023	1.023	1.044

No prime mover dynamics were considered in any of the simulation studies performed. The generator was assumed to have a constant input torque.

Two excitation systems were considered, a conventional alternator-rectifier excitation system, and a high-initial response thyristor (SCR) exciter. Block diagrams and data for the exciters are given in the Appendix.

The disturbance was introduced by simulating a stub[1] fault applied on the high voltage side of the generator's station transformer. A stub fault was used to provide the desired large disturbance without introducing the effect of additional system parameters which would result if a fault with subsequent line trip had been simulated.

Case I (Heavy Loading)

In order to study the performance of various models, the generator was represented by three different models. These were the FULL, one-axis, and two-axis models. As illustrated in Figure 6, the one-axis model proved to be inadequate for predicting the dynamic performance of this synchronous machine, and therefore was not used in the subsequent studies. The two-axis model, on the other hand, is in relatively good agreement with the FULL model. It predicts the first rotor swing with a fair degree of accuracy. More importantly, the frequencies of oscillation as indicated by the FULL and the two-axis models, are in good agreement.

Case II (Light Loading)

The synchronous machine was represented by the FULL and two-axis models, as shown in Figure 7. The FULL model correctly predicts the backswing phenomenon which is not indicated when the two-axis model is used. Nevertheless, the two models are in relatively good agreement. In fact, in Case II, the two models are in much better agreement than they

[1]A stub fault is defined as a fault applied at the end of a short stub section of line which has no apparatus connected to it. When fault is cleared, the post-fault system is identical to the pre-fault system.

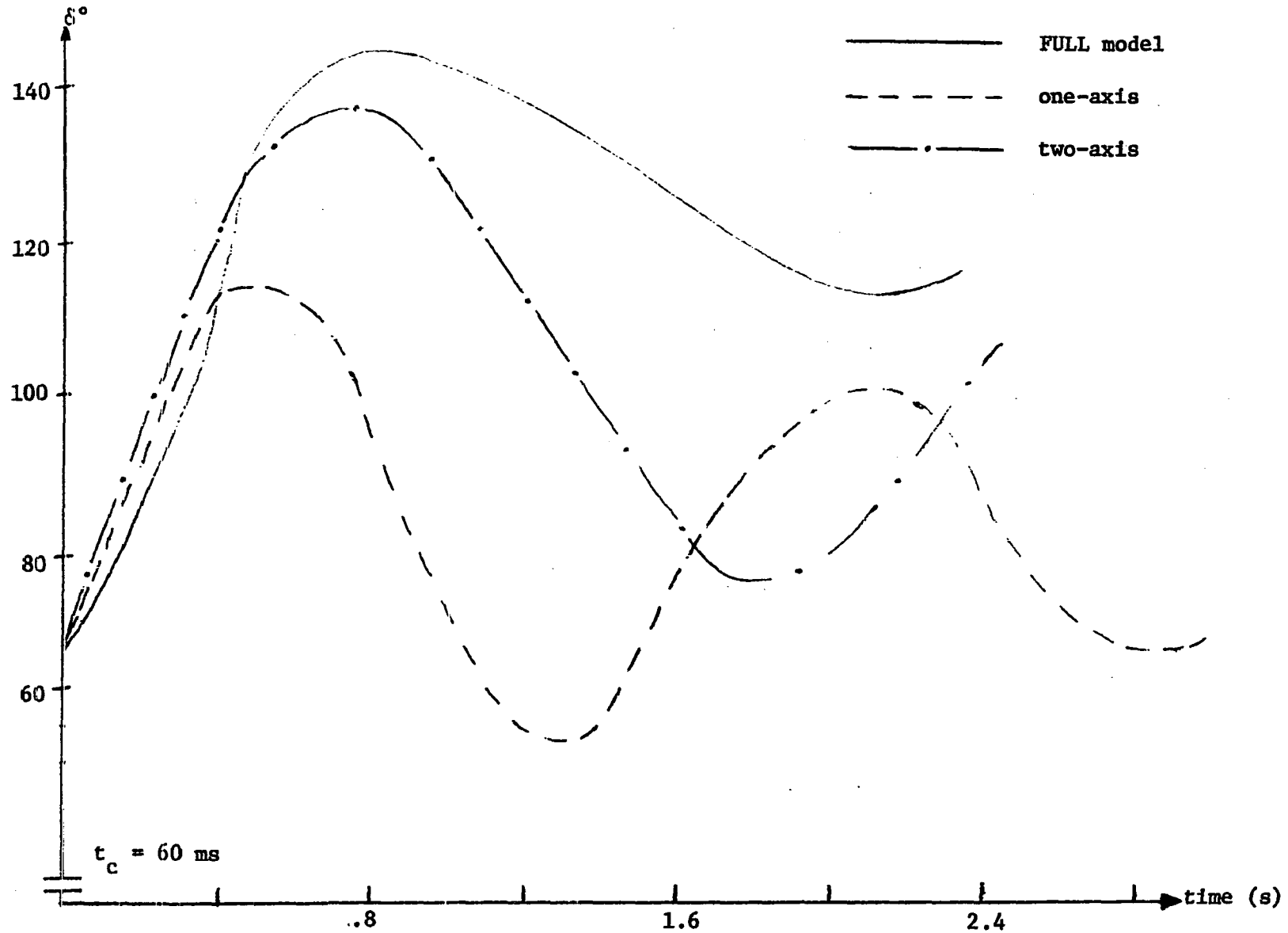

Figure 6. Plot of δ versus time (Case I). Simulation by the FULL, one-axis, and two-axis models

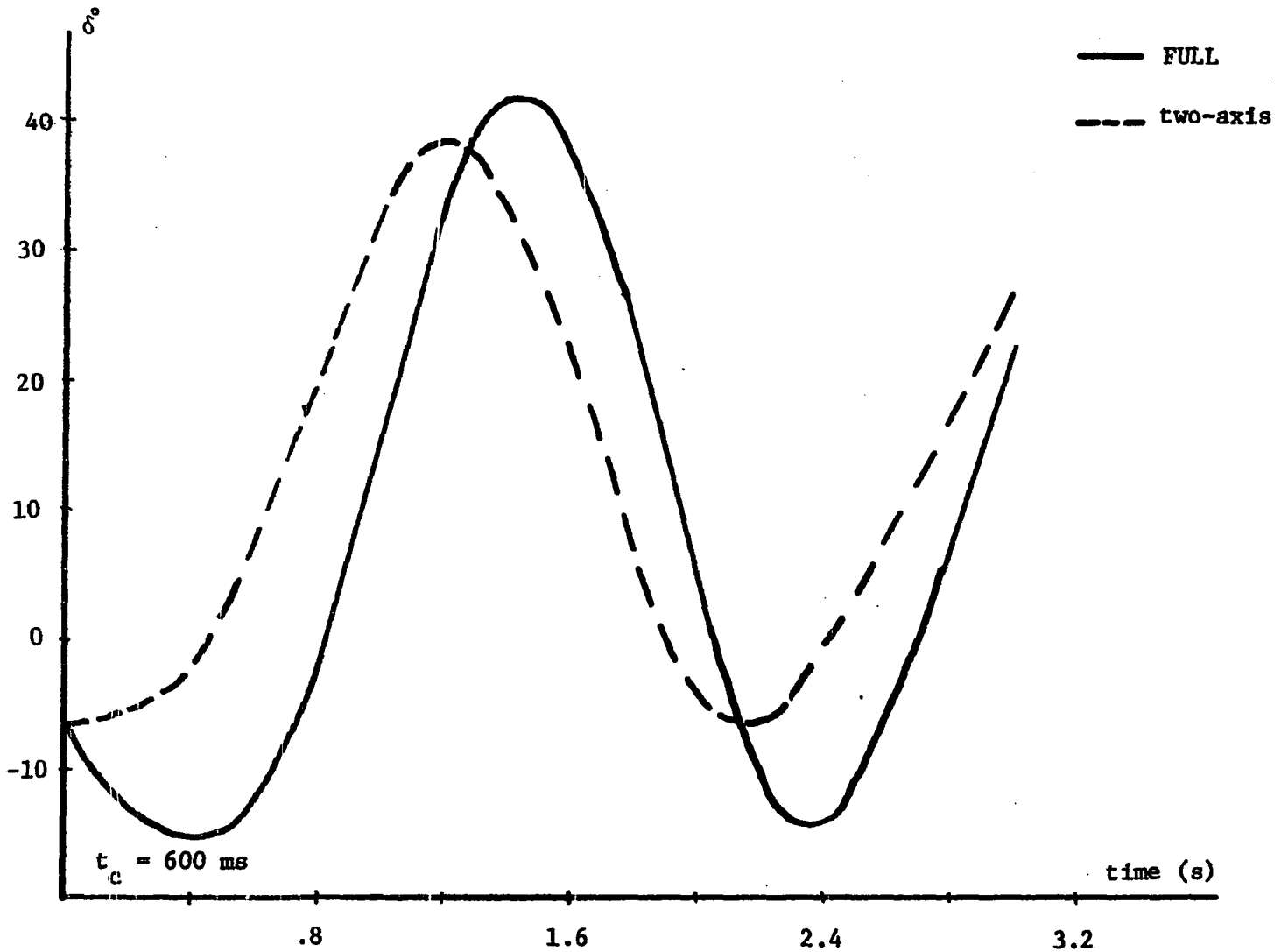

Figure 7. Plot of δ versus time (Case II). Simulation by the FULL and two-axis models

are in Case I. Since in Case I the generator is heavily loaded, it would be reasonable to expect that saturation of magnetic circuits would be more pronounced in Case I as opposed to Case II. This suggested that treatment of saturation might improve the agreement between the two models, particularly in Case I. Using the no-load saturation curve, the field current was modified to account for saturation which resulted, as illustrated in Figure 8, in improved agreement between the FULL and two-axis models.

Saturation could also be accounted for by adjusting the magnetizing inductances, L_{AD} and L_{AQ}. For hydro-machines, the q-axis inductance L_{AQ} seldom saturates, and is generally assumed to be constant (26).

The procedure for including saturation of magnetizing inductances is as follows. Let the unsaturated values of magnetizing inductances be L_{ADo} and L_{AQo}. The saturated values of these inductances for a solid iron rotor machine could be represented as:

$$L_{AD} = K_s L_{ADo}$$

$$L_{AQ} = K_s L_{AQo} \tag{27}$$

where

$$K_s = f(\lambda)$$

$$\lambda = (\lambda_{AD}^2 + \lambda_{AQ}^2)^{\frac{1}{2}} \tag{28}$$

and for hydro-machines

$$L_{AD} = K_s L_{ADo}$$

$$L_{AQ} = L_{AQo} \tag{29}$$

where

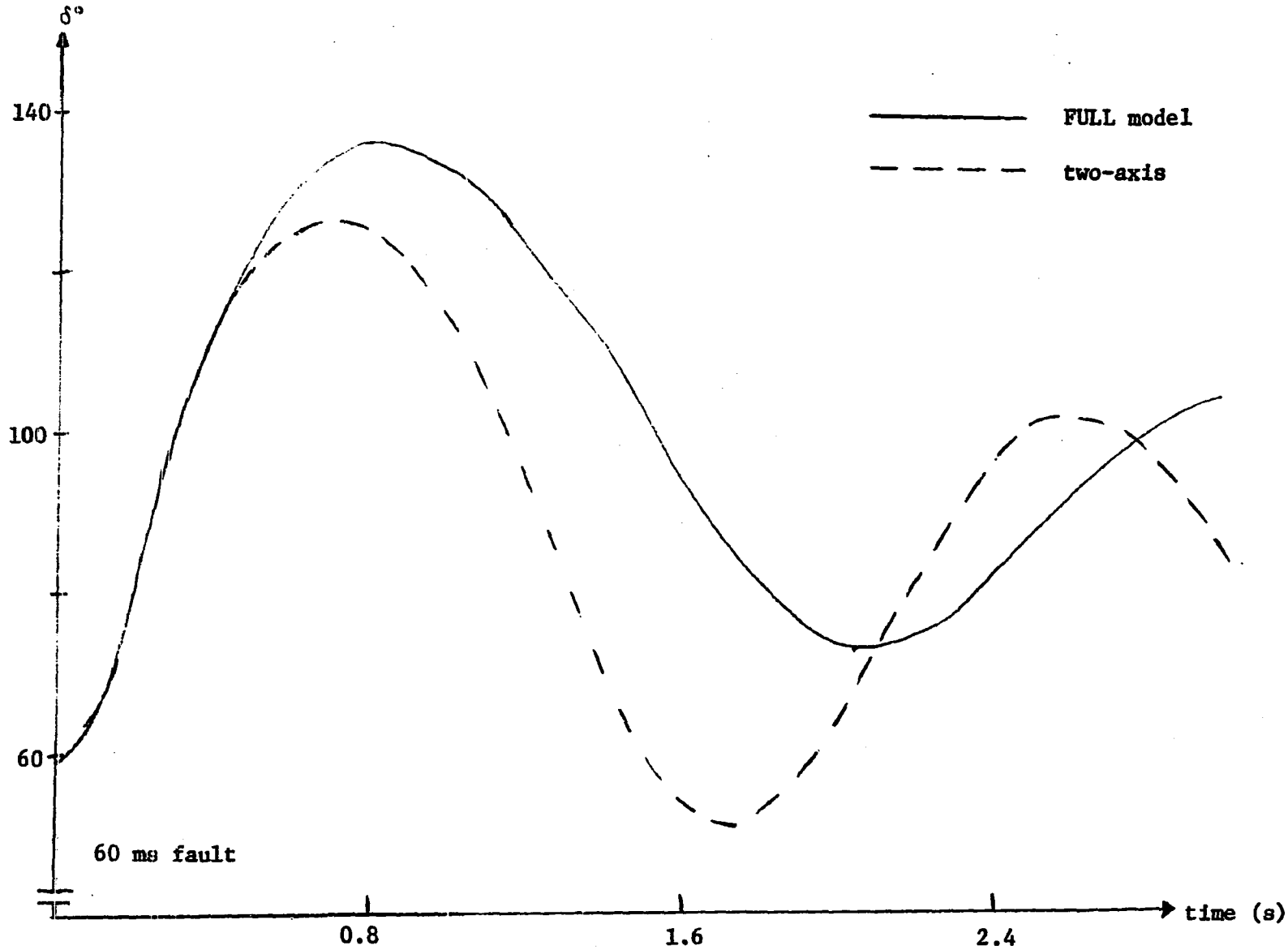

Figure 8. Plot of δ versus time (Case I). Simulation by the FULL and two-axis models. Saturation is accounted for by adjusting the field current

$$K_s = f(\lambda_{AD}) \tag{30}$$

where K_s is a saturation factor determined from the no-load magnetization curve of the machine. It must be noted that the procedure is an iterative process.

In order to provide for a uniform treatment of saturation in both models, the equations of the two-axis model were rewritten in terms of rotor variables, i.e., λ_f and λ_{Q1} instead of E'_q and E'_d. The model thus obtained was called the Approximate (APP) model.

The APP model, as illustrated in Figures 9 and 10, approximates the basic dynamic characteristics of synchronous machines, such as damping, magnitude of rotor swing, and frequency of oscillation, as indicated by the benchmark. It was, therefore, selected as the least complex model to be compared with the FULL model in the subsequent studies.

There are instances, as illustrated by Figure 10, when the APP model does not accurately represent the dynamic characteristics of the synchronous machine, as indicated by the FULL model. Close examination of the available data indicates that the discrepancy between the APP and the FULL models' swing curves develop during the fault period. The backswing phenomenon, which is indicated by the FULL model, is not present when the APP model is used. Figure 10 also indicates that after the fault is cleared, the two models perform in a similar manner. It would appear, therefore, that a combination of the FULL and the APP models might constitute a suitable modeling strategy. This concept is discussed in more detail in the next section.

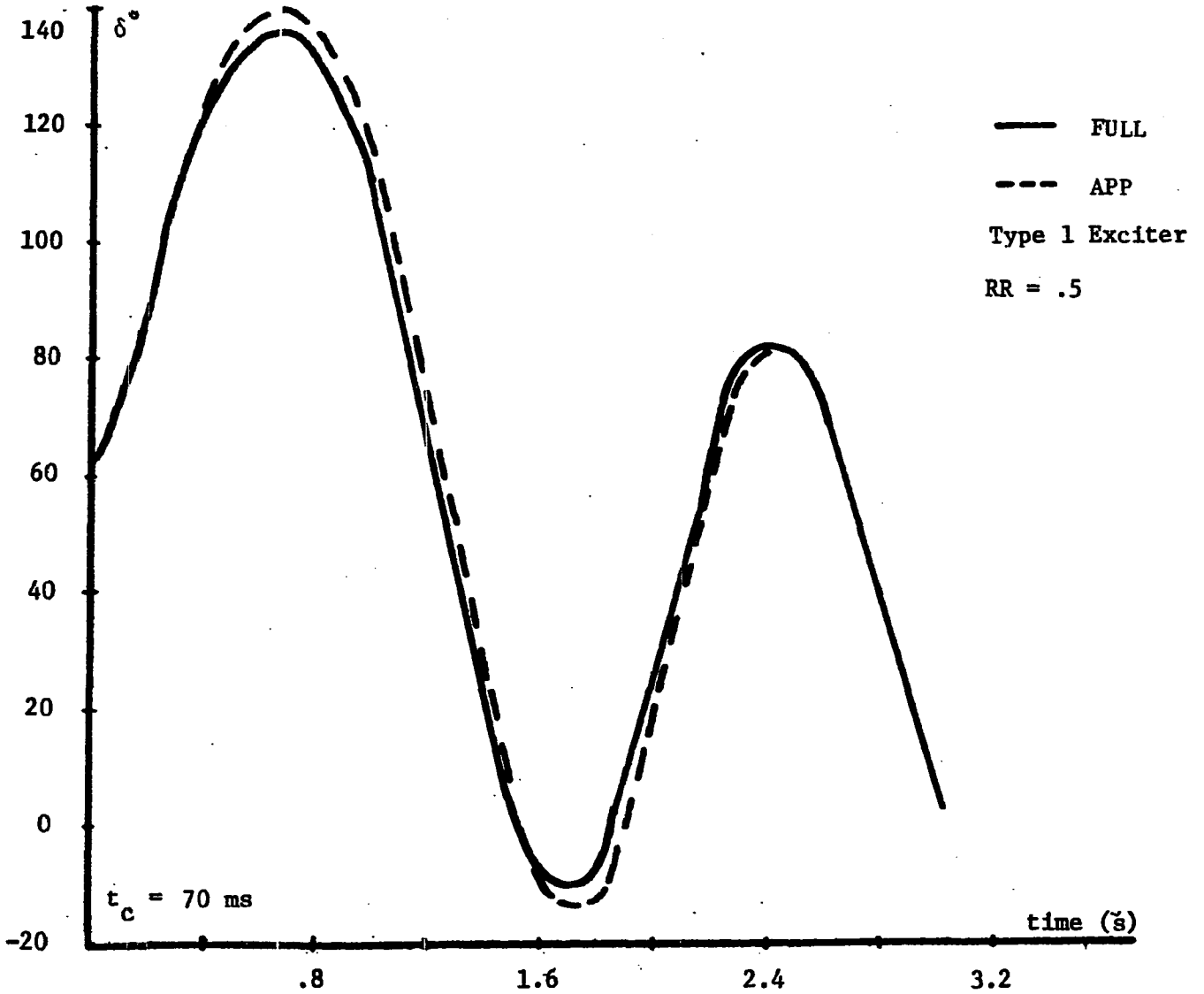

Figure 9. Plot of δ versus time (Case I). Simulation by the FULL and APP models

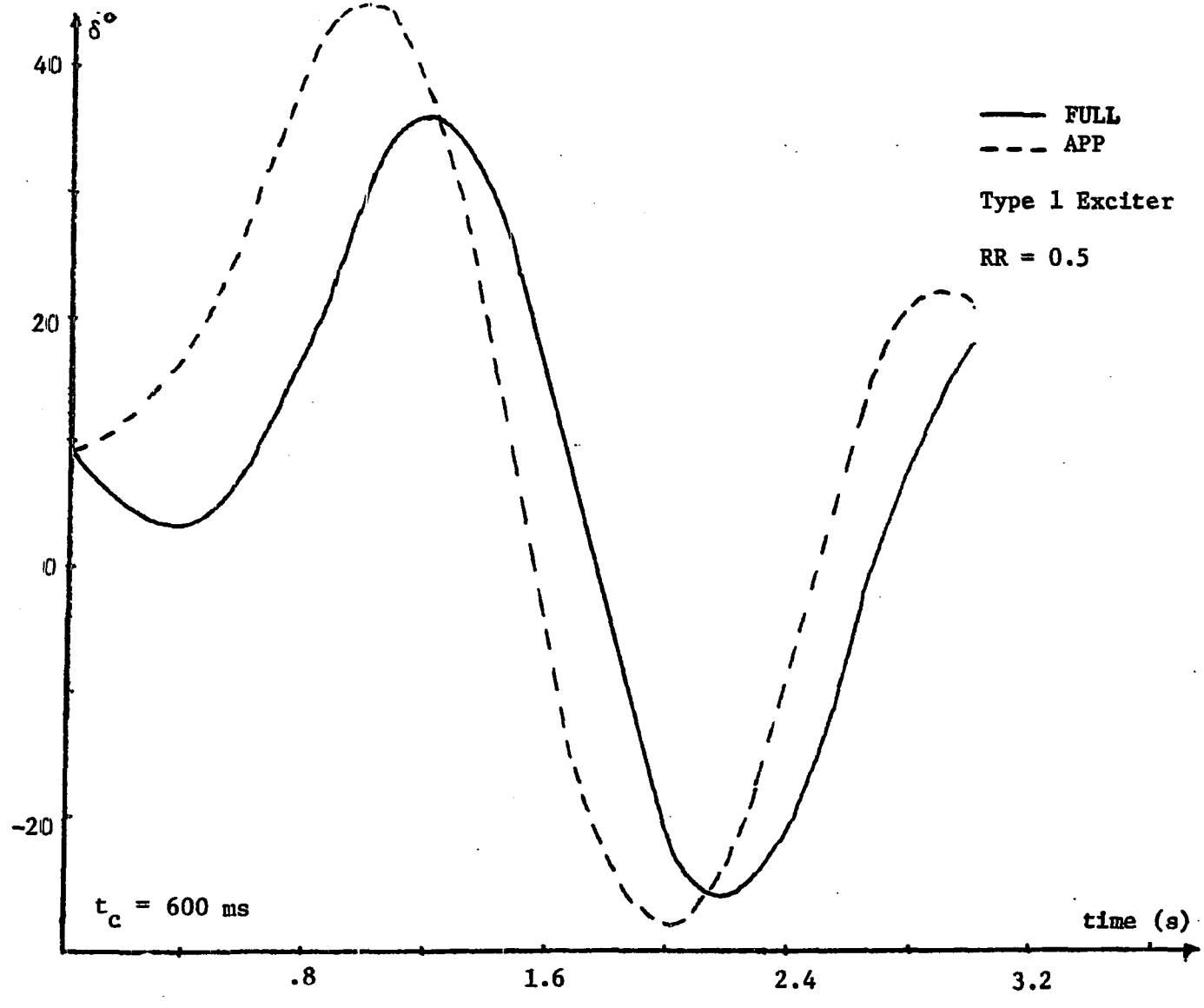

Figure 10. Plot of δ versus time (Case III). Simulation by the FULL and APP models

A. Model Switching

One of the ideas investigated in this project was the concept of model switching, which was the first step in developing an efficient transient stability program. The logic that leads to this concept, and justifications for using it, are described in this section.

At this stage, it might be helpful to point out that the FULL model is an 8th, or 7th, order model, where the APP model is a 4th, or 3rd, order model. To put it another way, the FULL model represents the synchronous machine with the aid of 8, or 7, first order differential equations as compared to 4, or 3, first order differential equations for the APP model. The four additional equations allow the FULL model to represent the machine more accurately than the APP model. However, the additional computer cost due to those four equations could be quite significant.

The four first order differential equations mentioned in the preceeding paragraph are:

$$\begin{aligned} \dot{\lambda}_d &= -v_d - r_a i_d - \omega\lambda_q \\ \dot{\lambda}_q &= -v_q - r_a i_q + \omega\lambda_d \\ \dot{\lambda}_D &= -r_D i_D \\ \dot{\lambda}_{Q2} &= -r_{Q2} i_{Q2} \end{aligned} \tag{31}$$

which account for stator transients ($\dot{\lambda}_d$ and $\dot{\lambda}_q$) and subtransient phenomenon ($\dot{\lambda}_D$ and $\dot{\lambda}_{Q2}$). Power system transient stability studies seek the response of the system when it is subjected to a disturbance. The disturbance is normally represented by a fault in the transmission system

(such as a three phase or a single phase fault) which results in the collapse of the terminal voltage (v_d and v_q) of the synchronous machine. The sudden change in the terminal voltage would require a readjustment in flux linkage levels, i.e., λ_d, λ_q, λ_D, λ_{Q2}, λ_f, and λ_{Q1}.

As shown in Figure 11, the flux linkages would be forced to go through oscillatory transients that decay with a time constant associated with the corresponding circuit, i.e., τ_a for λ_d and λ_q. This process repeats itself once the fault is removed. The time constants associated with stator transients and the subtransient phenomenon are relatively small. Typical figures are as follows:

τ_a	τ''_d	τ''_q
.180s	.03s	.03s

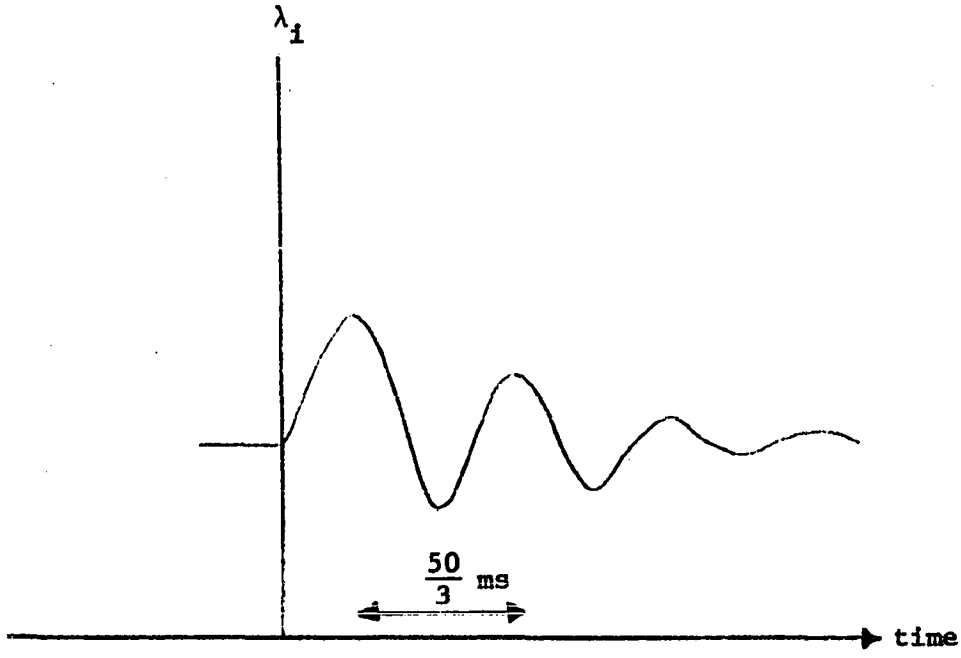

Figure 11. Transient response, plot of λ_i versus time

It follows that the fast transients associated with $\dot{\lambda}_d$, $\dot{\lambda}_q$, $\dot{\lambda}_D$ and $\dot{\lambda}_{Q2}$ subside after short periods of time, which are related to the appropriate time constants. From then on, it could be assumed that these transients are negligible or:

$$\dot{\lambda}_d = \dot{\lambda}_q = \dot{\lambda}_D = \dot{\lambda}_{Q2} = 0 \tag{32}$$

This reduces the FULL model to the APP model. The simulation period could, therefore, be divided into two time intervals (Figure 12). The first

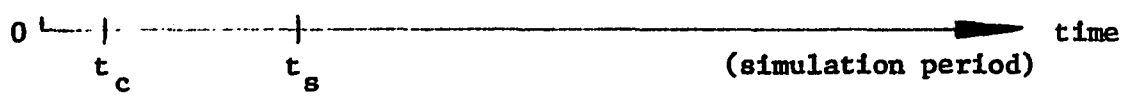

Figure 12. Schematic representation of the simulation period

time interval ($0 < t < t_s$) lasts until a relatively short time after the last switching operation (opening or closing of circuit breakers). During this time period, stator transients and subtransient phenomenon could play a major role in the dynamic performance of the synchronous machine, and therefore the synchronous machine may have to be represented by the FULL model. During the second time period ($t > t_s$), stator transients and subtransient phenomenon could be neglected, which means the APP model could adequately represent the synchronous machine.

The discussion presented so far suggests that, in addition to the two modeling strategies used so far (Figures 13a and 13b), there is a third alternative (Figure 13c) that combines the advantages of the first two alternatives in an extremely efficient manner. To put it another way, the third modeling strategy could be almost as accurate as the first alternative, but far less expensive.

The switching time (t_s) depends on the time constants associated with stator transients (τ_a) and subtransient phenomenon (τ''_d and τ''_q). These phenomena decay in an exponential manner. Therefore, after a period of approximately three to four times the largest time constant following the last switching operation, they could all be assumed to be negligible, at which time one could switch from the FULL to the APP model.

The model switching concept was extensively investigated. It proved to be consistently accurate and inexpensive as compared to when the FULL model is used for the entire simulation period (Figures 14 and 15).

The largest time constant of interest, for this machine, is τ_a, which is 172 ms. It follows that model switching should take place approximately 500 ms after the last switching operation, i.e.,

$$t_s - t_c \cong 3\tau_a \cong 500 \text{ ms}$$

This procedure is very accurate (Figure 16) and highly efficient.

The efficiency of model switching technique was measured by determining the execution time required for this modeling strategy as a percentage of the execution time needed when the FULL model was used for the entire simulation period. The figures thus obtained ranged from a

low of about 35% to a high of about 65%, thus making the model switching technique a highly efficient approach.

The examples presented thus far indicate that in some instances the results obtained with the FULL and the APP models are virtually the same. In such cases, it is unnecessary and inefficient to use the FULL model or to apply the concept of model switching. There is therefore, a need to identify such cases prior to actual stability studies so that proper modeling strategy could be selected. This subject will be discussed after the results of the multi-machine studies are presented.

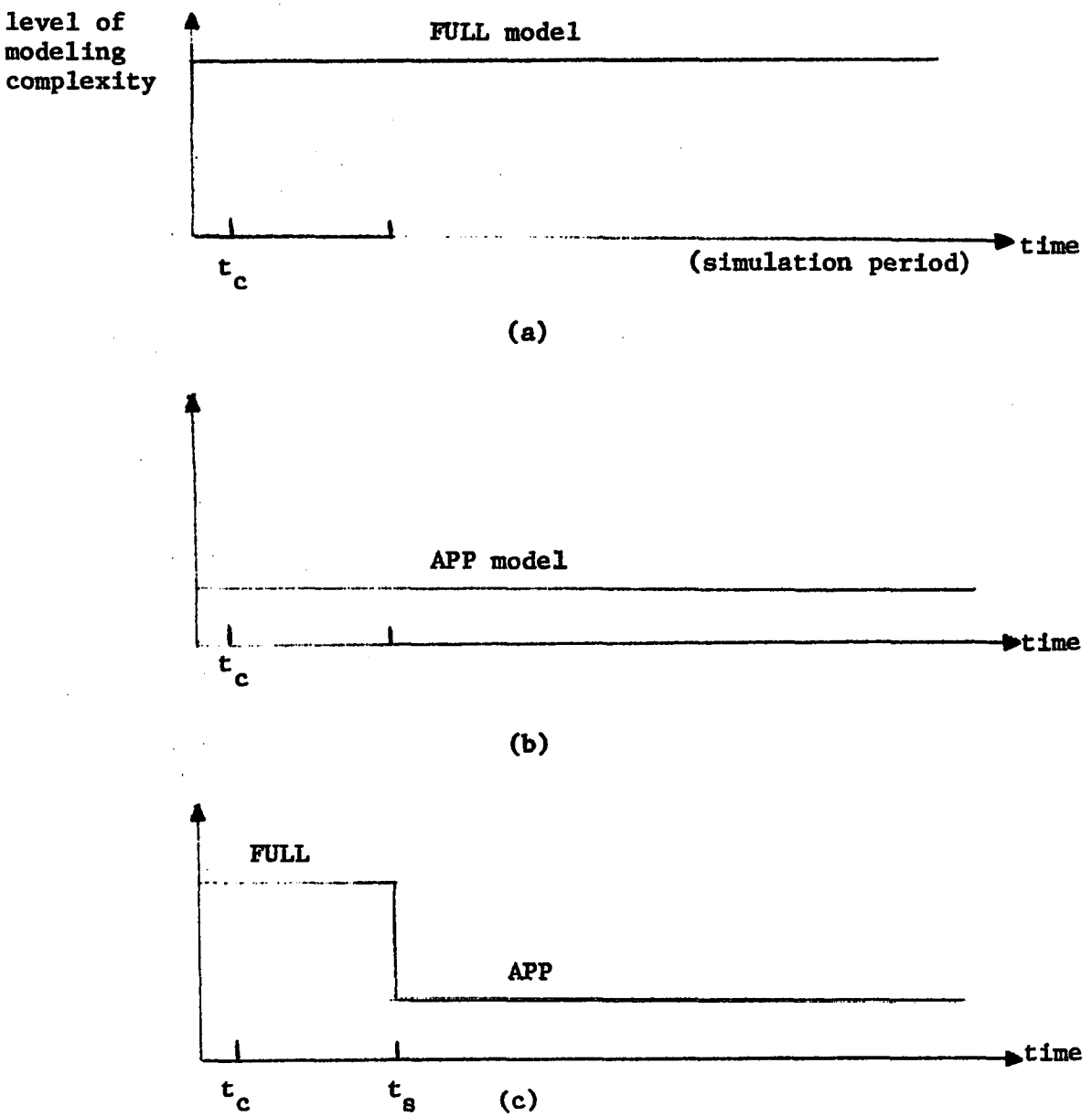

Figure 13. Schematic representation of the various modeling techniques

(a) Simulation by the FULL model

(b) Simulation by the APP model

(c) Model switching

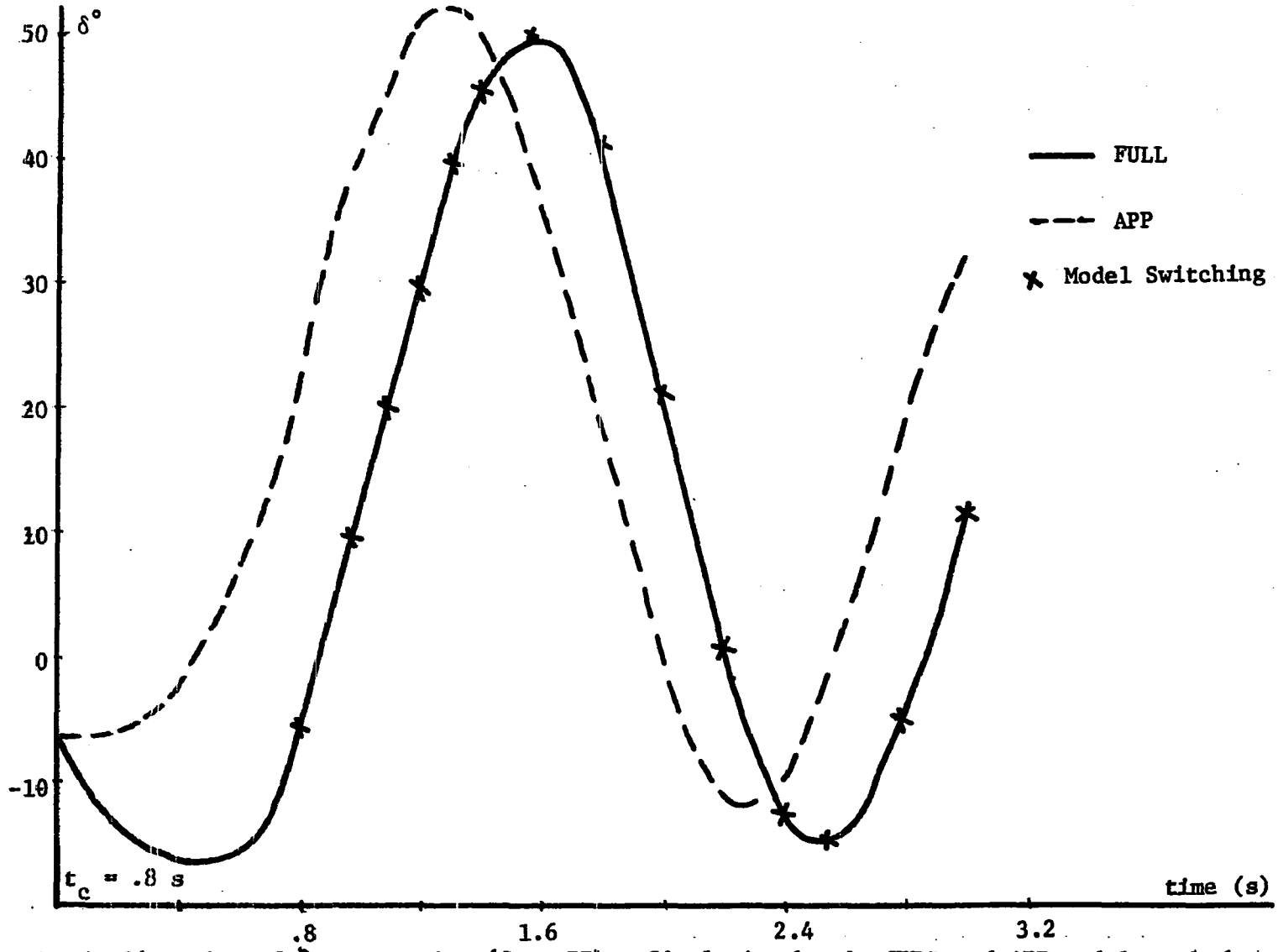

Figure 14. Plot of δ versus time (Case II). Simulation by the FULL and APP models and the model switching method

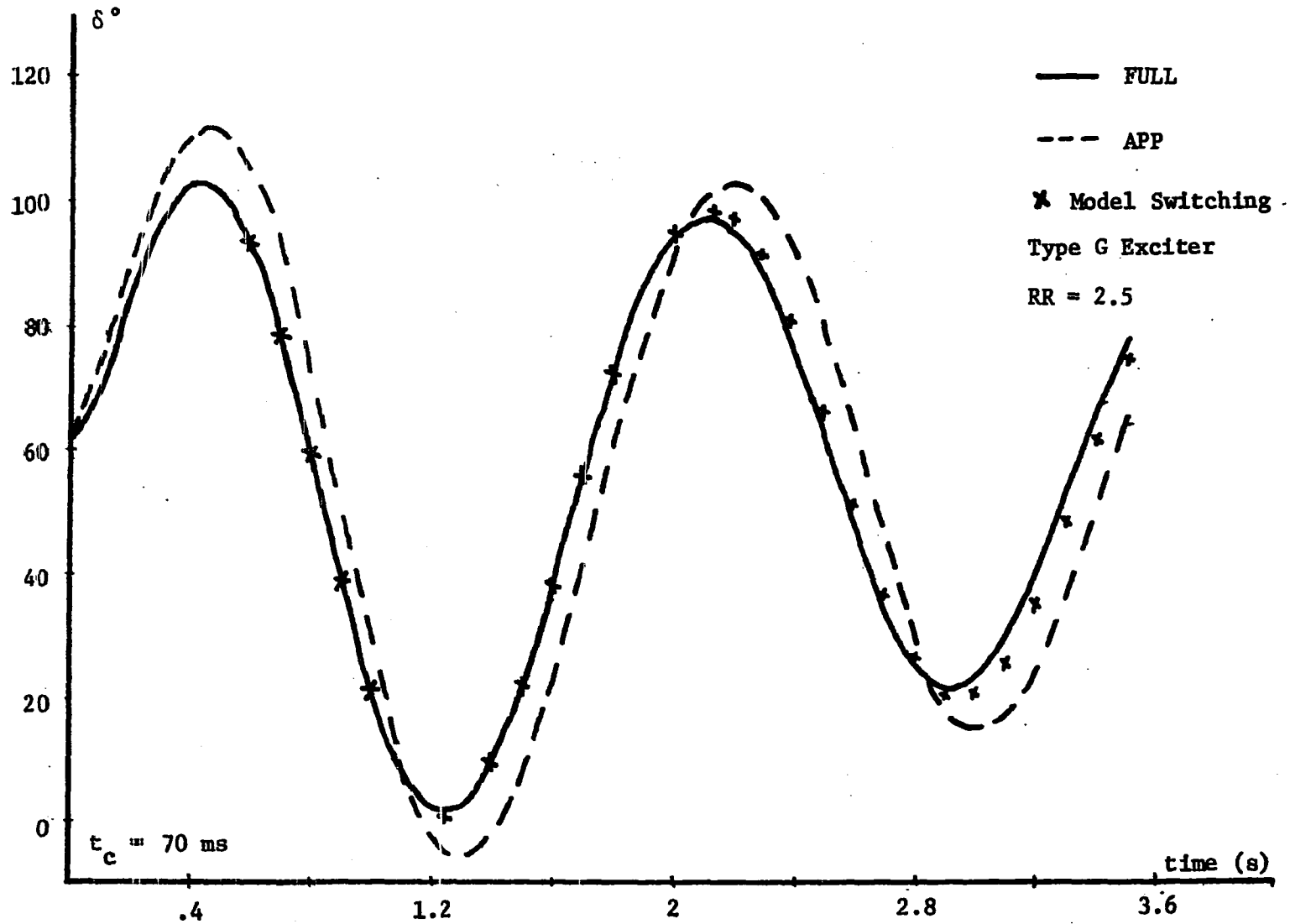

Figure 15. Plot of δ versus time (Case I). Simulation by the FULL and APP models and the model switching method

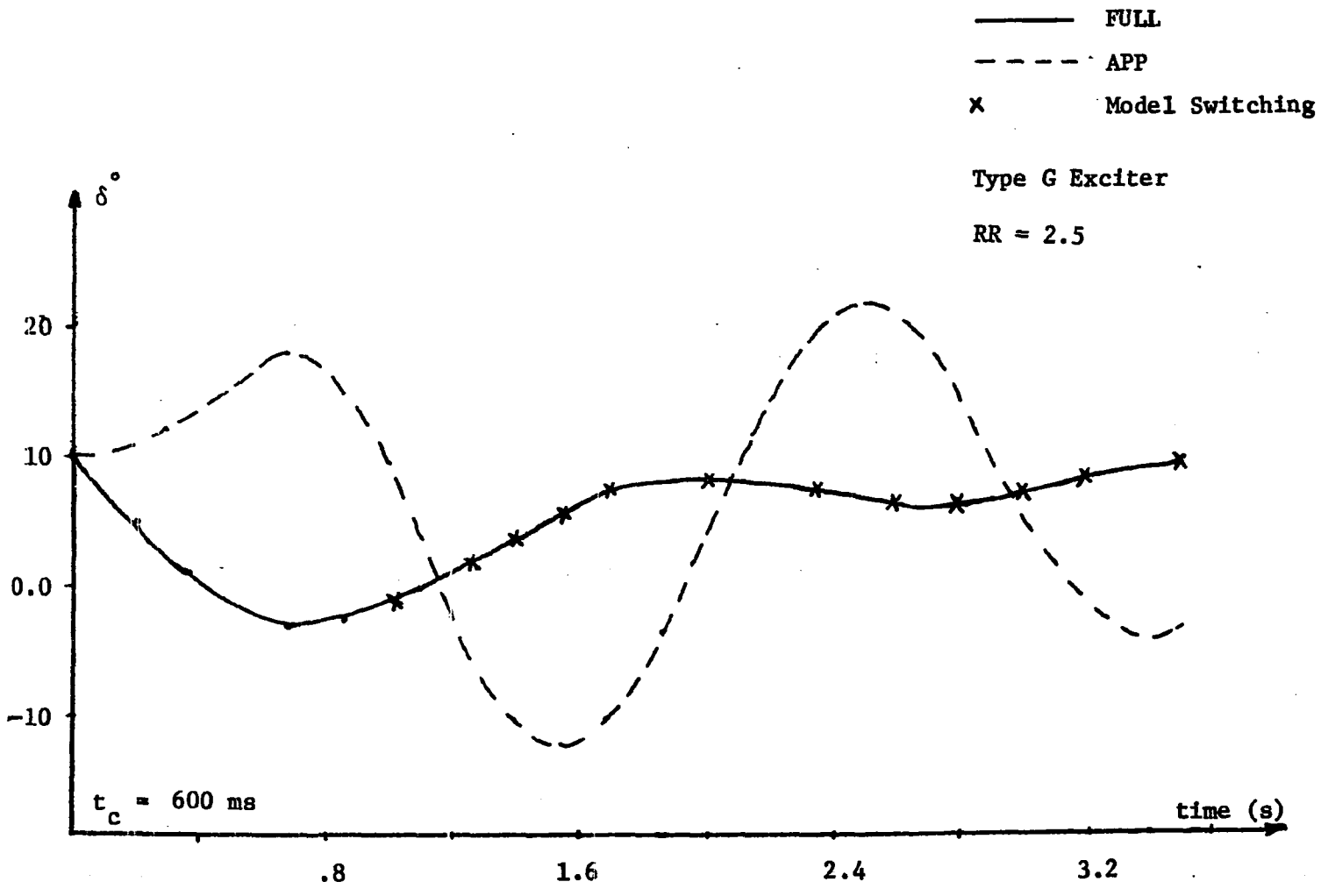

Figure 16. Plot of δ versus time (Case III). Simulation by the FULL and APP models and the model switching method

V. MODELING TECHNIQUES FOR MULTIMACHINE SYSTEM STUDIES

In Chapter IV, a simple model that would approximate basic dynamic characteristics of synchronous machines, as indicated by the FULL model, was developed. This model was called the APP model. It was also established that a combination of the FULL and APP models could greatly improve the efficiency of simulation. In this chapter, these concepts are applied to a 9-bus 3-machine system (26), which is shown in Figure 17.

One of the significant conclusions of Chapter IV is that in some cases the results obtained with either the FULL or the APP model are virtually the same. In such instances, the use of the FULL model or even the application of model switching technique is unnecessary. There is therefore, a need for a criterion that would enable us to choose the proper modeling strategy for a particular stability study. This subject will be pursued in this chapter. Finally, in this chapter we will introduce and examine a new modeling technique which is based on an approximate expression for the so-called retarding torque.

A. System Description

This power system, which is known in the literature as the Western System Coordinating Council (WSCC) nine bus test system, is shown in Figure 17. The system is comprised of 3 machines and 3 loads. Machines #2 and #3 are two-pole 3600 RPM generators, typical of fossil fuel thermal units. Machine #1, on the other hand, represents a large equivalent of hydro-machines with a rather high inertia constant. Data for the

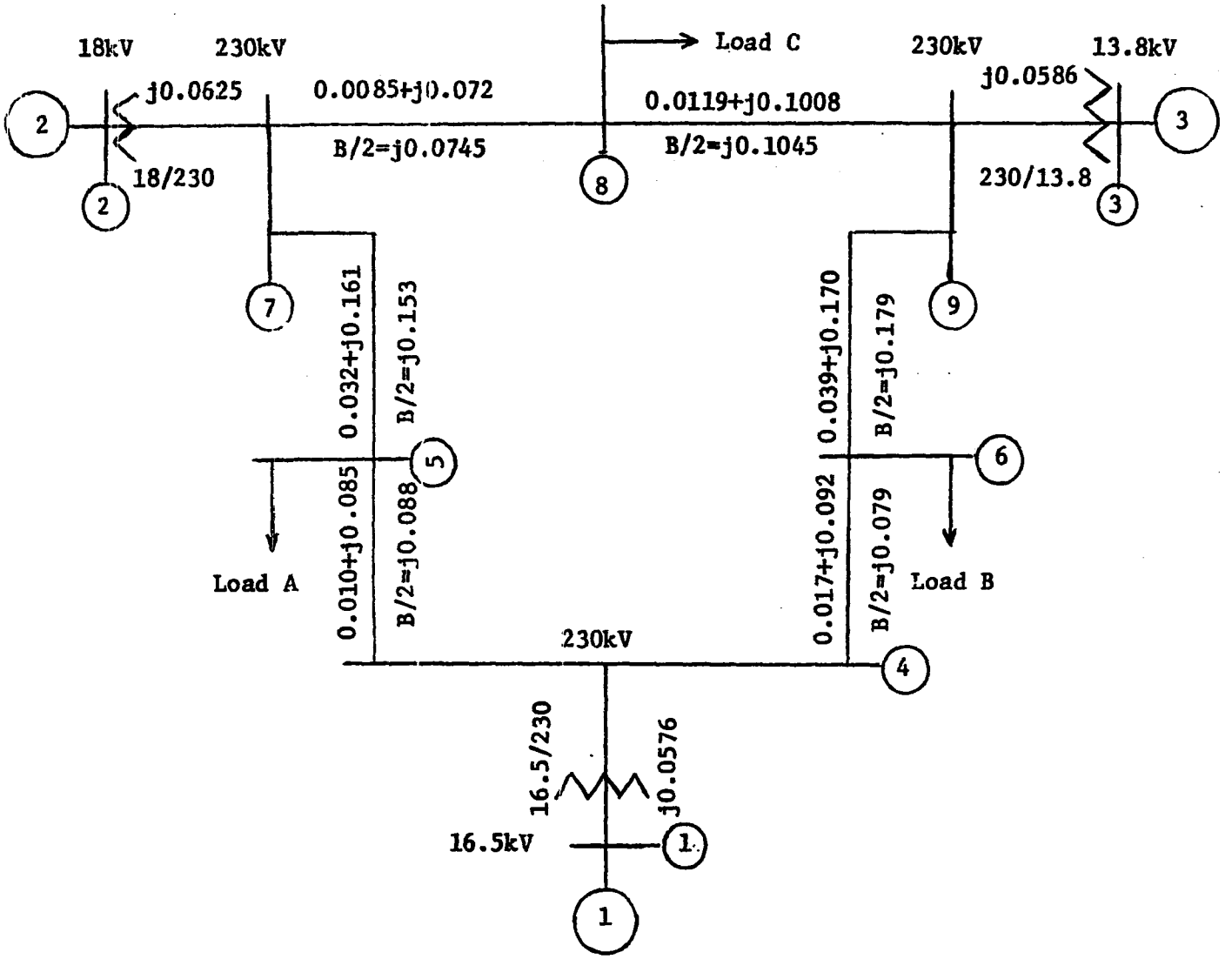

Figure 17. Nine bus system impedance diagram. All impedances in pu on 100 MVA base

generators are given in Table 3. The loads, which are represented by constant impedances, are described in Table 4. In these studies, two operating conditions, which are described in Table 5, were considered. These operating conditions represent wide variations in the initial loading of machines #1 and #2, which make it possible to examine the effect of different operating conditions on the dynamic behavior of these machines.

The disturbance was simulated by a three-phase fault placed at different locations in the system. In all cases, except when otherwise indicated, stub faults were used to provide the desired large disturbance without altering the structure of the transmission system. Also, the transmission system was simplified by eliminating all nodes, except for generator nodes, through the use of network reduction techniques (see Reference 26, section 2.10.2).

No prime mover dynamics were considered in any multi-machine studies. The generators were assumed to have constant input torques.

The excitation systems were all high-initial response type. Block diagrams and data for the excitation systems are given in the Appendix.

Table 3. Generator data[a]

Generator	1	2	3
Rated MVA	247.5	192	128
x_d	.1460	.8958	1.3125
x_d'	.0608	.1198	.1813
x_d''	.0483	.0891	.1072
τ_{do}'	8.96	6.0	5.89
τ_{do}''	.04	.033	.033
x_q	.0969	.8645	1.2587
x_q'	.0969	.1198	.1813
x_q''	.0483	.0891	.1072
τ_{qo}'	0	.535	.60
τ_{qo}''	.060	.08	.07
r_a	.0006	.0013	.0032
x_ℓ	.0336	.0521	.0742
H sec.	23.64	6.40	3.01

[a]Reactance values are in pu on a 100 MVA base. All time constants are in seconds. Values of the subtransient reactances and time constants are estimated.

Table 4. Description of the loads

Load	Location	MW	MVAR
A	bus #5	125	50
B	bus #6	90	30
C	bus #8	100	35

Table 5. Operating conditions

Generator	1	2	3
Condition 1			
P_o, MW	71.6	163	85
Q_o, MVAR	27	6.7	-10.9
v_t	1.040/0.0°	1.025/9.3°	1.025/4.7°
Condition 2			
P_o, MW	215	50	84
Q_o, MVAR	54.7	-15.6	-13
v_t	1.1118/0°	1.0473/-8.6°	1.0638/-5.7°

B. Multimachine Studies

The WSCC nine bus test system (Figure 17) was examined for transient stability by using different clearing times, fault locations, and operating conditions. A total of 20 cases were considered. A listing of some of the transient stability studies is presented in Table 6.

Table 6. Description of multimachine studies

Run Number	Figure	Fault Location	Clearing Time (ms)	Operating Condition
1	18	bus #4	220	1
2[a]	19	bus #7	60	1
3	20	bus #9	200	1
4	21	bus #6	300	1
4	22	bus #6	300	1
5	23	bus #7	200	2
6	24	bus #9	200	2

[a]In this case, fault was cleared by removing line 5-7. In all other cases, the disturbance was simulated by a stub fault.

The results of these studies are presented as plots of relative power angles, i.e., δ_{21} and δ_{31}, versus time (Figures 18-24). These plots offer a comparison of system's transient behavior as predicted by the FULL and APP models. Plots of δ_{21} versus time are given in Figures 18, 19, 22 and 23; corresponding curves for δ_{31} are presented in Figures 20, 21, and 24.

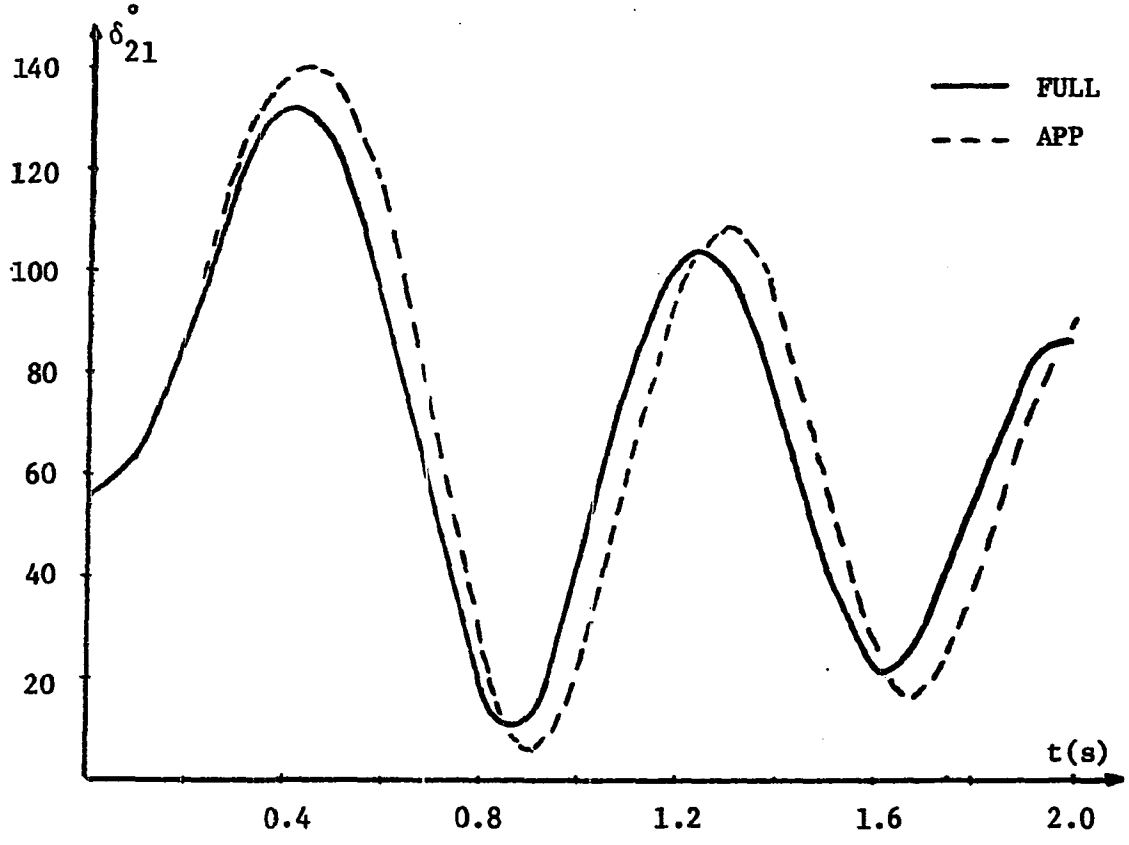

Figure 18. Plot of δ_{21} versus time for a 220 ms fault on bus #4 (Operating Condition 1). Simulation by the FULL and APP models

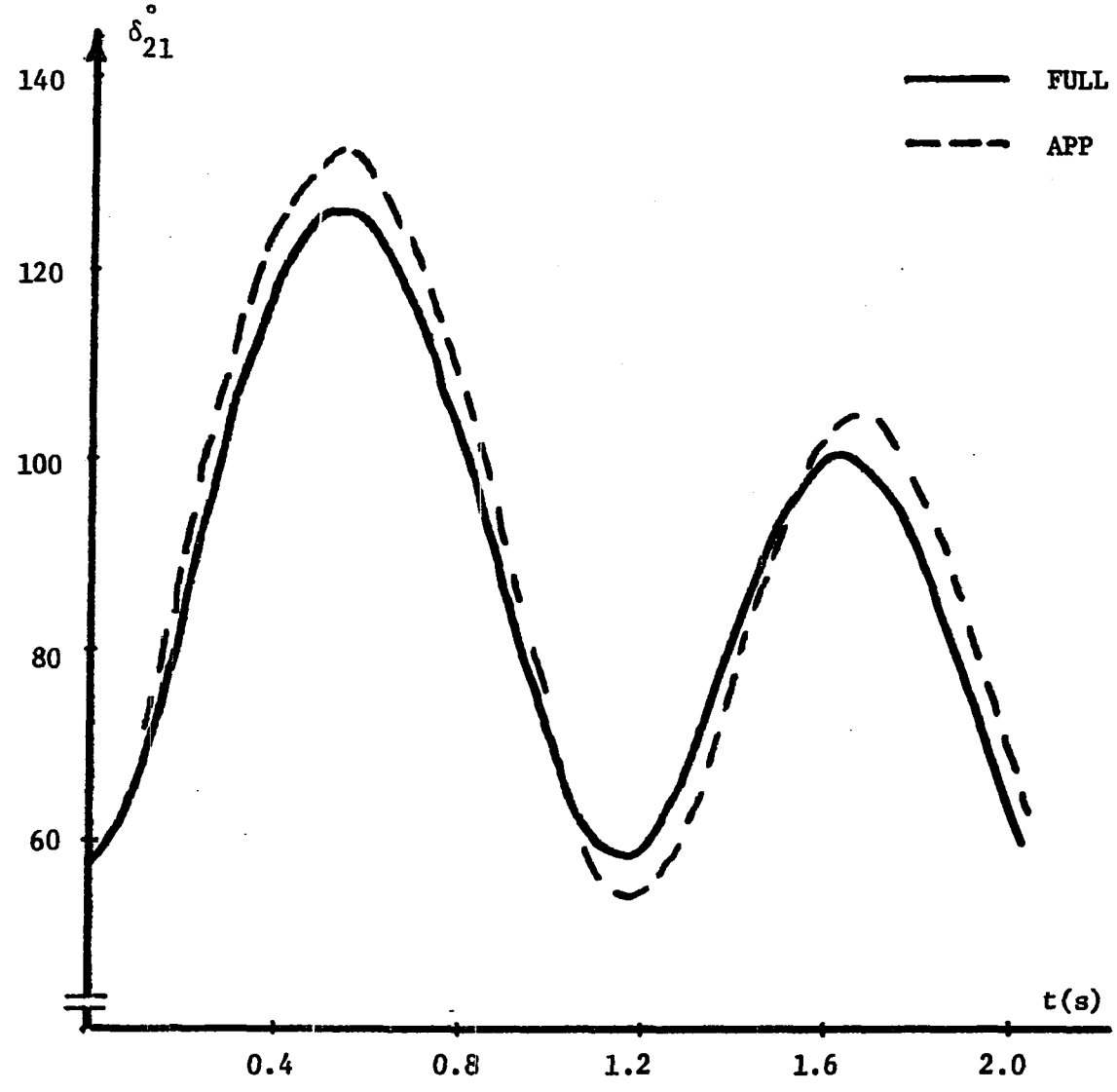

Figure 19. Plot of δ_{21} versus time for a 60 ms fault on bus #7 (Operating Condition 1). Simulation by the FULL and APP models

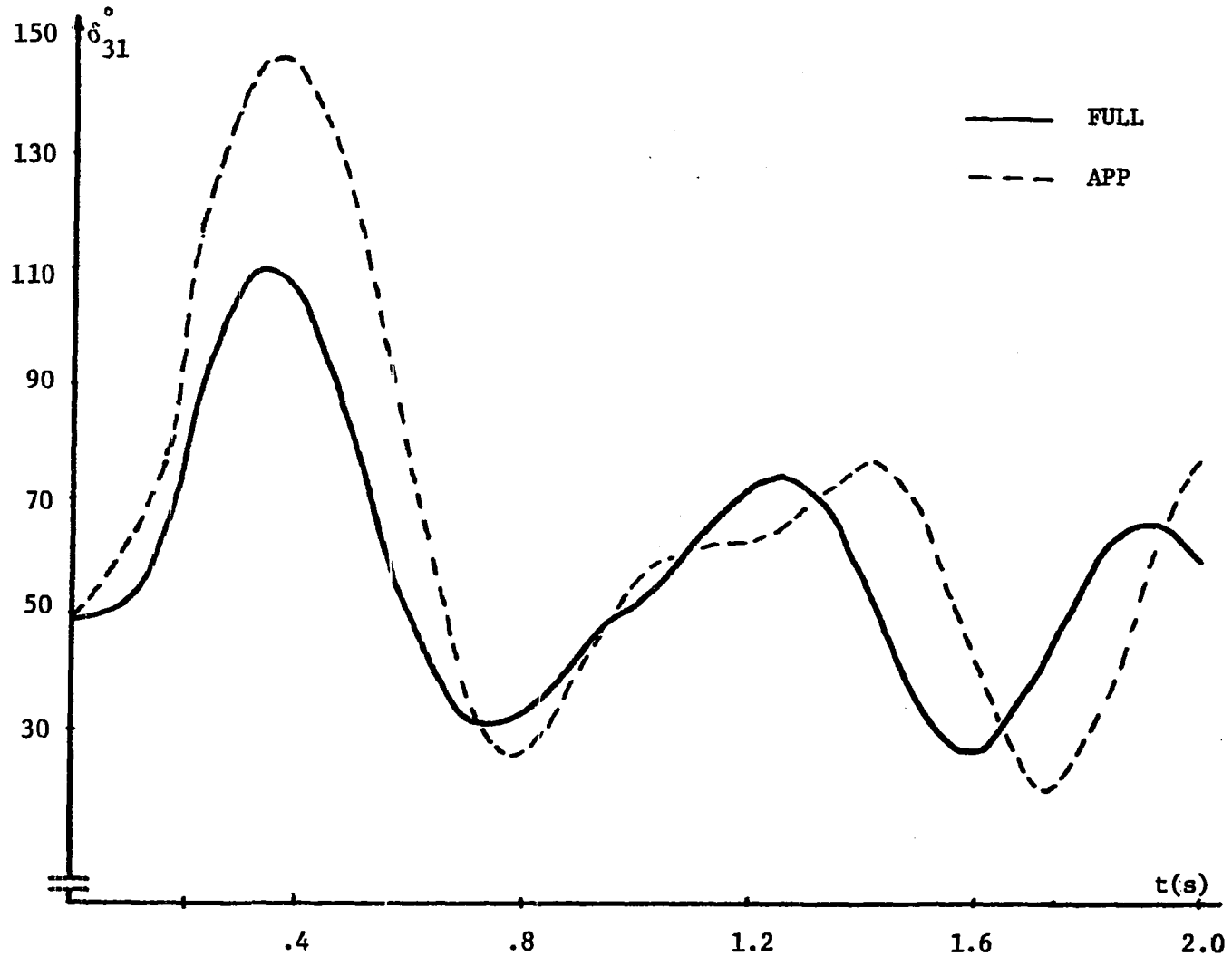

Figure 20. Plot of δ_{31} versus time for a 200 ms fault on bus #9 (Operating Condition 1). Simulation by the FULL and APP models

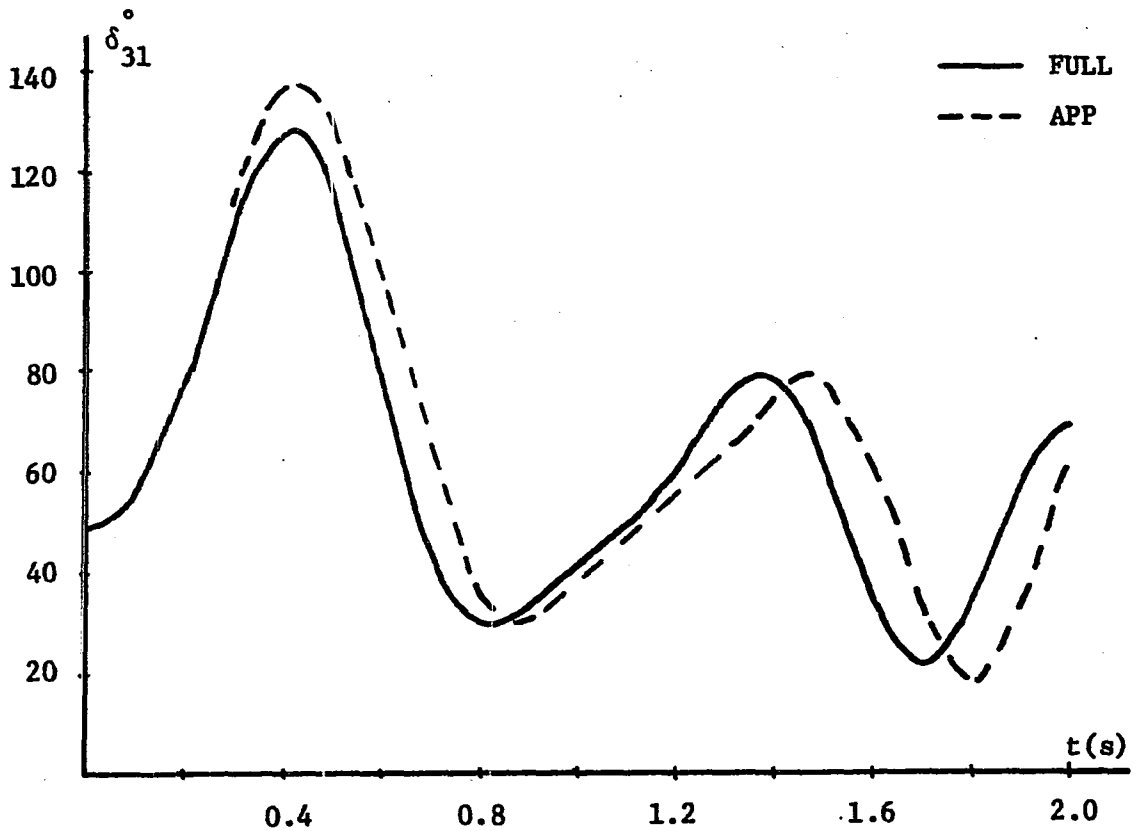

Figure 21. Plot of δ_{31} versus time for a 300 ms fault on bus #6 (Operating Condition_1). Simulation by the FULL and APP models

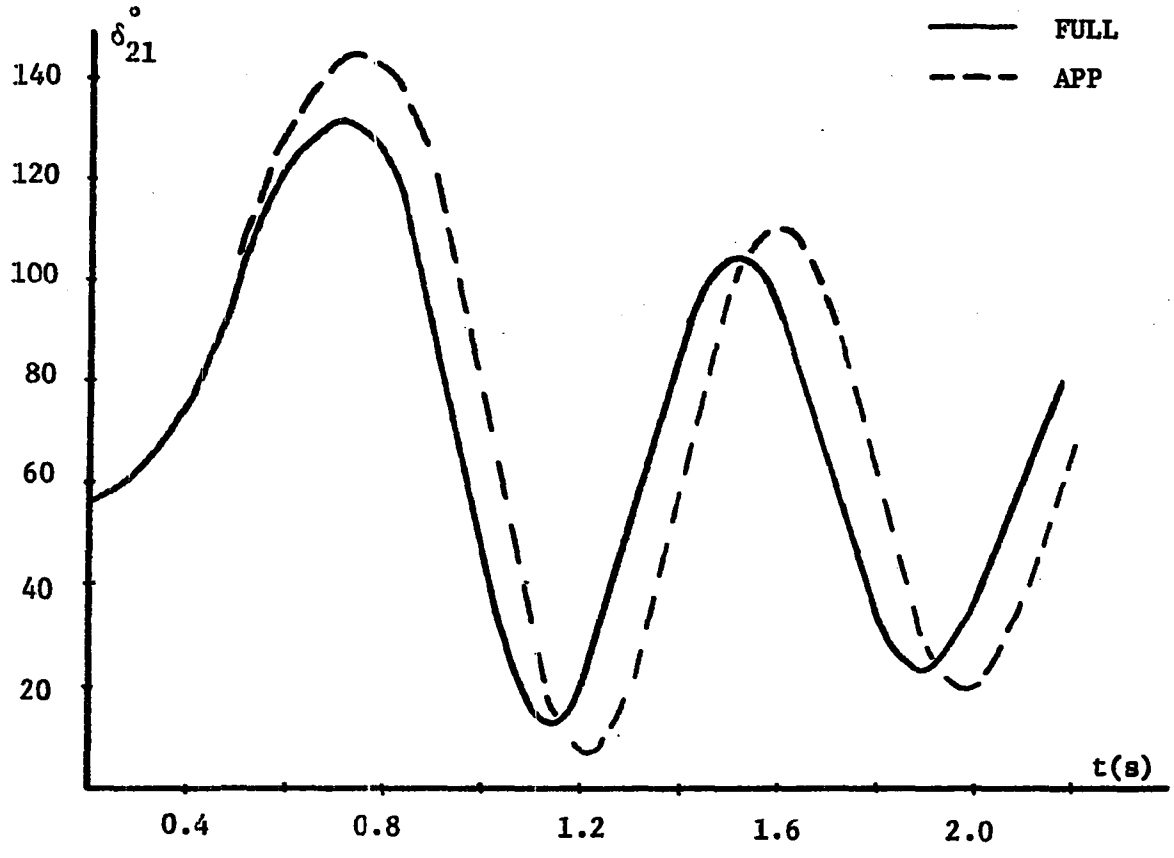

Figure 22. Plot of δ_{21} versus time for a 300 ms fault on bus #6 (Operating Condition 1). Simulation by the FULL and APP models

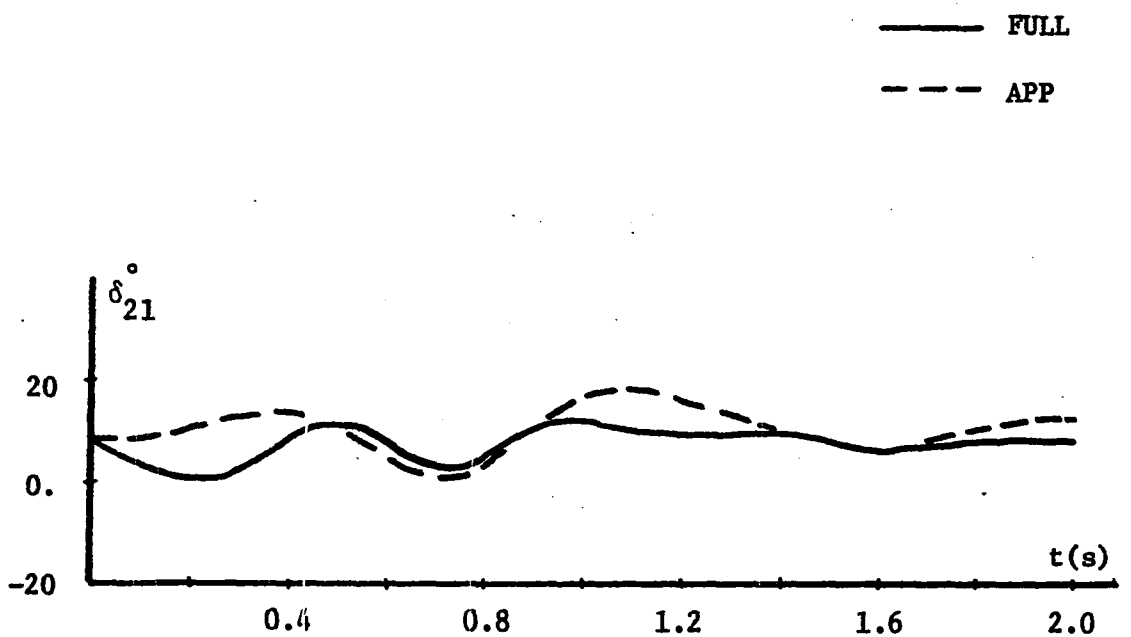

Figure 23. Plot of δ_{21} versus time for a 200 ms fault on bus #7 (Operating Condition 2). Simulation by the FULL and APP models

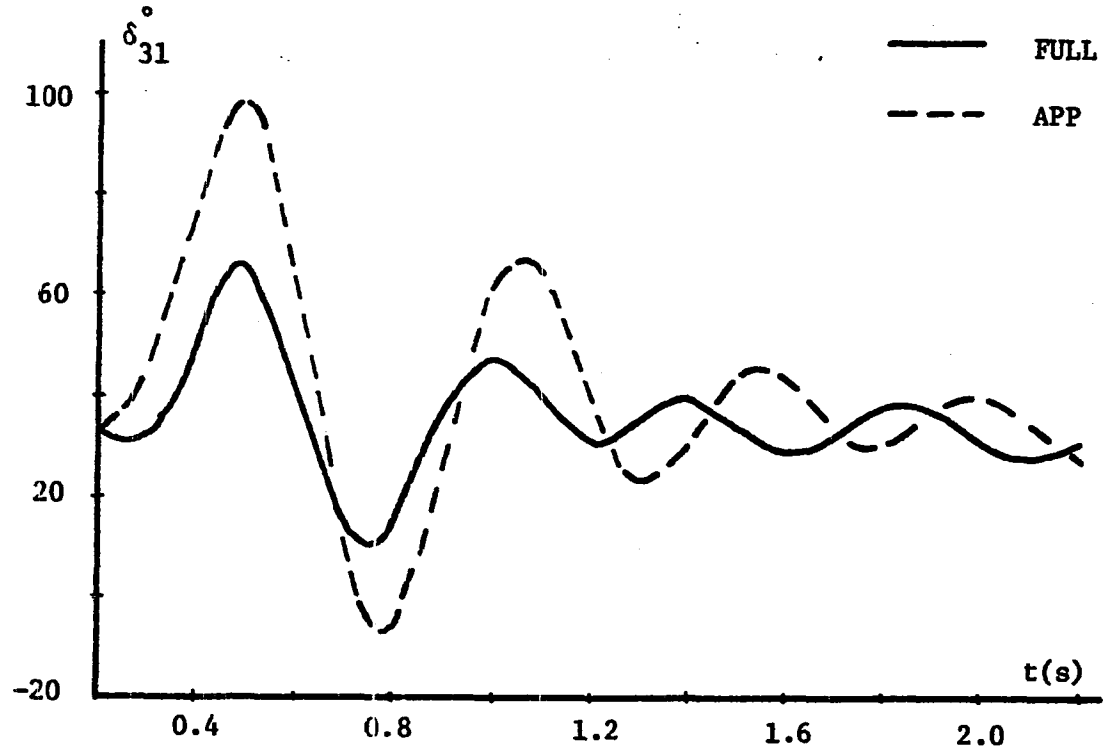

Figure 24. Plot of δ_{31} versus time for a 200 ms fault on bus #9 (Operating Condition 2). Simulation by the FULL and APP models

The results shown in Figures 18-24 clearly indicate that the APP model is indeed a proper least complex mathematical model when compared with the benchmark. For instance, the results presented in Figures 19 and 23, when the fault is close to Machine #2, indicate that the difference between the results obtained with the FULL and APP models is almost negligible. The same is true for the results presented in Figures 21 and 22 when the fault is on bus #6. We note that in all of the aforementioned cases there is good agreement between the FULL and APP models with regard to factors such as magnitude of rotor swing, damping, and frequency of oscillation.

In some instances, such as the cases displayed in Figures 20 and 24, there is a significant difference between the results obtained with the FULL and APP models. For instance, in Figure 20, there is a considerable discrepancy between the FULL and APP models with regard to the predicted magnitude of the first rotor swing. The same is true for the results presented in Figure 24. In these cases there are basically two possibilities for improving the results. The first approach takes advantage of the model switching technique which was described in Chapter IV. The second alternative is based on an approximate expression for the retarding torque which is incorporated in the APP model swing equations.

Finally, close examination of these results (Figures 18-24) indicates a potential problem with the procedure commonly used in a selective modeling technique which is widely used in large-scale transient stability studies. This subject is discussed in the next section.

1. Selective modeling technique

In large scale power system transient stability studies, it is common to represent the synchronous machines by models of varying details (26; 28; 32). This modeling method is basically a selective modeling approach which is used to reduce computational cost without sacrificing accuracy of the simulation. This is done by dividing the synchronous machines into two groups. One group consists of those synchronous machines that are considered to be near the disturbance. Another group contains those synchronous machines that are judged to be remote from the disturbance. The synchronous machines that are in the first group are regarded to be severely disturbed and are, therefore, represented by complex models. On the other hand, machines in the latter group are simulated by simple representations such as the classical model. The synchronous machines at an intermediate location may be represented by still other models.

The selective modeling method is a viable technique for improving the efficiency of transient stability studies. It is intended to allow power system engineers to select the proper mathematical model for each synchronous machine and, thus, make intelligent use of computer models that are available to them. However, although the selective modeling method is a sound concept, it may be made inefficient due to the criterion that is used to classify the synchronous machines. There is no concrete procedure available for this purpose. It is usually assumed that machines far away from the disturbance are not severely disturbed and thus simple models, such as the classical model, would adequately represent them.

The machines close to the fault, on the other hand, are regarded to be severely disturbed and therefore represented by complex models.

The results of multimachine studies, some of which are illustrated in Figures 18 through 24, indicate that the above described procedure is not correct in all cases. For example, the results presented in Figures 19 and 23, where the fault is located near Machine #2, clearly indicate that there is no need to represent Machine #2 by the FULL model. In these cases, the APP model predicts the dynamic performance of Machine #2 quite accurately, as indicated by the benchmark model, despite the fact that the fault is near it. The same holds true for the results presented in Figure 18, where the disturbance is near Machine #1. Again for this case, there is clearly no need to represent Machine #1 by the FULL model. Figure 20, on the other hand, indicates that there is a definite need for representing Machine #3 by the FULL model. In this case, the disturbance is located near Machine #3.

The discussion presented thus far clearly suggests that selection of synchronous machine models, for selective modeling approach, cannot be solely based on location of the fault. There are obviously other factors that affect the selection of the proper model. These factors must be identified and incorporated in the model selection process so that the efficiency of the selective modeling method can be greatly improved.

A close review of the available data indicates that the difference between the results obtained with the FULL and APP models, in addition to fault location, is related to the clearing time, initial loading, and the parameters of the synchronous machines. This, in turn, suggests that all those factors must be incorporated in the model selection process.

In order to gain further insight, those factors were varied one at a time and their effects on the swing curves were studied.

a. Effect of fault location (electrical proximity) In order to investigate the effect of the fault location, $|Z_{ii}|$ was used to provide a measure of electrical distance between machine i and the disturbance, where Z_{ii} is the i^{th} diagonal element of the faulted system impedance matrix. In these studies, 200 ms stub faults were used to simulate the disturbance. The initial loading of the machines corresponds to Operating Condition 2 (Table 5). The results of these studies, which are plots of δ_{31} versus time, are given in Figure 25. The difference between the results obtained with the FULL and APP models, particularly the predicted magnitude of the first rotor swing, is greater when the fault is on bus #9, as indicated by Figure 25a, than when the fault is on bus #7, as indicated by Figure 25b. As was mentioned earlier, $|Z_{33}|$ represents the electrical distance between Machine #3 and the fault, i.e., the fault on bus #9 is electrically closer to Machine #3 than the fault on bus #7. These results are in agreement with the view that the severity of the disturbance varies inversely with the electrical distance from the fault.

b. Effect of clearing time (t_c) In these studies, a stub fault was placed on bus #9 and cleared at different times so that the effect of clearing time could be documented. The machine loadings correspond to Operating Condition 1 (Table 5).

Figure 26 gives a plot of δ_{31} versus time for three values of clearing time. The results indicate that as the clearing time increases,

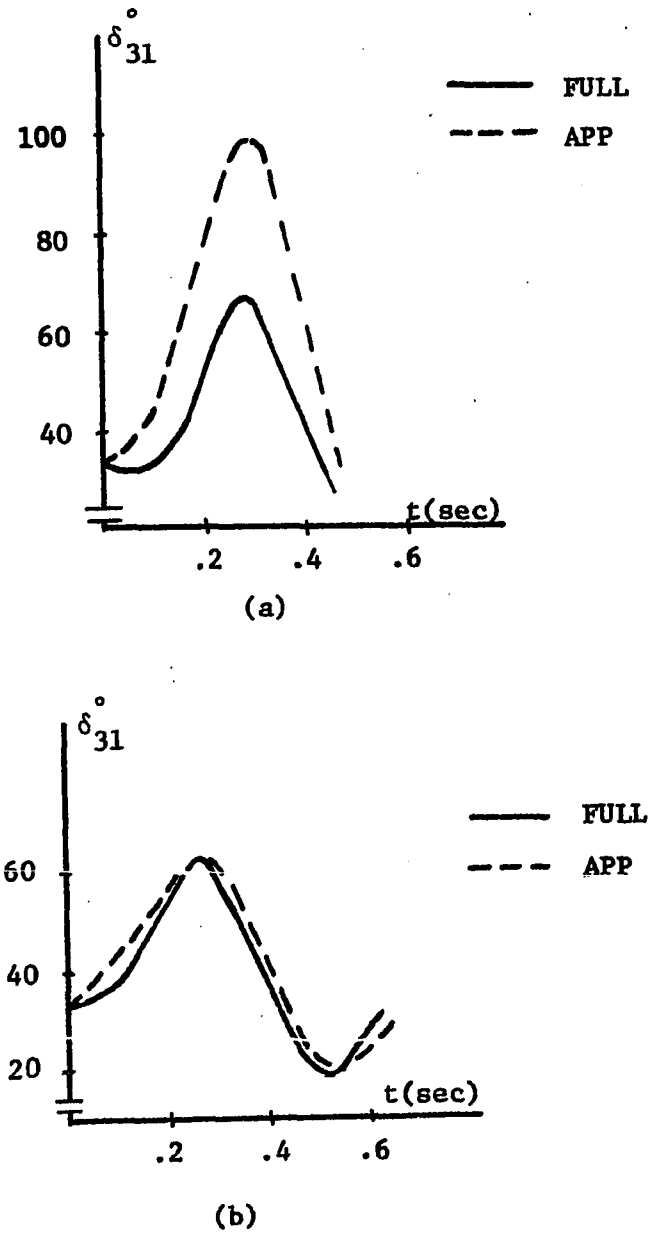

Figure 25. Effect of fault location. Plots of δ_{31} versus time for a 200 ms fault (Operating Condition 2). Simulation by the FULL and APP models

(a) Fault on bus #9, $|Z_{33}|$ = 0.06 pu

(b) Fault on bus #7, $|Z_{33}|$ = 0.19 pu

there is a greater discrepancy between the results obtained with the FULL and APP models.

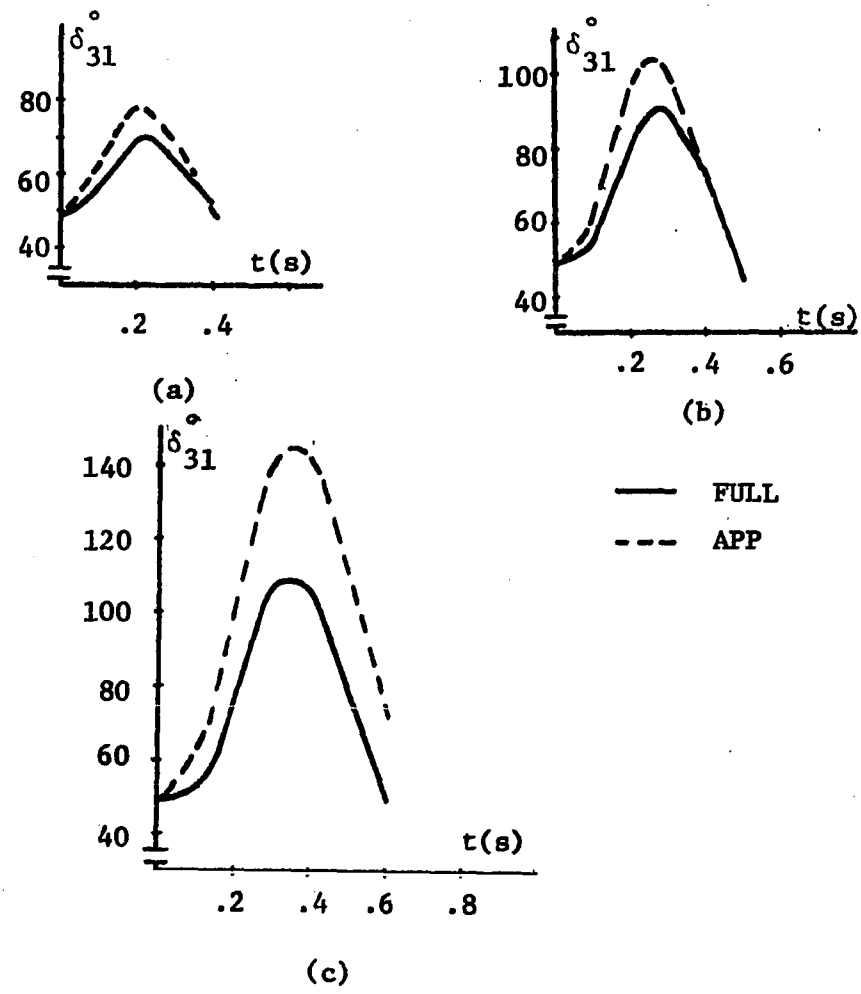

Figure 26. Effect of clearing time. Plots of δ_{31} versus time for faults on bus #9 (Operating Condition 1). Simulation by the FULL and APP models

(a) t_c = 100 ms

(b) t_c = 150 ms

(c) t_c = 200 ms

c. Effect of initial loading Initial loading of the machines could offer qualitative information concerning synchronizing torque coefficients. These coefficients are measures of the changes in the electrical torques of the machines for small changes in rotor angles. When a power system is disturbed, the electrical torques of the generators will change in such a way so that the state of equilibrium could be restored. High synchronizing torque coefficients, i.e., large changes in the electrical torques, are indicative of a strong power system. Low synchronizing torque coefficients, on the other hand, indicate a weak power system. For a particular power system, synchronizing torque coefficients are functions of system's operating conditions. therefore, a power system, depending on its operating conditions, can be in a strong, or a weak mode of operation. A strong mode of operation, as opposed to a weak mode of operation, implies that the electrical torques of the generators, in response to a disturbance, will change drastically in order to restore the state of equilibrium. Consequently, for identical disturbances, a strong mode of operation will result in smaller swings than a weak mode of operation.

As was mentioned earlier, in these studies two operating conditions were considered. In order to make a comparison between the synchronizing torque coefficients of the two cases, δ_2 and δ_3 were increased by one degree and the changes in the electrical torques were recorded. These variations in the electrical torques (ΔT_e's), which are measures of synchronizing torque coefficients, are presented in Table 7.

Table 7. Comparison of the changes in the electrical torques[a]

Operating Conditions	ΔT_{e1} (pu)	ΔT_{e2} (pu)	ΔT_{e3} (pu)
1	-.053	.026	.022
2	-.055	.032	.026

[a] ΔT_{ei} is the amount by which T_{ei} varies, from its initial value, due to changes in δ_2 and δ_3.

As illustrated in Table 7, Operating Condition 2 represents a stronger mode of operation than Operating Condition 1. It could, therefore, be expected that for identical faults, Operating Condition 2 would indicate smaller swings, and smaller differences between the results obtained with the FULL and APP models, than Operating Condition 1. This could be seen by studying the results presented in Figures 27a and 27b. In both cases, a 200 ms stub fault was placed on bus #9. Figure 27a presents plots of δ_{21} versus time, when the machines' initial loading correspond to Operating Condition 1. Plots of δ_{21} corresponding to Operating Condition 2 are given in Figure 27b. We note that, with regard to the predicted magnitude of the first rotor swing, the FULL and APP models are in much better agreement in Figure 27b than they are in Figure 27a.

d. Effect of machine parameters There is a large number of machine parameters that could be investigated. The inertia constant (H) was chosen for the purpose of these studies. The inertia constant

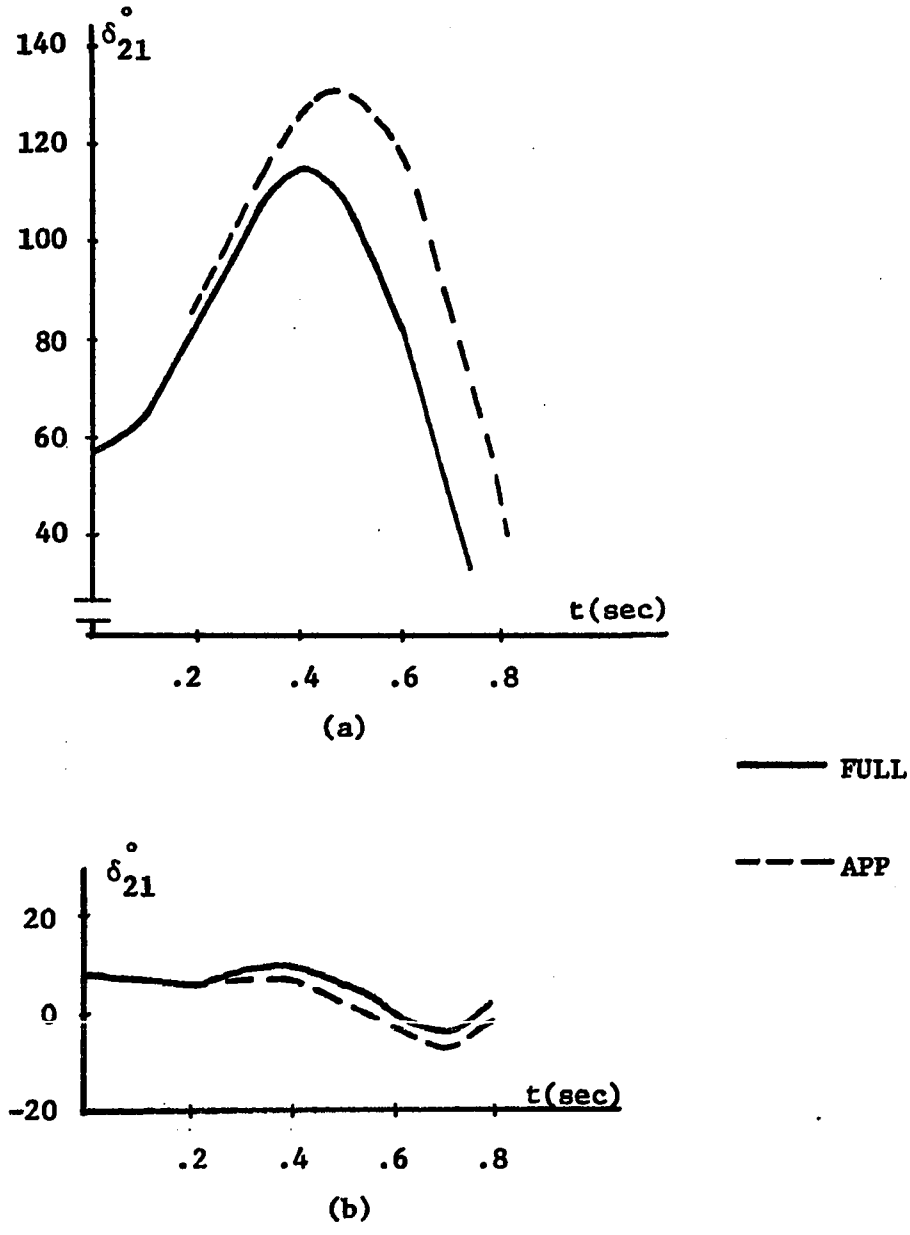

Figure 27. Effect of initial loading. Plots of δ_{21} versus time for a 200 ms fault on bus #9. Simulation by the FULL and APP models

(a) Operating Condition 1

(b) Operating Condition 2

of machine #3 was reduced by a factor of 2.5 times, i.e., $H_3/2.5$, and its effects on the swing curves were recorded. In these studies 200 ms stub faults were placed on bus #6. The machines' initial loading corresponds to Operating Condition 1. The results of these studies, which are plots of δ_{31} versus time, are presented in Figure 28. These results indicate that the discrepancy between the results obtained with the FULL and APP models, particularly the estimated magnitude of the first rotor swing increases when the inertia constant is decreased.

The data presented in Figures 25-28 clearly indicate a clear relationship between the aforementioned four factors, and the difference between the results obtained with the FULL and APP models. However, none of these factors by itself could provide us with adequate information needed for choosing the proper machine model for selective modeling technique. For instance, Figure 25 indicates that when the fault is near or at the terminals of Machine #3, that machine would have to be represented by the FULL model. This, however, does not mean that if the fault is near any machine, then that machine must be represented by the FULL model. In fact, it is quite conceivable that under different circumstances, even a fault on Bus #9 will not require simulation of Machine #3 by the FULL model.

The discussion presented thus far indicates that the choice of proper machine model must be based on all of the aforementioned four factors. To put it another way, a criterion is needed that will relate the difference between the results obtained with the FULL and APP models to those four factors. One such method will be presented in Chapter VI.

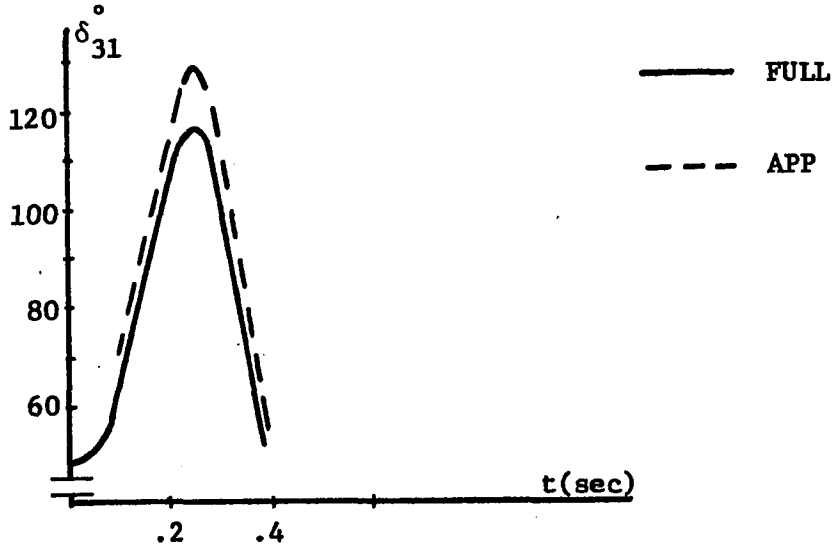

(a)

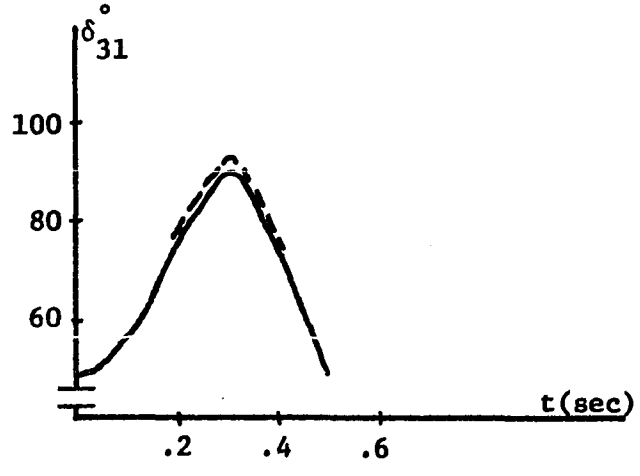

(b)

Figure 28. Effect of inertia constant. Plots of δ_{31} versus time for a 200 ms fault on bus #6 (Operating Condition 1). Simulating by the FULL and APP models

(a) $\frac{H_3}{2.5}$

(b) H_3

It will then become possible to classify the machines based on how severely they are disturbed, and thus to select the proper machine model to represent each category of generators. It is hoped that such a technique will greatly increase the efficiency of power system transient stability studies.

2. Model switching technique

One of the ideas investigated in Chapter IV was the model switching concept which proved to be consistently accurate and inexpensive, as compared to when the FULL model was used for the entire simulation period. This technique is investigated for multimachine system studies. A summary of these studies is presented in Table 8.

Table 8. Description of model switching studies

Run Number	Figure	Fault Location	Clearing Time (ms)	Operating Condition
1	29	bus #4	220	1
2	30	bus #7	60	1
3	31	bus #9	200	1
4[a]	32	bus #9	125	1

[a] In this case, for demonstration purposes, the inertia constant of of machine #3 was reduced by a factor of 2.5 times, i.e., $H_3/2.5$

The results of these studies are illustrated in Figures 29-32. Figures 29 and 30 present plots of δ_{21} versus time. Plots of δ_{31} versus time are given in Figures 31 and 32. These plots offer a comparison of the system's transient performance as predicted by the FULL and APP models and model switching technique. The results indicate that model switching technique is a highly accurate method, as compared to when the FULL model is used for the entire simulation period. For instance, with regard to the magnitude of the first rotor swing, Figures 31 and 32 indicate a significant discrepancy between the results obtained with the FULL and APP models. On the other hand, the results obtained by the model switching method are highly accurate, when compared with the benchmark. We note that in all these cases the results obtained with the FULL model and model switching technique are in good agreement with regard to factors such as frequency of oscillation, damping, and magnitude of rotor swing.

The efficiency of model switching technique can be determined by studying data presented in Table 9. As the presented data indicate, the execution time required by the model switching technique is generally less than 50% of the required execution time when the FULL model is used for the entire simulation period. This confirms the premise that the model switching technique is a highly efficient method.

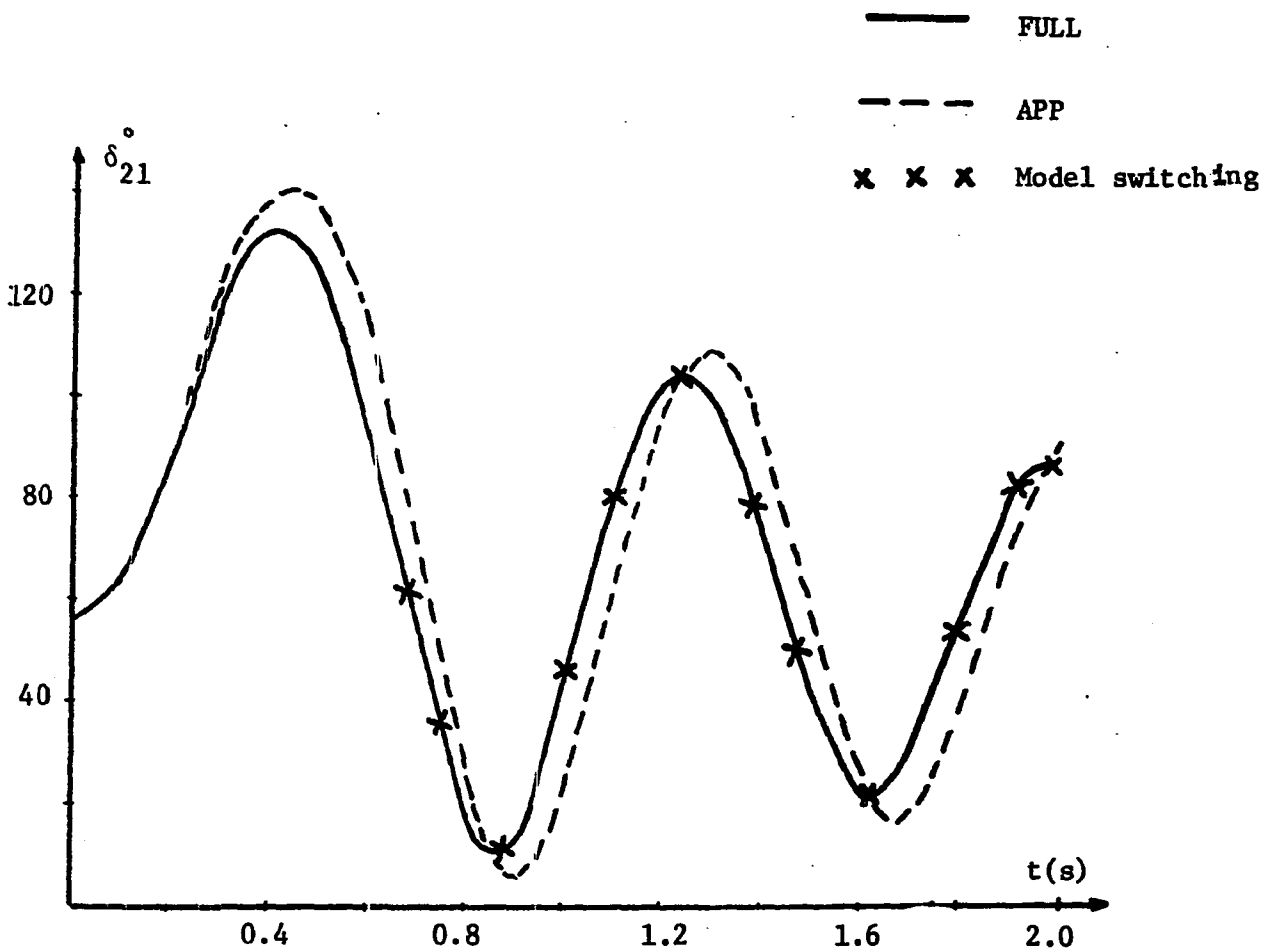

Figure 29. Plot of δ_{21} versus time for a 220 ms fault on bus #4 (Operating Condition 1). Simulation by the FULL and APP models, and the model switching technique

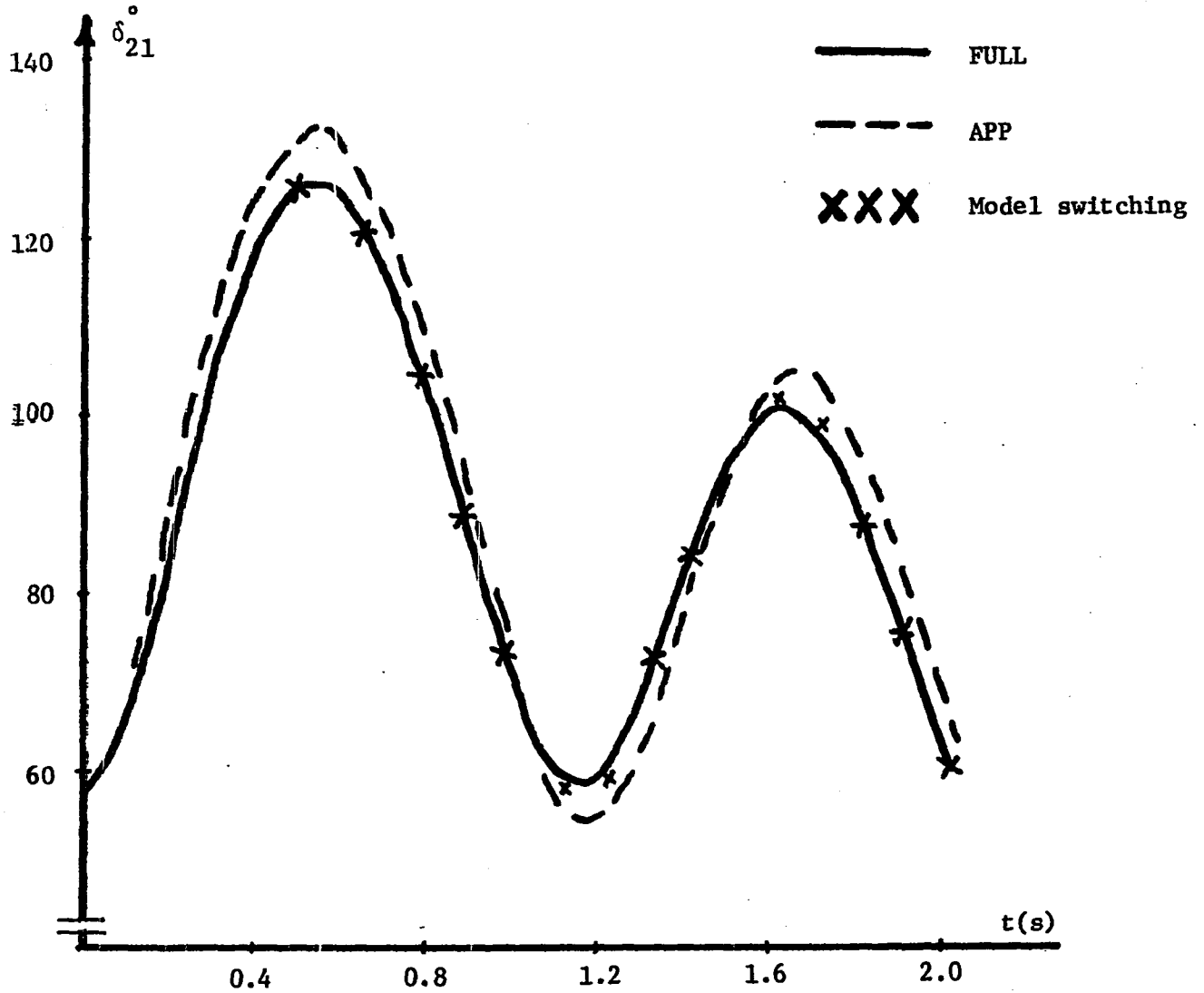

Figure 30. Plot of δ_{21} versus time for a 60 ms fault on bus #7 (Operating Condition 1). Simulation by the FULL and APP models, and the model switching technique

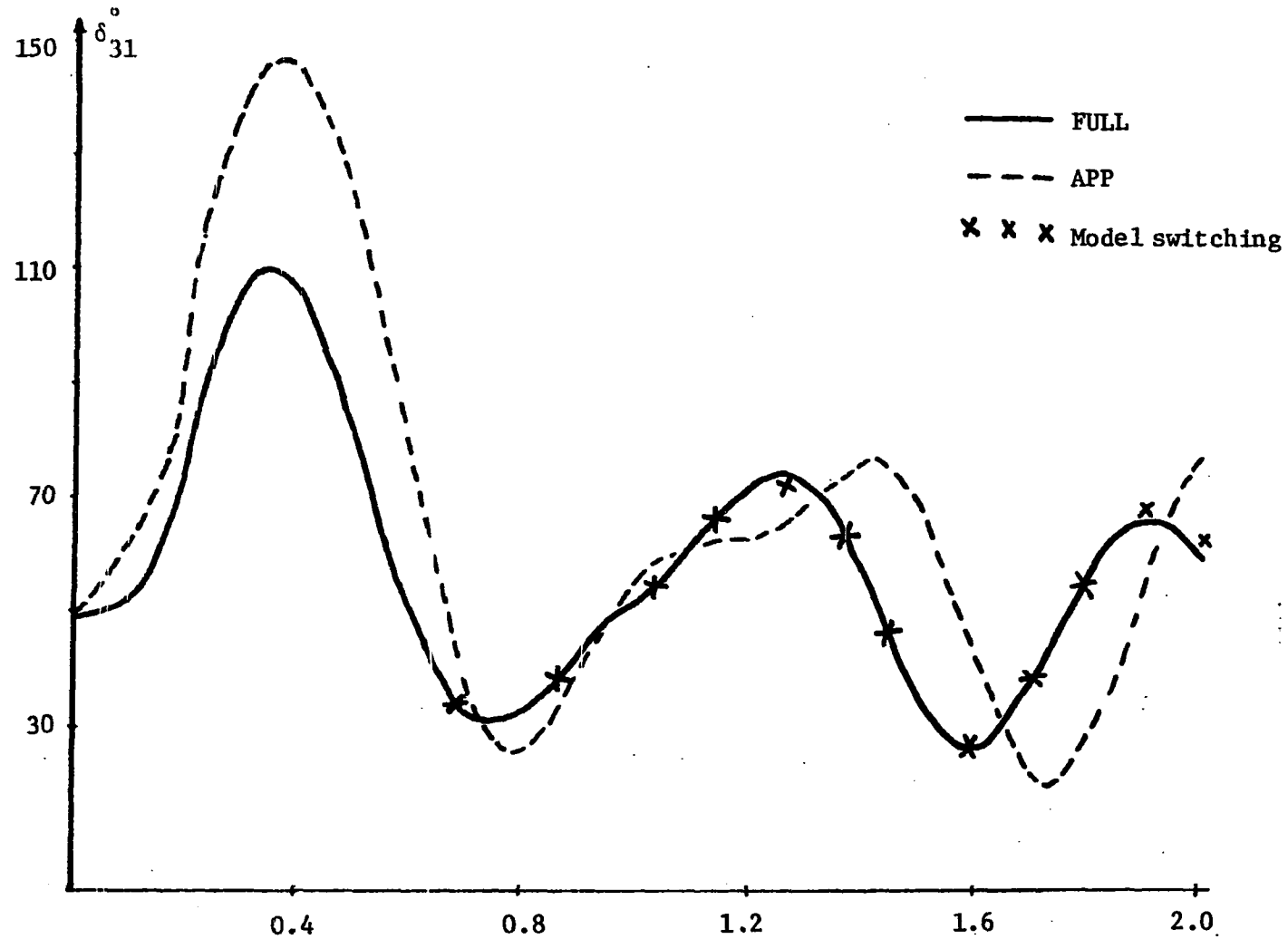

Figure 31. Plot of δ_{31} versus time for a 200 ms fault on bus #9 (Operating Condition 1). Simulation by the FULL and APP models, and the model switching technique

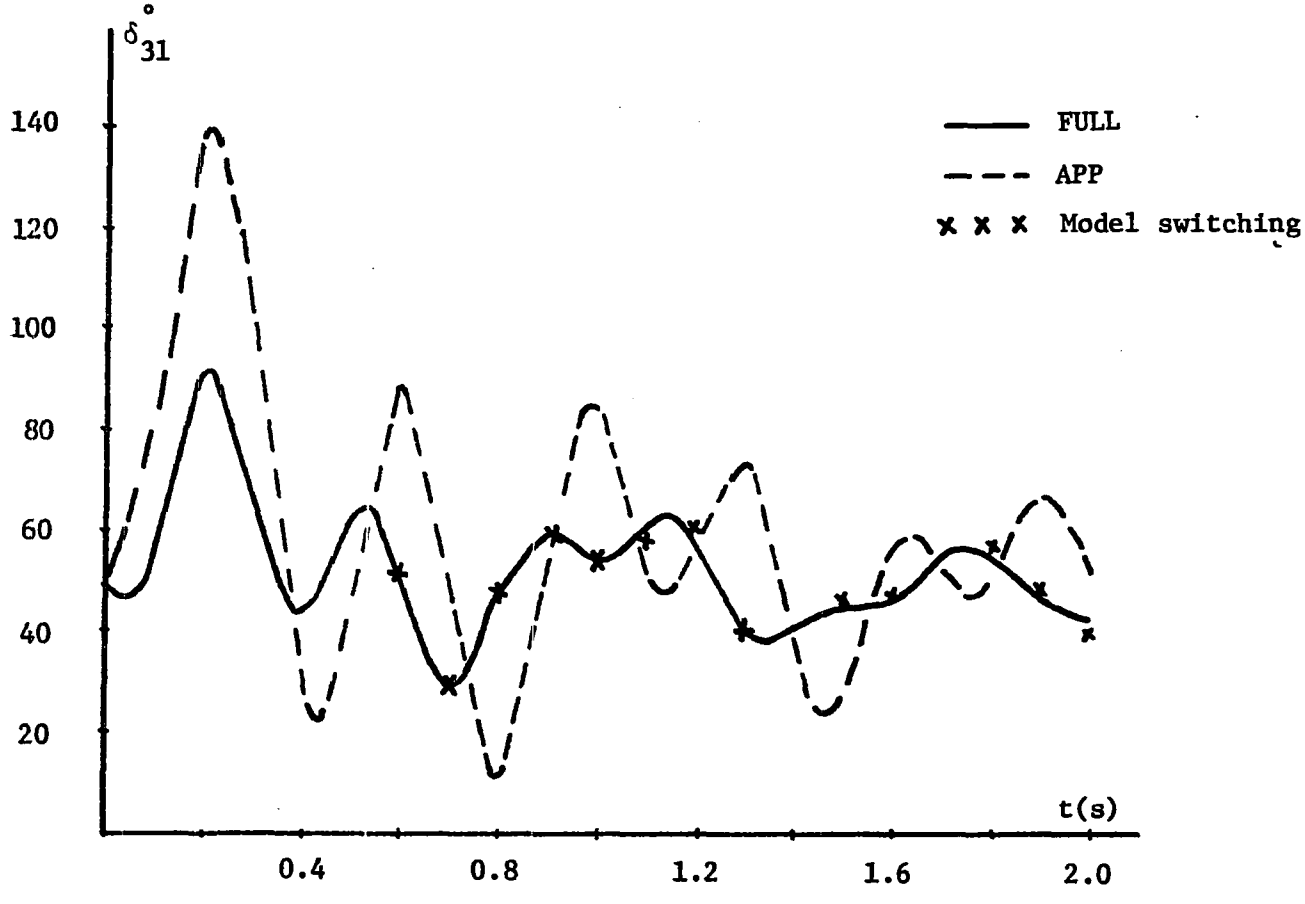

Figure 32. Plot of δ_{31} versus time for a 125 ms fault on bus #9 (Operating Condition 1). Simulation by the FULL and APP models, and the model switching technique

Table 9. Comparison of the execution times

model / run number	Simulation Execution Time in Seconds		
	FULL	APP	Model Switching
1	26	8	13
3	30	7	13
4	43	9	20

In the next section we will introduce a novel approach for improving the efficiency of transient stability studies. This technique takes advantage of an approximate expression for the so-called retarding torque.

3. Accounting for the effect of the retarding torque

Electrical torque of a synchronous machine, when it is subjected to a three-phase terminal fault, could be analytically derived and used to improve the efficiency of transient stability studies. These concepts are described in this section.

a. Short circuit torques For a three-phase fault at the machine's terminals, electrical torque (T_e) could be expressed as:

$$T_e = T_1 + T_2 + T_3 \tag{34}$$

where T_1 and T_2 are due to copper losses in rotor and stator circuits respectively, and T_3 is a decaying torque that oscillates at 60 Hz (assuming that rotor speed remains constant during the fault). Closed

form expressions for T_1, T_2, and T_3 were derived by both Concordia (24) and Adkins and Mehta (33), and are as follows:

$$T_1 = \frac{V_o^2}{2\omega_R}\left(\frac{x_d - x_d'}{x_d' x_d \tau_d} + \frac{x_d' - x_d''}{x_d'' x_d \tau_d} + \frac{x_q - x_q'}{x_q' x_q \tau_q} + \frac{x_q' - x_q''}{x_q'' x_q \tau_q}\right) e^{-2t/\tau_a} \quad (35)$$

$$T_2 = r_a\left[(i_{dt} - i_{do})^2 + (i_{qt} + i_{qo})^2\right] \quad (36)$$

and,

$$T_3 = \left(V_{qo}(i_{dt} - i_{do}) + V_{do}(i_{qt} + i_{qo})\right)e^{-t/\tau_a} \sin\omega_R t - \left(V_{do}(i_{dt} - i_{do}) - V_{qo}(i_{qt} + i_{qo})\right)e^{-t/\tau_a}\cos\omega_R t \quad (37)$$

where subscript o refers to prefault values, and,

$$i_{dt} = V_{qo}\left(\frac{1}{x_d} + \left(\frac{1}{x_d'} - \frac{1}{x_d}\right)e^{-t/\tau_d'} + \left(\frac{1}{x_d''} - \frac{1}{x_d'}\right)e^{-t/\tau_d''}\right)$$

$$i_{qt} = V_{do}\left(\frac{1}{x_q} + \left(\frac{1}{x_q'} - \frac{1}{x_q}\right)e^{-t/\tau_q'} + \left(\frac{1}{x_q''} - \frac{1}{x_q'}\right)e^{-t/\tau_q''}\right) \quad (38)$$

When the synchronous machine is represented by the FULL model, all three components of the short circuit torque are accounted for, i.e.,

$$T_{e,FULL} = T_1 + T_2 + T_3 \quad (39)$$

where $T_{e,FULL}$ is the calculated electrical torque when the FULL model is used to represent the synchronous machine. On the other hand, T_1, which represents copper losses in rotor circuits as a result of induced voltages due to dc offset of stator current, and T_3 will not be

accounted for if the APP model is used to represent the synchronous machine. Therefore,

$$T_{e,APP} = T_1' \tag{40}$$

where T_1' represents stator copper losses, and $T_{e,APP}$ is the calculated electrical torque when the APP model is used. We note that T_2 and T_1' are not equal. However, since stator resistance (r_a) is very small, we can write

$$T_2 \cong T_1' \cong 0 \tag{41}$$

Incorporating Equation 41 into Equation 39, we obtain

$$T_{e,FULL} \cong T_{e,APP} + T_1 + T_3 \tag{42}$$

Equation 42 indicates that the combined effect of T_1 and T_3 is the main cause of the discrepancy in the calculated electrical torque when different models are used to represent the synchronous machines.

Since T_1 and T_3 tend to retard the rotor, their combined effect can be approximated by a so called retarding torque (T_{ret}) that could be defined in the following manner:

$$T_{ret} \cong Ae^{-2/\tau_a} \tag{43}$$

where A, which is a constant, is determined by equating the combined effect of T_1 and T_3, and T_{ret}, as shown below:

$$\int_o^\infty T_{ret}\, dt = \int_o^\infty (T_1 + T_3)\, dt \tag{44}$$

Integrating the left hand side of Equation 44, we will get

$$\frac{A}{-2}\tau_a e^{-2t/\tau_a} \Big|_o^\infty \cong \int_o^\infty (T_1 + T_3)\, dt \tag{45}$$

which yields

$$\frac{A}{2}\tau_a \cong \int_o^\infty (T_1 + T_3)\, dt \tag{46}$$

or,

$$A \cong \frac{2}{\tau_a} \int_o^\infty (T_1 + T_3)\, dt \tag{47}$$

The discussion presented thus far is concerned with a special case in which a generator is subjected to a terminal fault. A more general treatment of this subject for nonterminal faults will now be presented.

Consider a power system with n machines. The interface equation for the i^{th} generator is

$$v_i = Z_{i1}\, i_1 + \ldots + Z_{ii}\, i_i + \ldots + Z_{in}\, i_n \tag{48}$$

where Z_{ij}'s are elements of reduced system impedance matrix. The above equation can be written as

$$v_i = Z_{ii}\, i_i + \sum_{\substack{j=1 \\ j \neq i}}^{n} Z_{ij}\, i_j \tag{49}$$

or,

$$v_i = Z_{th,i}\, i_i + v_{th,i} \tag{50}$$

where

$$Z_{th,i} = Z_{ii}$$

and

$$v_{th,i} = \sum_{\substack{j=1 \\ j \neq i}}^{n} Z_{ij}\, i_j \tag{51}$$

In other words, the i^{th} generator sees the rest of the power system as a single voltage source at the end of a line with an impedance of Z_{ii}, as shown in Figure 33.

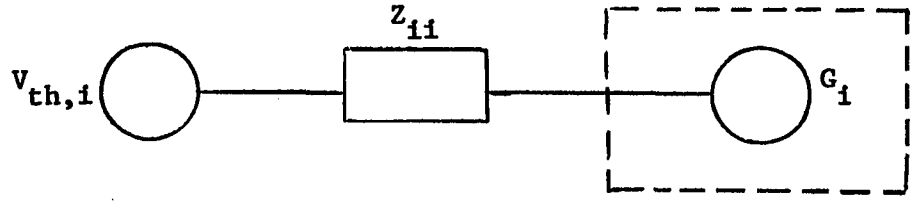

Figure 33. Equivalent representation of a multimachine system

When the power system is subjected to a fault, $v_{th,i}$'s, although nonzero, will be very small. If it is assumed that $v_{th,i}$'s are all zero, then a fault in the transmission system will appear as a fault at the terminals of all generators if their terminals are extended out by treating Z_{ii}'s as an extension of their stator windings, as shown in Figure 34.

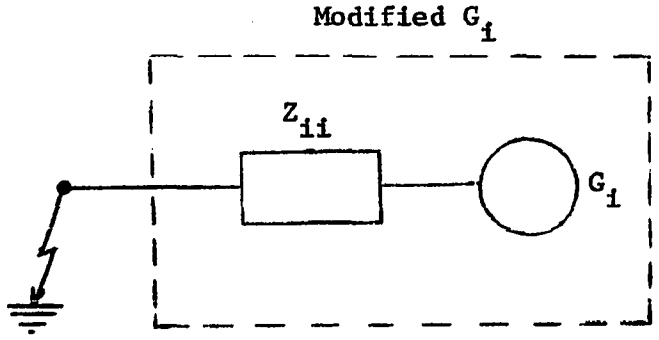

Figure 34. Schematic representation of a modified generator

Such a procedure makes it possible to obtain an approximate expression for the retarding torque of every machine in the system.

Once an approximate expression for the retarding torque is obtained, it could be incorporated in the swing equation of the APP model in the following manner:

$$\frac{2H}{\omega_R}\ \dot{\omega}_{APP} = T_m - (T_{e,APP} + T_{ret}) \tag{52}$$

where ω_{APP} is the calculated rotor speed when the APP model is used to represent the machine. If, on the other hand, the FULL model was used in the simulation, the swing equation will be:

$$\frac{2H}{\omega_R}\ \dot{\omega}_{FULL} = T_m - T_{e,FULL} \tag{53}$$

Since the net effects of $T_{e,FULL}$ and $(T_{e,APP} + T_{ret})$ are nearly the same, it follows that Equations 52 and 53 will lead to approximately the same swing curves.

b. Simulation by the APP model, and the retarding torque — Inclusion of the effect of the retarding torque in the swing equations of the APP model, as illustrated in Figure 35-37, greatly improves the performance of the APP model, as compared with the benchmark. The presented results are plots of δ_{21} (Figure 36) and δ_{31} (Figures 35 and 37) versus time. These plots make it possible to compare the transient behavior of the system as indicated by the FULL and APP models, and the proposed modeling technique, i.e., including the effect of the retarding torque in the swing equations of the APP model. We note that in some cases (Figures 35 and 37) there is considerable difference between the FULL and APP models with regard to the predicted magnitude of the first rotor

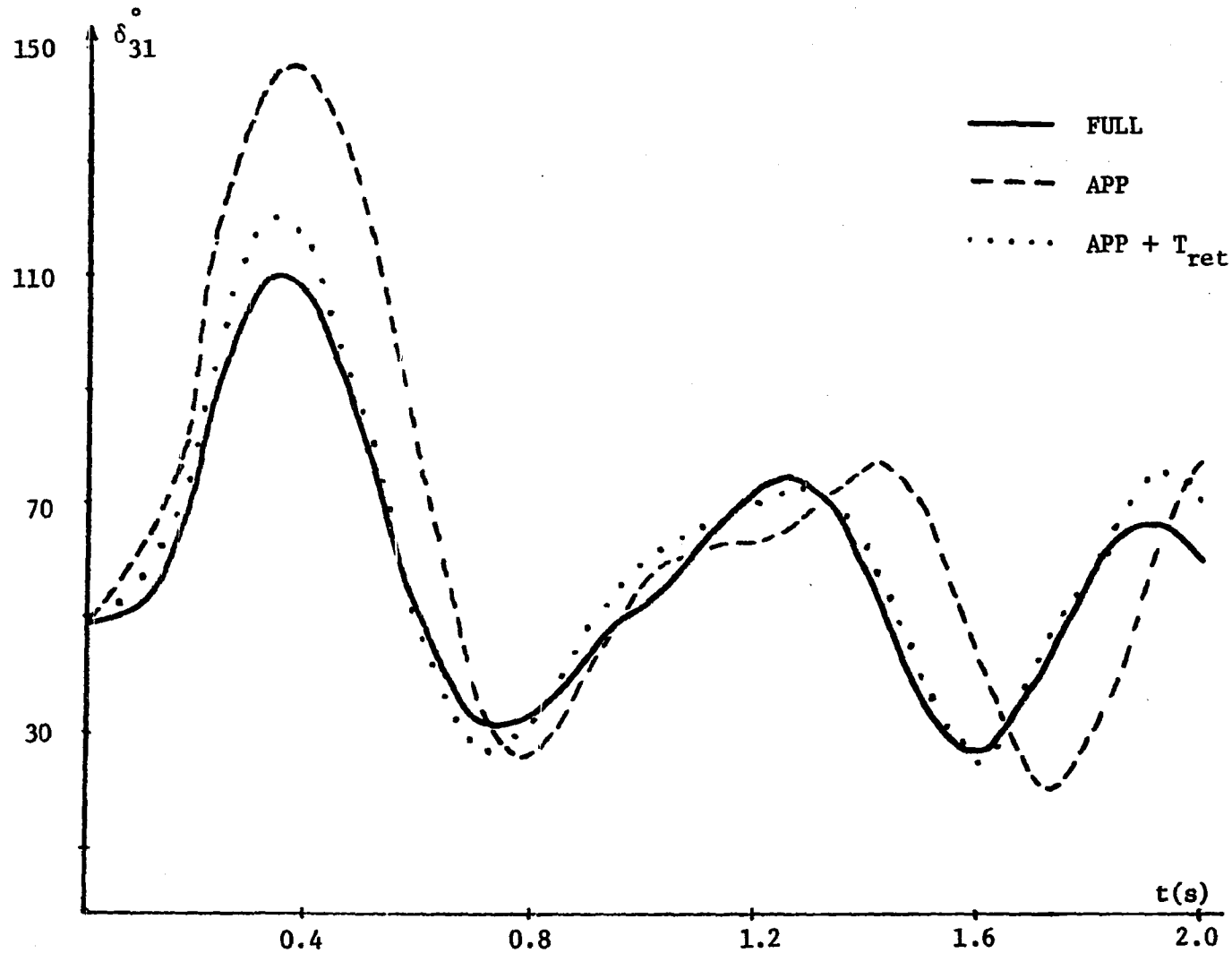

Figure 35. Plot of δ_{31} versus time for a 200 ms fault on bus #9 (Operating Condition 1). Simulation by the FULL and APP models, and the (APP + T_{ret}) method

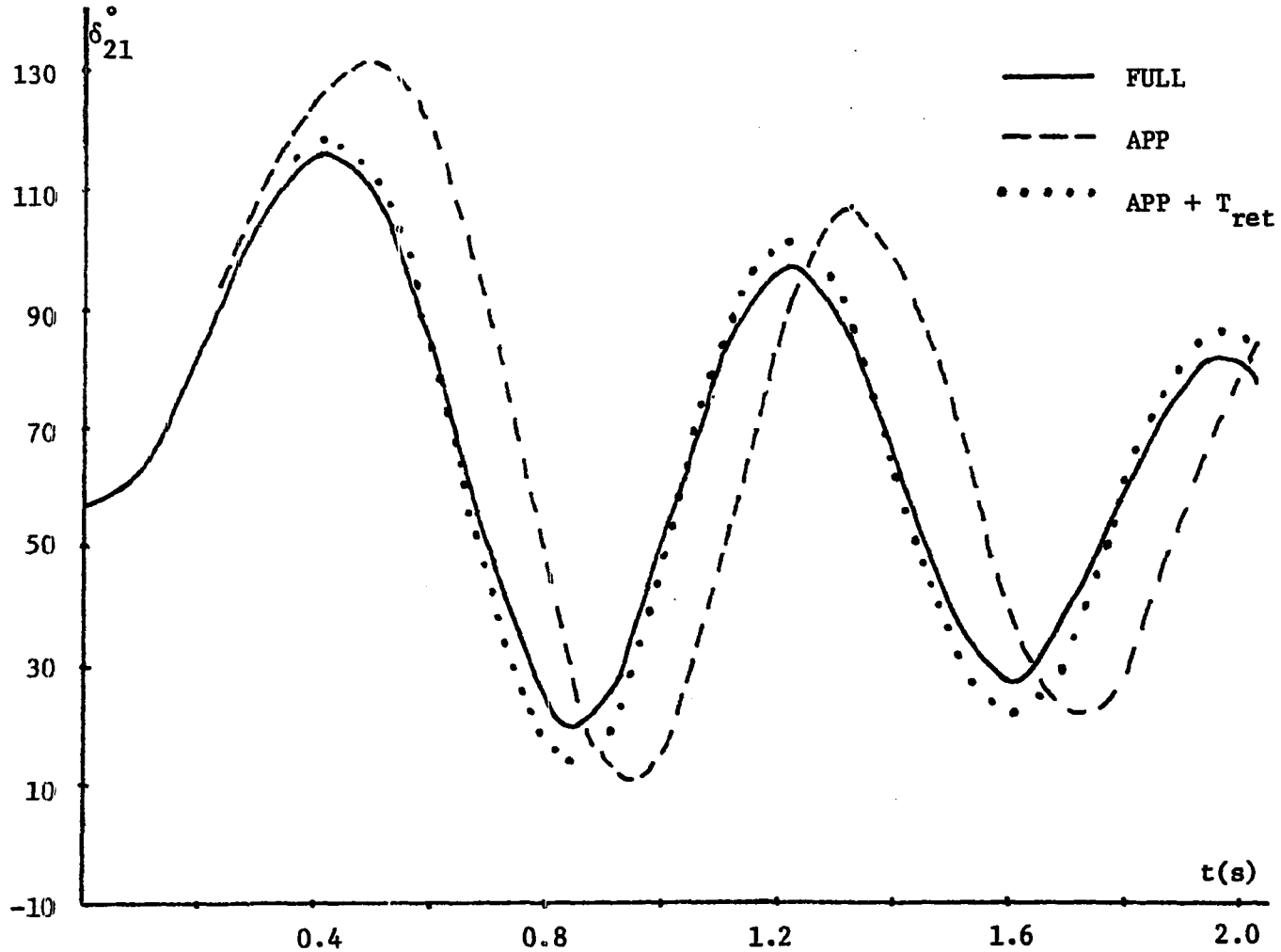

Figure 36. Plot of δ_{21} versus time for a 200 ms fault on bus #9 (Operating Condition 1). Simulation by the FULL and APP models, and the (APP + T_{ret}) method

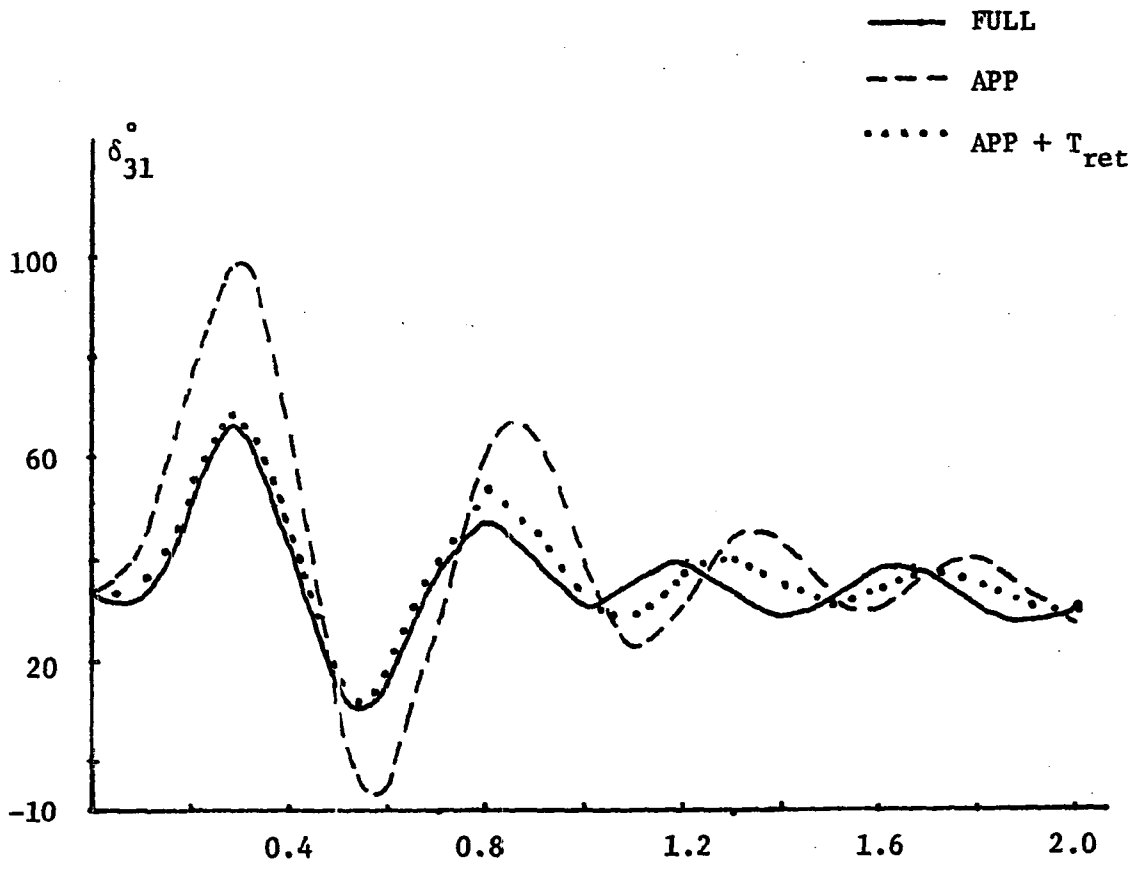

Figure 37. Plot of δ_{31} versus time for a 200 ms fault on bus #9 (Operating Condition 2). Simulation by the FULL and APP models, and the (APP + T_{ret}) method

swing. However, when the effect of the retarding torque is accounted for, there is a great improvement in the performance of the APP model, as compared with the benchmark, with regard to factors such as magnitude of the first rotor swing, damping, and frequency of oscillation.

In these studies, 200 ms stub faults on bus #9 were used to simulate the disturbance. The results presented in Figures 35 and 36 correspond to Operating Condition 1. Figure 37 illustrates the results corresponding to Operating Condition 2.

It must be noted that although this modeling technique is not as accurate as the model switching method, it is, however, much less expensive. The increase in the required execution time, as compared with when the APP model is used for the entire simulation period, is estimated to be only 10%. This compares very favorably with the corresponding figure for the model switching technique which is about 100%. Therefore, accounting for the effect of the retarding torque could constitute the first step toward improving the efficiency of transient stability studies. This method could be used in preliminary transient stability studies which are made to identify those cases that require closer scrutiny. Once such cases are identified, the model switching technique could then be utilized to further improve the accuracy of the simulation.

At this point, it might be helpful to emphasize once again that in many cases, the APP model does adequately represent the synchronous machine for transient stability studies. In such cases, there is obviously no need to account for the effect of the retarding torque, or using model switching technique. In the next chapter, a method will be

presented that will make it possible to select the proper modeling strategy for a particular transient stability study.

4. Review of modeling techniques

In this section, we will briefly review the various modeling methods that have been discussed thus far and state how and when each of these methods could be used.

Figure 38 graphically describes various modeling approaches that were discussed in this and the previous chapter. The presented alternatives are in descending order of accuracy and computational cost.

The first alternative, Figure 38a, employs the FULL model for the entire simulation period. Due to high computational cost associated with this approach, it is used only when justified, i.e., in special studies.

The second, Figure 38b, when used selectively, could prove to be an appropriate modeling technique when a high degree of accuracy is desired.

The third, using the APP model plus the retarding torque, is shown in Figure 38c. It requires slightly more execution time than when the APP model is used for the entire simulation period. This technique could greatly improve the performance of the APP model and could be regarded as the first step toward improving the efficiency of transient stability studies.

And finally, the fourth alternative is using the APP model for the entire simulation period, as shown in Figure 38d. This is the least

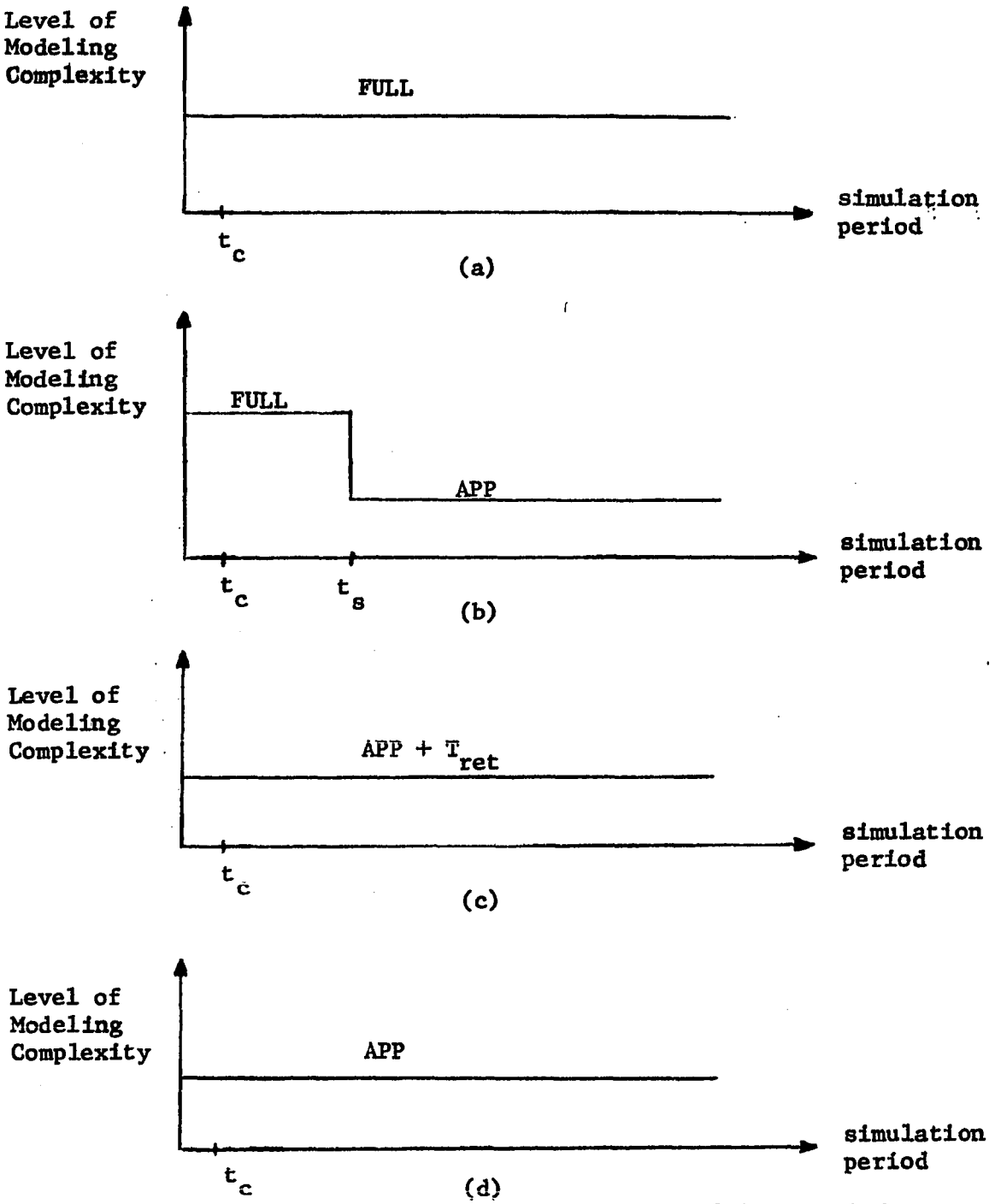

Figure 38. Schematic representation of various modeling techniques

(a) simulation by the Full model
(b) model switching
(c) simulation by the APP model plus retarding torque
(d) simulation by the APP model

expensive approach, and in most cases, offers a fair degree of accuracy when compared with the first alternative.

The aforementioned modeling approaches need not be applied uniformly throughout the power system. In practice, only a selected few of the machines may be represented by the method depicted in Figure 38b. Another group of generators would be represented by the APP model shown in Figure 38d. The third alternative, Figure 38c, may be applied to still another group of synchronous machines. Such a highly selective modeling strategy will greatly improve the efficiency of transient stability studies. There is, however, a definite need for a criterion that will make it possible to select the proper modeling approach for each group of machines. One such criterion will be presented in the next chapter.

VI. CRITERION FOR SELECTIVE MODELING

In Chapters IV and V, various modeling techniques for transient stability studies were discussed. It was established that some of those approaches, i.e., model switching method, can greatly improve the efficiency of simulation. It was also demonstrated that selective modeling approach can result in further gains in simulation efficiency. In this chapter, we will develop a criterion for selective modeling that will lead to a three tiered modeling strategy. This criterion is based on the machine's additional rotor displacement at the instant of fault clearing due to the retarding torque.

A. Measuring Severity of the Disturbance to the Synchronous Machine

We seek to develop a method that will enable us to select the proper modeling approach for each generator for a particular transient stability study. Such a criterion will provide qualitative information, regarding the discrepancy between the results obtained with the FULL and APP models, for each generator. The choice of the proper modeling technique for each machine could then be based on the expected difference between the performance of the FULL and APP models.

In Chapter V, it was illustrated that, following a three-phase fault, the electrical torque obtained using the FULL model can be approximated by three torque components:

$$T_{e,FULL} \cong T_{e,APP} + T_1 + T_3 \tag{54}$$

and the combined effects of T_1 and T_3 could be approximately represented by the retarding torque (T_{ret}), i.e.,

$$T_{e,FULL} \cong T_{e,APP} + T_{ret} \tag{55}$$

We can therefore write

$$\frac{2H}{\omega_R} \dot{\omega}_{APP} = T_m - T_{e,APP}$$

$$\frac{2H}{\omega_R} \dot{\omega}_{FULL} = T_m - T_{e,FULL} \cong T_m - (T_{e,APP} + T_{ret}) \tag{56}$$

Where ω_{APP} represents the calculated rotor speed when the APP model is used, ω_{FULL} is defined in a similar manner. It follows that

$$\frac{2H}{\omega_R} (\dot{\omega}_{APP} - \dot{\omega}_{FULL}) \cong T_{ret} \tag{57}$$

or,

$$\frac{2H}{\omega_R} \int_o^{t_c} (\dot{\omega}_{APP} - \dot{\omega}_{FULL})\, dt \cong \int_o^{t_c} T_{ret}\, dt \tag{58}$$

which is equivalent to

$$\Delta\omega(t_c) \triangleq \frac{\omega_{APP}(t_c) - \omega_{FULL}(t_c)}{\omega_R} \cong \frac{\int_o^{t_c} T_{ret}\, dt}{2H} \tag{59}$$

and

$$\Delta\delta(t_c) \triangleq \delta_{APP}(t_c) - \delta_{FULL}(t_c) \cong \frac{\int_o^{t_c} \int_o^{t} T_{ret}\, dt}{2H} \tag{60}$$

where $\Delta\omega(t_c)$ and $\Delta\delta(t_c)$ are the amounts by which rotor speed and power angle of a machine are overestimated (at $t = t_c$) if the APP model, as opposed to the FULL model, is used to represent that machine. Finally, we can write

$$\Delta\omega_{ij}(t_c) = \Delta\omega_i(t_c) - \Delta\omega_j(t_c) \tag{61}$$

and

$$\Delta\delta_{ij}(t_c) = \Delta\delta_i(t_c) - \Delta\delta_j(t_c) \tag{62}$$

where subscripts i and j refer to Machines i and j.

As indicated in Chapter V, the approximate expression for the retarding torque accounts for fault location, parameters and initial loading of the machine. It follows that $\Delta\omega_{ij}(t_c)$ and $\Delta\delta_{ij}(t_c)$ depend on fault location, clearing time, parameters and initial loading of the machines. We note that these are the four factors that, in Chapter V, were shown to affect the difference between the results obtained with the FULL and APP models.

Close examination of the available data indicates that the difference between the results obtained with the FULL and APP models is related to the magnitudes of $\Delta\delta_{ij}(t_c)$'s. This can be seen by examining the swing curves presented in Figure 39, which are plots of δ_{31} versus time for a 200 ms fault (Fig. 39a), and a 100 ms fault (Fig. 39b), on bus #9. The machines' initial loading correspond to Operating Condition 1. These plots indicate that the discrepancy between the FULL and APP models, particularly with regard to the predicted magnitude of the first rotor swing, is directly proportional to the values of $\Delta\delta_{31}(t_c)$. To put it another way, high values of $\Delta\delta_i(t_c)$ indicate that Machine i is severely disturbed. On the other hand, low values of $\Delta\delta_i(t_c)$ would mean that Machine i is not severely disturbed.

The choice of the appropriate modeling approach for a machine, or a group of machines, could now be based on how severely those machines are disturbed.

We propose that, prior to any transient stability study, $\Delta\delta(t_c)$ be computed for each synchronous machine. As will be shown in the final

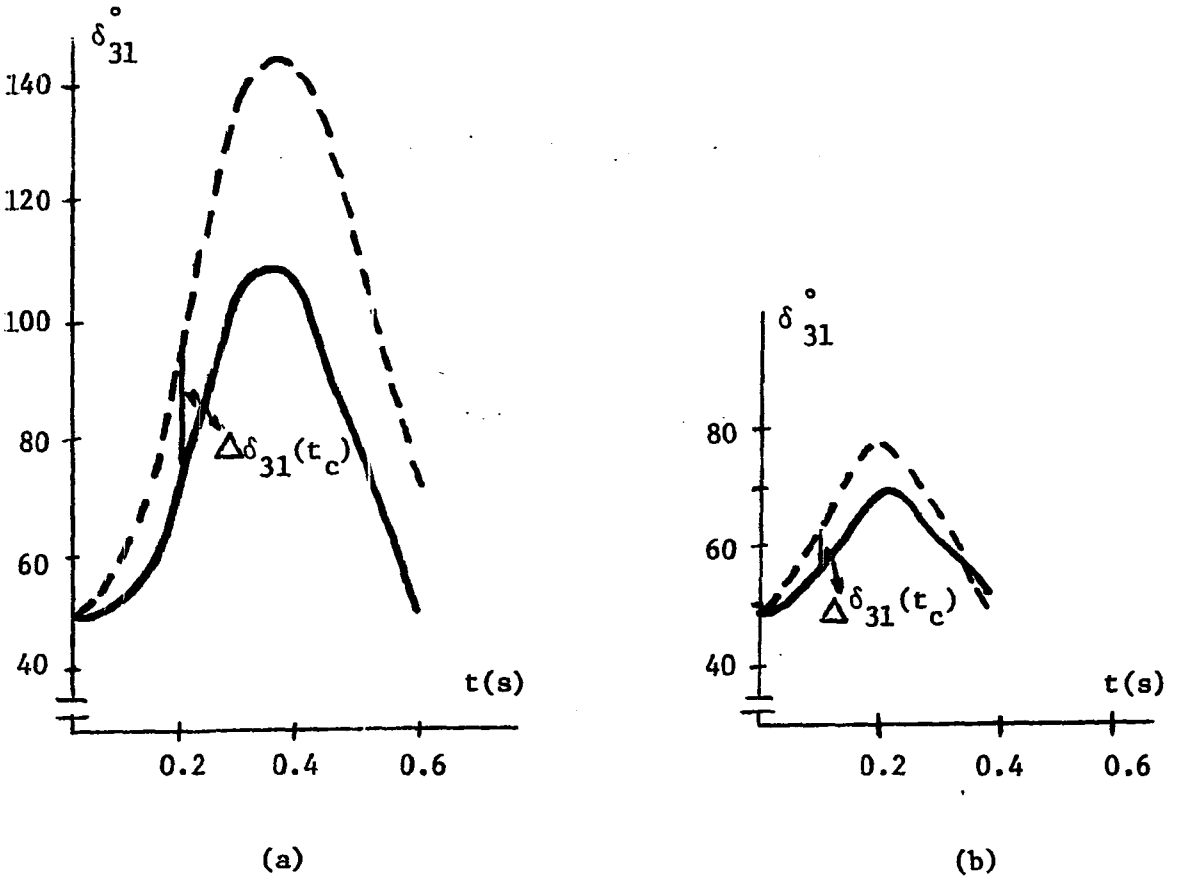

Figure 39. Plots of δ_{31} versus time for a fault on bus #9 (Operating Condition 1). Simulation by the FULL and APP models

(a) t_c = 200 ms

(b) t_c = 100 ms

section of this chapter, this step requires an almost negligible amount of additional computer time. Once all $\Delta\delta(t_c)$'s are calculated, those values could be used to classify the synchronous machines into three different groups (Figure 40) in the following manner:

Group I $\quad \Delta\delta(t_c) \leqslant \rho$

Group II $\quad \rho < \Delta\delta(t_c) \leqslant \beta$

Group III $\quad \Delta\delta(t_c) > \beta$

where machines in Group I are among the least severely disturbed and could therefore be represented by the APP model. We note in passing that it may be desirable to have a fourth group, i.e., Group 0, which contains those machines that are virtually undisturbed. Those machines would be represented by the classical model.

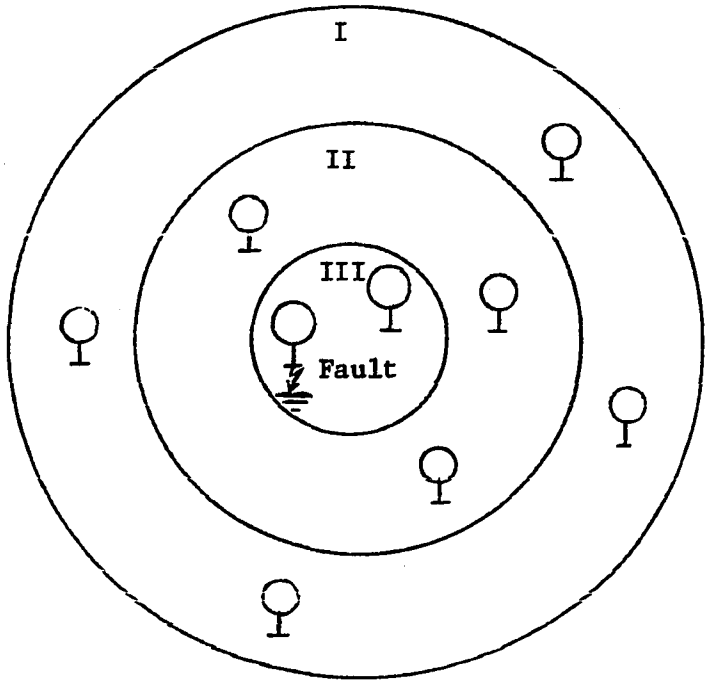

Figure 40. Pictorial representation of generator grouping

B. Three-Tiered Modeling Strategy

Once the synchronous machines are divided into different groups, the proper modeling method for each group of machines could be selected in the following manner:

Group I the APP model

Group II the APP model + T_{ret}

Group III model switching technique

Understandably for each power system, the values of ρ and β must be determined empirically. In practice, a considerable amount of prior knowledge and experience with a particular power system is usually available to system engineers which enables them to decide the appropriate boundaries of $\Delta\delta(t_c)$'s for generator grouping. For instance, for the multimachine system that was examined in Chapter V, it was found that $\rho = 5^\circ$ and $\beta = 10^\circ$ were quite appropriate for this purpose. We propose, however, that such figures for ρ and β be allowed to vary based on the following considerations.

1. Type of the transient stability study

Transient stability studies, based on period of simulation, could be divided into three categories: short, medium, and long term. In case of a long term transient stability study, due to the cumulative nature of the error, more emphasis must be placed on model switching technique and inclusion of the effect of the retarding torque, i.e., lower values for ρ and β.

2. (Expected) margin of stability

In case of a (expected) marginally stable system, a rather high degree of accuracy may be desirable. Consequently, more emphasis must be placed on model switching technique and inclusion of the effect of the retarding torque, i.e., lower values for ρ and β.

3. Computational resources

Capacity of the computer memory system and the required execution time could place a limit on the size of the system's mathematical model, i.e., higher values for ρ and β.

C. Numerical Example

In this section, we will investigate the effectiveness of the proposed selective modeling technique by applying it to the WSCC nine bus test system.

Table 10 presents the predicted values of $\Delta\delta_i(t_c)$'s for a 150 ms fault on bus #9. The machines' initial loading corresponds to Operating Condition 1.

Table 10. $\Delta\delta_i(t_c)$'s for a 150 ms fault on bus #9

$\Delta\delta_1(t_c)$	$\Delta\delta_2(t_c)$	$\Delta\delta_3(t_c)$
0.67°	2.22°	10°

The data presented in Table 10 indicate that Machine #3 is severely disturbed. Machines #1 and #2, on the other hand, are virtually unaffected. Consequently, if values of ρ and β, as recommended in the preceding section, are chosen to be 5° and 10° respectively, we will have the following modeling strategy:

Group I	Machines #1 and #2	the APP model
Group II	Machine #3	the (App + T_{ret}) method

We note that if a higher degree of accuracy is desirable, the model switching method could be used to simulate Machine #3.

The validity of this modeling strategy could be determined by examining the swing curves of this study shown in Figures 41 and 42. As incidated in Figure 41, which presents a plot of δ_{31} versus time, there is a substantial discrepancy between the FULL and APP models, particularly with respect to the magnitude of the first rotor swing. It follows that the APP model does not adequately represent Machine #3, which is in agreement with the proposed modeling approach. The plot of δ_{21} versus time, which is shown in Figure 42, indicates that there is a good agreement between the FULL and APP models. In other words, the APP model adequately represents these two machines, which confirms the validity of the proposed modeling strategy.

The effectiveness of the proposed selective modeling technique greatly depends on the efficiency of the procedure used to compute $\Delta\delta_i(t_c)$'s. The required execution time for calculating $\Delta\delta_i(t_c)$ is under 0.01 s per machine, or under 1.00 s for a 100 machine power system. As illustrated in Chapter V, the approximate expression for

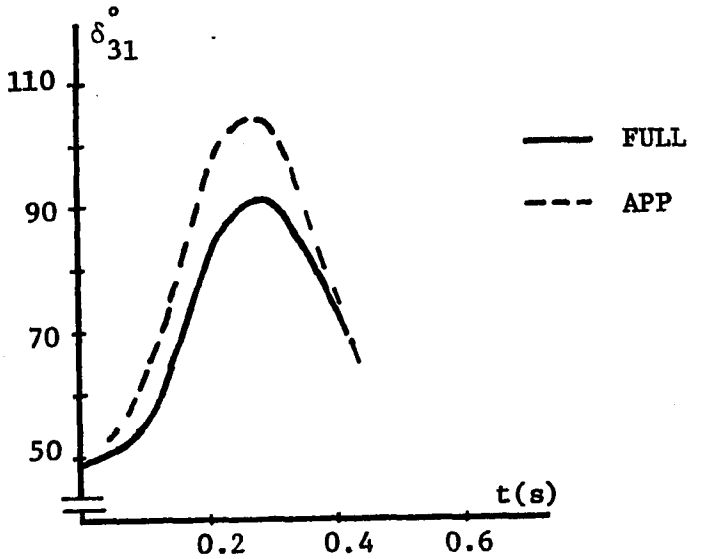

Figure 41. Plot of δ_{31} versus time for a 150 ms fault on bus #9 (Operating Condition 1). Simulation by the FULL and APP models.

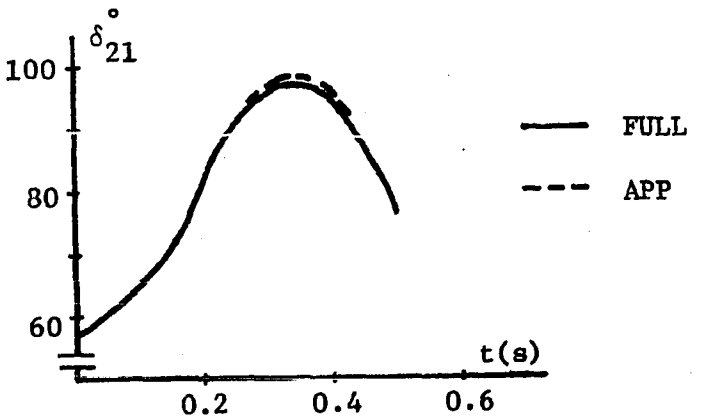

Figure 42. Plot of δ_{21} versus time for a 150 ms fault on bus #9 (Operating Condition 1). Simulation by the FULL and APP models

the retarding torque is based on calculation of Z_{ii}'s of the faulted system impedance matrix. These calculations will add approximately 4 s to the required execution time. Thus, for a 100 machine power system, it will take less than 5 s to obtain $\Delta\delta_i(t_c)$'s for all generators, which is practically negligible when compared with the overall computational cost of transient stability studies. The accuracy of this procedure can be determined by examining the information presented in Table 11. In this table $\Delta\delta_{ij}(t_c)$'s represent values obtained from actual simulation and are used as the benchmark. On the other hand, $\Delta\delta^*_{ij}(t_c)$'s were obtained by the procedure based on the approximate expression for the retarding torque. We note, that in most cases $\Delta\delta_{ij}(t_c)$ and $\Delta\delta^*_{ij}(t_c)$ are in very good agreement. In some instances, such as when the fault is on bus #6, there is some discrepancy between $\Delta\delta_{31}(t_c)$ and $\Delta\delta^*_{31}(t_c)$. However, even in that case, $\Delta\delta^*_{31}(t_c)$ is in reasonably good agreement with the benchmark value of $\Delta\delta_{31}(t_c)$.

Table 11. Comparison of $\Delta\delta_{ij}(t_c)$ and $\Delta\delta^*_{31}(t_c)$

Fault Location, t_c	$\Delta\delta_{21}(t_c)$	$\Delta\delta^*_{21}(t_c)$	$\Delta\delta_{31}(t_c)$	$\Delta\delta^*_{31}(t_c)$
bus #9, 100 ms	0.70°	0.99°	7.60°	4.91°
bus #9, 150 ms	1.00°	1.55°	11.70°	9.40°
bus #6, 200 ms	2.20°	1.16°	2.70°	5.29°

The criterion for selective modeling technique, which is presented in this chapter, could very easily be incorporated into commercially available transient stability programs. The needed computations are quite straightforward, and require a minimal amount of computer time. It is hoped that this criterion will encourage the selective use of the various modeling techniques that were discussed in the previous chapters.

VII. CONCLUSIONS AND RECOMMENDATIONS

The goal of this research work, as indeed it is the purpose of many engineering projects, is to improve the efficiency of a certain computational procedure, namely transient stability studies. More specifically, we seek to develop improved modeling methods for synchronous machines in transient stability studies. To that extent, as was mentioned earlier, we sought to achieve the following:

i) To develop and examine the least complex mathematical model, suitable for transient stability studies.

ii) To identify and analyze efficient modeling techniques.

iii) To develop and investigate a selective modeling approach.

Based on study results, which were presented in the preceding chapters, we wish to make the following comments about the findings of this research project.

A. Summary and Conclusions

1. Least complex model

Such a model must meet two specific requirements, that is

i) It must approximate the basic dynamic characteristics of the synchronous machines, as indicated by the benchmark model.

ii) It must be structured so that it will be inexpensive to use.

The APP model proved to be an inexpensive and, in many cases, a fairly accurate model when compared with the benchmark model. Therefore, the APP model could be regarded as an appropriate least complex model.

The fact that the APP model provides an inexpensive representation of the synchronous machines should come as no surprise. This model was obtained by modifying an existing inexpensive model, i.e., the two-axis (the one-axis for hydromachines) model. We note that the APP model does not account for the subtransient effects. Consequently, in some instances, i.e., when the subtransient effects may not be neglected, the APP model would not adequately represent the synchronous machines. In such cases, which are identified by the criterion presented in Chapter VI, other modeling techniques are recommended.

Finally, we note that the one-axis model may not adequately represent machines with solid iron rotors, i.e., turboalternators (Figure 6), as compared with the two-axis model. This could be expected since the one-axis model includes only one rotor circuit which represents the field winding. The two-axis model, on the other hand, has an additional rotor circuit which accounts for the currents that could flow in a solid iron rotor. Therefore, when turboalternators, which generate the bulk of electric power in the U.S., are modeled for transient stability studies, when the subtransient effects are neglected, it may be desirable to represent them by the two-axis model. We note in passing that some of the commercially available transient stability programs permit only the one-axis or the classical representation (4). There are, however, more advanced programs that offer the two-axis or more detailed representations (21).

a. Treatment of saturation There are basically two methods for treatment of saturation in synchronous machines. One approach involves

adjusting the field current, based on the no-load saturation curve. Another method is based on modifying L_{AD} and, for solid iron rotor machines, L_{AQ} (Chapter IV). The first method basically accounts for the saturation of magnetic circuits along the d-axis, and thus may be acceptable for machines with salient rotors, i.e., hydromachines. In solid iron rotor machines, however, it is reasonable to expect that saturation would occur along both d- and q-axes. Consequently, adjustment of the field current may not adequately account for saturation in turboalternators (Figures 8 and 9). The second method, on the other hand, allows both d- and q-axes mutual inductances to saturate. Therefore, when turboalternators are modeled for transient stability studies, it may be desirable to represent saturation by the second method. We note, however, that the second method is an iterative process and consequently more expensive than the first approach. It remains to be seen whether the additional accuracy gained by using the second method justifies the extra computer cost.

2. Efficient modeling techniques

There are basically two possibilities for improving the efficiency of synchronous machine modeling for transient stability studies. These are model switching and accounting for the effect of the retarding torque when the APP model is used.

Model switching technique is a highly accurate method, giving results comparable to those obtained when the FULL model is used for the entire simulation period. However, at the present time, to the best of our knowledge, there are only very few, if any, commercial transient

stability programs that permit FULL representation of the synchronous machines. Therefore, there is a need for modifying many existing transient stability programs to allow for a selected few of the machines to be represented by the FULL model. Such a program must also make it possible to switch machine models during the simulation period. Inclusion of the effect of the retarding torque in the swing equations of the APP model is an inexpensive technique for improving the performance of the APP model. This technique, although not as accurate as model switching method, is nevertheless an attractive modeling approach. In particular, this technique could probably be incorporated into the existing commercial programs with minimal modifications.

3. Selective modeling approach

The examples presented in Chapters IV and V clearly demonstrate the need for a selective modeling approach. A three-tiered modeling strategy is presented in Chapter VI, which could greatly improve the efficiency of transient stability studies. This modeling strategy is based on a highly efficient criterion which provides for a fast and fairly accurate evaluation of how severely each machine is disturbed. This is achieved by calculating the expected difference between the FULL and APP models, with regard to rotor angle at clearing time ($\Delta\delta_i(t_c)$), for each machine. This information makes it possible to select the proper modeling approach for each generator. Finally, we note that this criterion can very easily be incorporated into the existing commercial programs.

B. Suggestions for Future Work

The results of this research project will hopefully encourage more detailed representation of synchronous machines for transient stability studies. If so, we recommend that:

1. The techniques for representing the external system also be improved and made compatible with the detailed generator models used. If this is not the case, satisfactory interfacing between the models may not be possible.
2. The performance of the proposed modeling techniques when other types of external system representations are used be examined.
3. The outcome of system studies will depend, in addition to the system's mathematical model, on system parameters. Therefore, an industry-wide research effort for improving data acquisition techniques for power systems is needed to assure that we are not attempting ten-place accuracy answers with two-place accuracy data.

VIII. REFERENCES

1. Kimbark, E. W. Power System Stability. Vol. 1. New York: John Wiley & Sons, Inc., 1948.

2. Undrill, J. M. "Equipment and Load Modeling in Power System Dynamic Simulation." Paper presented at Energy Foundation Conference, Henniker, New Hampshire, August 1975 on "System Engineering for Power," sponsored by U.S. Energy Research and Development Administration. ERDA Report No. CONF-750867: 394-418.

3. Dyrkacz, M. S., C. C. Young, and F. J. Maginniss. "A Digital Transient Stability Program Including the Effects of Regulator Exciter and Governor Response." AIEE Transactions PAS-79 (1961):1245-57.

4. Philadelphia Electric Company. Philadelphia Electric Company Power System Stability Program. Power System Planning Division. Users Guide UG004-2 (1971).

5. Dandeno, P. L., R. L. Hauth, and R. P. Schulz. "Effects of Synchronous Machine Modeling in Large Scale System Studies." IEEE Transactions PAS-92 (1973): 574-82.

6. Adkins, B., and R. G. Harley. "Calculation of Angular Back Swing Following a Short Circuit of a Loaded Alternator." Proceedings IEE 117 (1970): 377-86.

7. Adkins, B., and S. S. Kalsi. "Transient Stability of Power Systems Containing both Synchronous and Induction Machines." Proceedings IEE 118 (1971): 1467-1474.

8. Harley, R.G., and D. J. N. Limebeer. "Synchronous Machine Stability Using Composite Governor and Voltage Regulator Models." University of Natal, Durban, South Africa. Private communication.

9. Neilson, R., and G. Shackshaft. "Results of Stability Tests on an Underexcited 120 MW Generator." Proceedings IEE 119 (1972): 175-88.

10. NPCC Report. "Effects of Synchronous Machine Modeling in Large Scale System Studies." Private communication.

11. Manchur, G., and W. Watson. "Synchronous Machine Operational Impedances from Low Voltage Measurements at the Stator Terminals." IEEE Transactions PAS-93 (1974): 777-84.

12. Dandeno, P.L., and P. Kundur. "Stability Performance of 555 MVA Turboalternators - Digital Comparisons with System Operating Tests." IEEE Transactions PAS-93(1974): 767-76.

13. Dommel, H. W., and N. Sato. "Fast Transient Stability Solutions." IEEE Transactions PAS-91 (1972): 1643-50.

14. Lee, S. T. Y., and F. C. Schweppe. "Distance Measures and Coherency Recognition Transient Stability Equivalents." IEEE Transactions PAS-92 (1973): 1550-57.

15. Goudie, D. B., B. D. Spalding, and H. Yee. "Coherency Recognition for Transient Stability Studies Using Singular Points." IEEE Transactions PAS-96 (1977): 1368-75.

16. Brown, H. E., D. Coleman, R. E. Nied, and R. B. Shipley. "A Study of Stability Equivalents." IEEE Transactions PAS-88 (1969): 200-07.

17. Elangovan, S., and A. Kuppurajulu. "Simplified Power System Models for Dynamic Stability Studies." IEEE Transactions PAS-90 (1971): 11-23.

18. Lee, Y. W., W. D. Humpage, and K. P. Wong. "Numerical Integration Algorithms in Power System Dynamic Analysis." Proceedings IEE 121 (1974): 467-73.

19. Talukdar, S. N., and K. N. Stanton. "New Integration Algorithms for Transient Stability Studies." IEEE Transactions PAS-89 (1970): 985-91.

20. Henrici, P. Discrete Variable Methods in Ordinary Differential Equations. New York: John Wiley & Sons, Inc., 1961.

21. Electric Power Research Institute. "Power System Dynamic Analysis Phase I." EPRI Report. Palo Alto, California. Private communication.

22. Clarke, E. Circuit Analysis of A-C Power Systems. Vol. 2. New York: John Wiley & Sons, Inc., 1950.

23. Kimbark, E. W. Power System Stability. Vol. 3. New York: John Wiley & Sons, Inc., 1956.

24. Concordia, C. Synchronous Machines - Theory and Performance. New York: John Wiley & Sons, Inc., 1951.

25. Adkins, B., and R. G. Harley. The General Theory of Alternating Current Machines: Application to Practical Problems. London: Chapman and Hall, 1975.

26. Anderson, P. M., and A. A. Fouad. Power System Control and Stability. Ames, Iowa: Iowa State University Press, 1977.

27. Park, R. H. "Two Reaction Theory of Synchronous Machines." AIEE Transactions PAS-48 (1929): 716-30.

28. Prabhashankar, K., and W. Janischewsyj. "Digital Simulation of Multimachine Power Systems for Stability Studies." IEEE Transactions PAS-87 (1968): 73-81.

29. Stevenson, W. D. Elements of Power System Analysis. New York: McGraw-Hill, Inc., 1975.

30. Anderson, P. M. Analysis of Faulted Power Systems. Ames, Iowa: Iowa State University Press, 1973.

31. Matsch, L. W. Electromagnetic and Electromechanical Machines. New York: A. Dun - Donnelley, 1977.

32. Young, C. C. "Equipment and System Modeling for Large-Scale Stability Studies." IEEE Transactions PAS-91 (1972): 99-109.

33. Adkins, B. and D. B. Mehta. "Transient Torque and Load Angle of a Synchronous Generator Following Several Types of System Disturbance." Proceedings IEE 107 (1960): 61-74.

IX. ACKNOWLEDGMENTS

The author wishes to express his appreciation to members of his committee, Dr. A. A. Fouad (chairman), Dr. R. G. Brown, Dr. A. N. Michel, Dr. A. G. Potter, and Dr. G. Seifert.

Sincere thanks are also due Dr. K. C. Kruempel and Dr. R. J. Lambert for their assistance regarding computer programming.

The author also wishes to thank Gretchen Triplett for her patience in the typing of this manuscript.

X. APPENDIX. EXCITATION SYSTEMS

Block diagrams and data for the excitation systems that were used in single machine and multimachine studies are presented in this Appendix.

A. Block Diagrams and Data for Excitation Systems of Single Machine Studies

In these studies, two excitation systems were used. These were Type 1 and Type G exciters. Data for these exciters are given in Tables 10.1 and 10.2. The block diagrams are shown in Figures 10.1 and 10.2.

Table 10.1. Data for Type 1 Exciter (RR = 0.5)[a]

$\bar{K}_A$	$\bar{K}_F$	$\bar{K}_E$	$\bar{S}_E$	$\bar{V}_{RMAX}$	$\bar{V}_{RMIN}$	$\bar{T}_A$	$\bar{T}_F$	$\bar{T}_E$	$\bar{T}_R$
25	.16	-.0445	$.0016e^{1.465E_{FD}}$	1	-1	.06	1.0	.5	0.

[a]All time constants are in seconds; all other parameters are in pu.

Block diagram for Type 1 exciter is given in Figure 10.1.

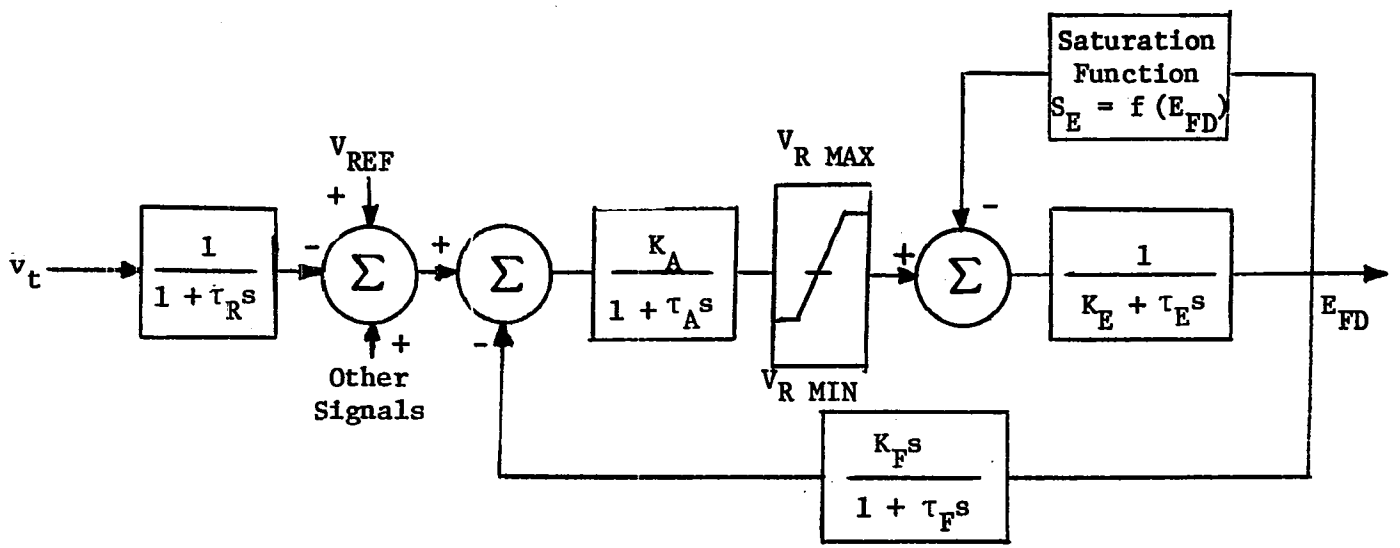

Figure 10.1. Type 1 - alternator - rectifier exciter

Table 10.2. Data for Type G Exciter (RR = 2.5)[a]

K_A	K_F	τ_{A1}	τ_{A2}	τ_F	V_{RMAX}	V_{RMIN}
250	.036	.2	0.	1.	5.15	-5.15

[a]Time constants are in seconds; all other parameters are in pu.

Block diagram for Type G exciter is given in Figure 10.2.

B. Block Diagram and Data for Excitation Systems of Multimachine Studies

Type A exciters were used in multimachine studies. Data for these exciters are given in Table 10.3. Block diagram for a Type A exciter is shown in Figure 10.3.

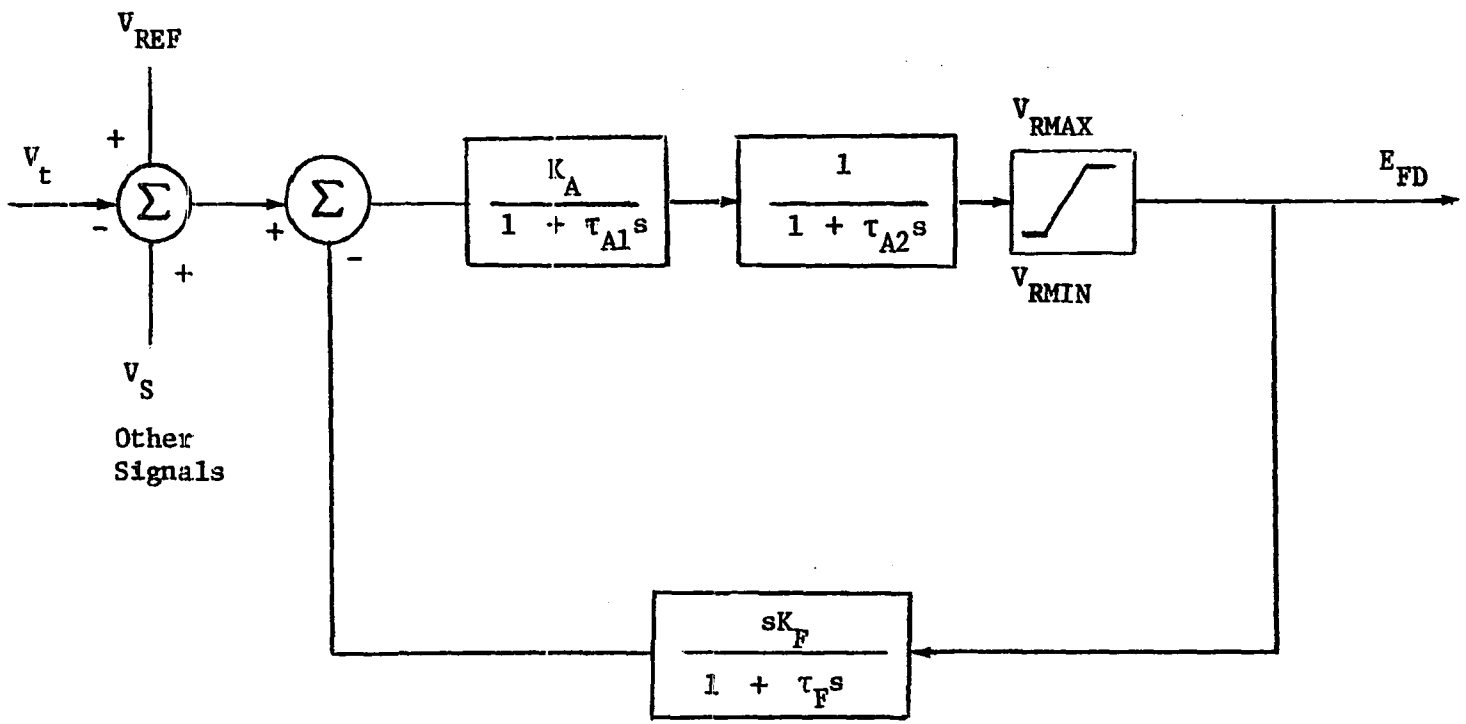

Figure A.2. Type G - Thyristor (SCR) exciter

Table 10.3. Data for Type A exciters

Exciter		1	2	3
RR		1.5	1.5	1.5
τ_R	s	0	0	0
K_A	pu	54	400	400
τ_{A1}	s	.105	.05	.05
τ_{A2}	s	0	0	0
V_{RMAX}	pu	3.850	.6130	.6130
V_{RMIN}	pu	-3.850	-.6130	-.6130
K_E	pu	-.062	-.0769	-.0769
τ_E	s	.732	1.370	1.370
A_{EX}		.0195	.0137	.0137
B_{EX}		1.1274	.6774	.6774
K_F	pu	.140	.040	.040
τ_F	s	1.0	1.0	1.0
S_E .75 max		.410	.1120	.1120
$S_{E\,max}$		1.131	.2254	.2254

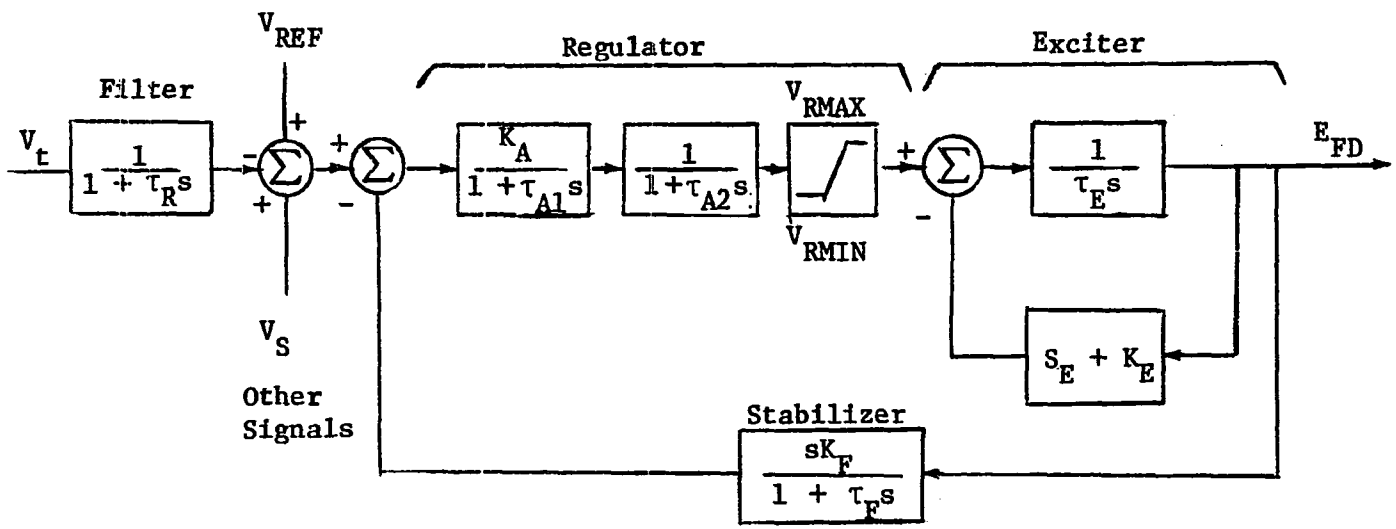

Figure 10.3. Type A - Continuously acting dc rotating excitation system